



中国科学院国家天文台

NATIONAL ASTRONOMICAL OBSERVATORIES, CHINESE ACADEMY OF SCIENCES

the SILK ROAD PROJECT at NAOC

丝绸之路计划



RECRUITMENT PROGRAM OF GLOBAL EXPERTS

LIGO black hole merger events in NBODY6++GPU; current status of stellar evolution

Rainer Spurzem*, Peter Berczik ... and Silk Road Team

Astronomisches Rechen-Inst., ZAH, Univ. of Heidelberg, Germany

National Astronomical Observatories (NAOC), Chinese Academy of Sciences

Kavli Institute for Astronomy and Astrophysics (KIAA), Peking University

spurzem@nao.cas.cn <http://silkroad.bao.ac.cn>

with collaborators: Mirek Giersz, Chris Belczynski, Agostino Leveque...

Sambaran Banerjee, Thorsten Naab, Francesco Rizzuto ...

*Research Fellow at



FIAS Frankfurt Institute for Advanced Studies



VolkswagenStiftung

Picture:
Tian Shan
Mountain
Kazakhstan
(R.Sp.)

Strategic Priority Program
'Pilot-B' on Gravitational Wave
Research in China



中国科学院国家天文台

National Astronomical Observatories, CAS

the **SILK ROAD PROJECT** at NAOC

丝绸之路计划



Rainer Spurzem

CAS Visiting Professor, Senior International Scientists
Professor at Heidelberg University (on partial leave)



Gareth Kennedy

Postdoc (CAS Fellow)

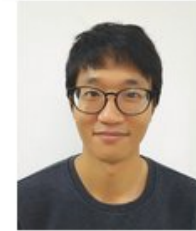
(now Shanghai)



Xiaoying Pang

Postdoc at NAOC

(now Suzhou)



Jongsuk Hong

KIAA Postdoc

from Oct. 1, 2016



Shuo Li

Postdoc (NAOC)



Shiyan Zhong

Ph. D. Student (NAOC)

(now Kunming)



Qi Shu

Ph.D. student KIAA/PKU



Peter Berczik

Senior Silk Road Project Postdoc

Bhusan Kayastha
Ph.D student



Yohai Meiron

Postdoc (KIAA-PKU)

(now Toronto)



Long Wang

Ph. D. Student (Peking University)

(now Bonn)



Matthias Kühtreiber

Ph.D. Student Observatory

Univ. Vienna, Austria

Visiting Student
KIAA/PKU/NAOC



Thijs Kouwenhoven

Balren research professor at KIAA

(now Suzhou)



Jose Fiestas

Postdoc at NAOC

(now Lima)



Maxwell Tsai (aka. Xu CA¹¹)

Ph. D. Student (NAOC)

(now Leiden)



Austria: Gerhard Hensler, Matthias Kühtreiber
Kazakhstan: Chingis Omarov, Bekdaulet Shukirgaliyev, Mukhagaly Kalambay, ...
Germany: Andreas Just, Fabian Klein, Taras Panamarev, ...
Ukraine: Peter Berczik, Margaryta Sobolenko, Alexander Veles

RECRUITMENT
PROGRAM OF GLOBAL EXPERTS

Kavli Institute for Astronomy and Astrophysics, Peking Univ.



北京大學
PEKING UNIVERSITY



Regular Openings:
Postdoc
Faculty
Visitors
(see AAS Job Reg,
search KIAA)

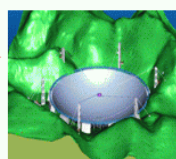
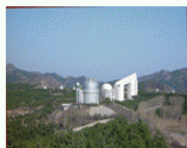
Total ~25 postdocs; 2/3 are non-Chinese.



中国科学院国家天文台

NATIONAL ASTRONOMICAL OBSERVATORIES, CHINESE ACADEMY OF SCIENCES

NAOC
CAS

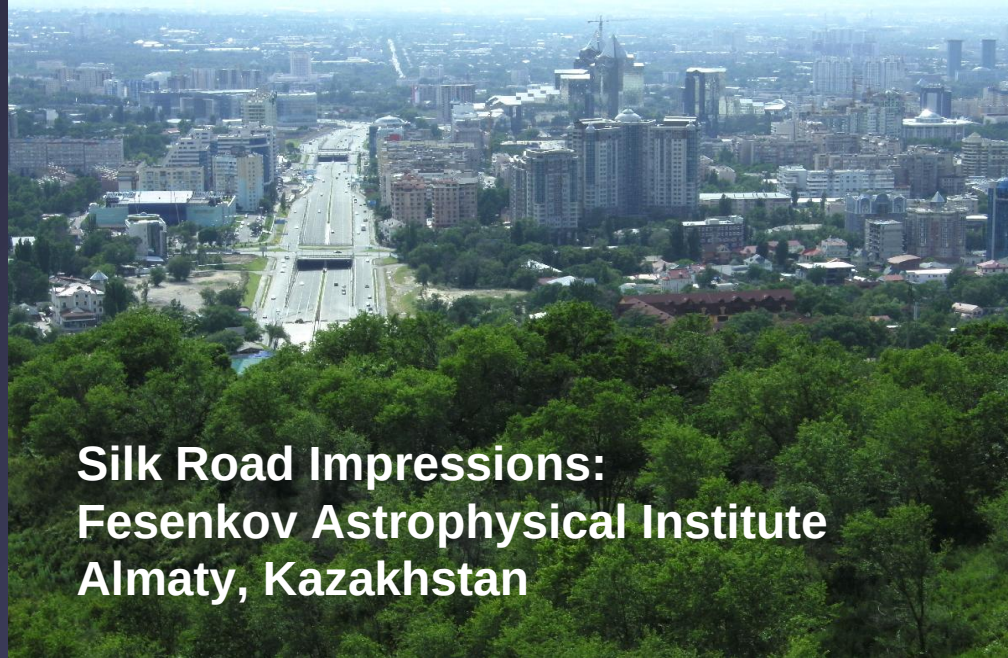


Top: NAOC Headquarter Beijing
Bottom: LAMOST Site



**Silk Road Project =
Computational Science Project...**



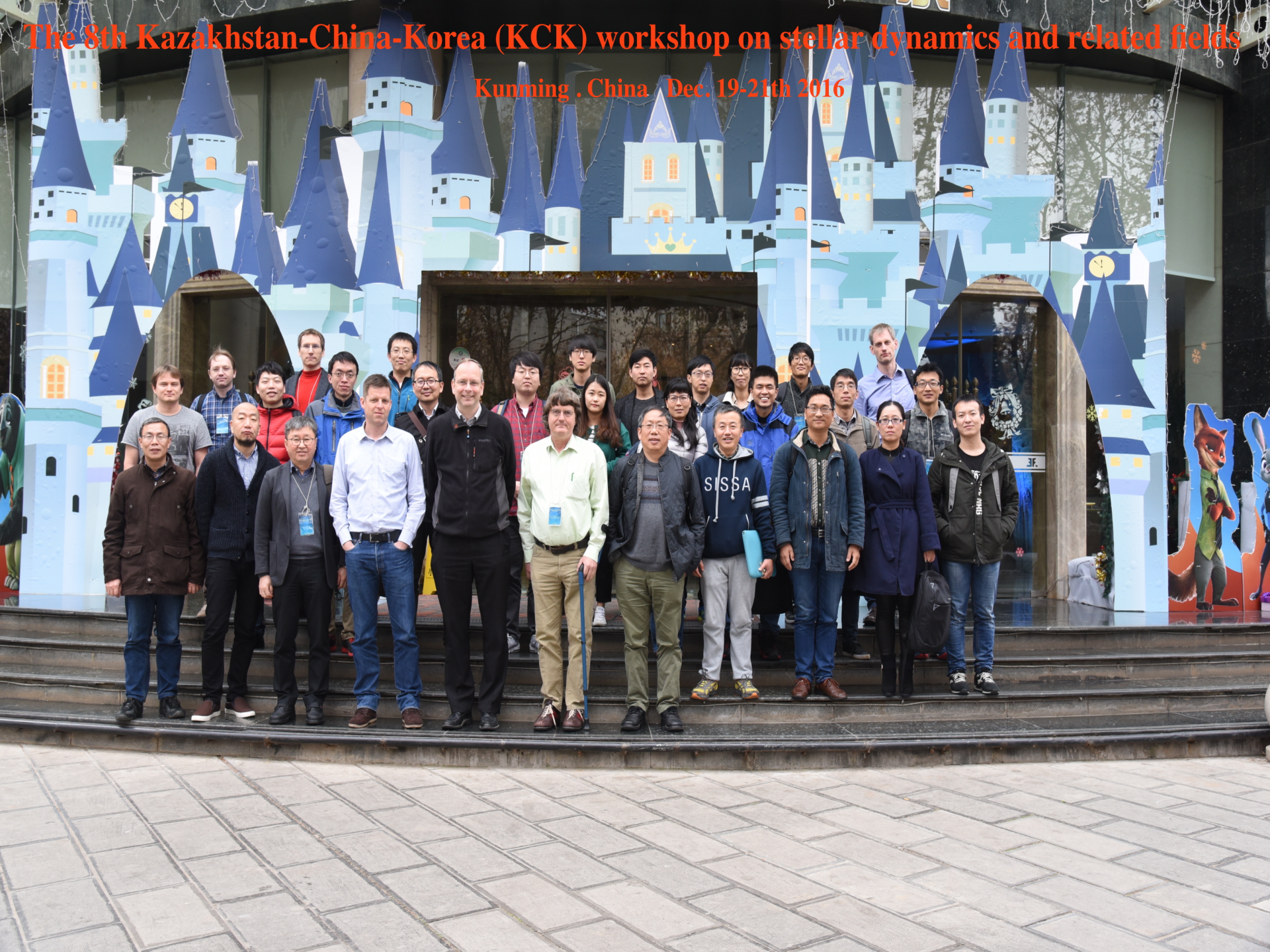


**Silk Road Impressions:
Fesenkov Astrophysical Institute
Almaty, Kazakhstan**



The 8th Kazakhstan-China-Korea (KCK) workshop on stellar dynamics and related fields

Kunming, China, Dec. 19-21th 2016



1) Star Cluster Dynamics

2) Post-Newtonian Theory

3) Black Hole Binaries – Grav. Waves

4) Supermassive Black Hole Binaries

5) Computational Instruments

On the Evolution of Stellar Systems

V. A. Ambartsumian

(George Darwin Lecture, delivered on 1960 May 13)

IN THIS lecture we shall consider some aspects of the problem of the evolution of stellar systems. We shall concentrate chiefly on *galaxies*. However, at the same time we shall treat here some questions connected with *star clusters* as component members of galaxies.



Concepts discussed:

- Total Energy of grav. star clusters NOT additive
- No thermodynamical equilibrium
- Statistical Theory of Gases to be used with care
(large mean free path)
- Locally truncated Maxwellian distribution.

(Credit: X-ray: NASA/CfA/J. Grindlay et al.,
Optical: NASA/STScI/R. Gilliland et al.)

X-ray binaries
with neutron stars
and black holes

Globular Cluster 47 Tuc
~ one million stars

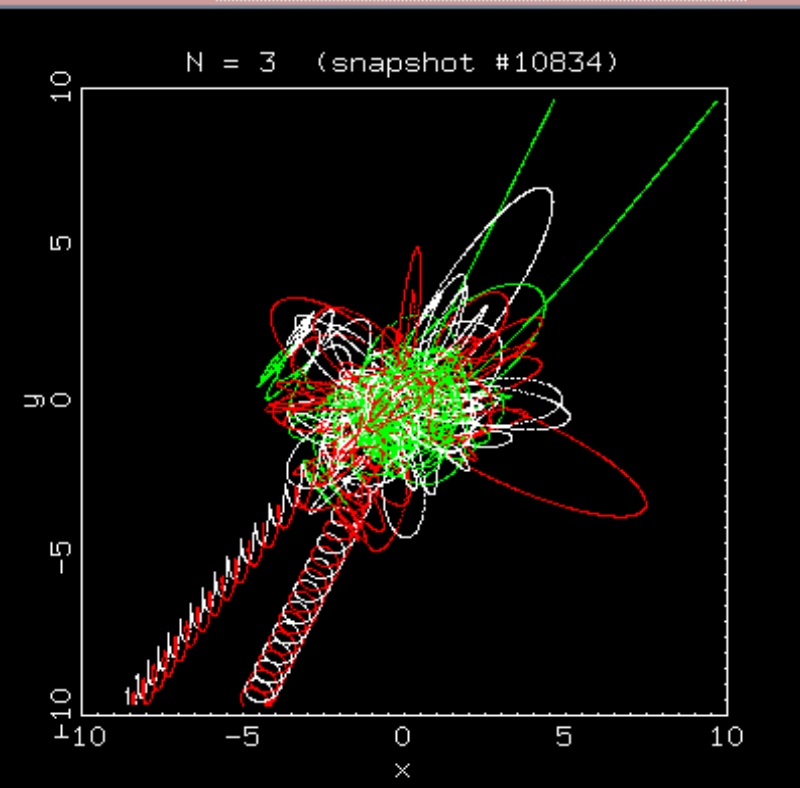
$$\vec{a}_0 = \sum_j Gm_j \frac{\vec{R}_j}{R_j^3} ; \quad \vec{a}_0 = \sum_j Gm_j \left[\frac{\vec{V}_j}{R_j^3} - \frac{3(\vec{V}_j \cdot \vec{R}_j)\vec{R}_j}{R_j^5} \right]$$

3-body Encounters Starlab Simulation (S.L.W. McMillan)

<http://www.physics.drexel.edu/~steve/>

-> Three-Body-Problem

StarLab



**Gravothermal Oscillations -
Attractor in Phase Space
Spurzem 1994, Giersz & Spurzem 1994
Amaro-Seoane, Freitag & Sp. 2004**

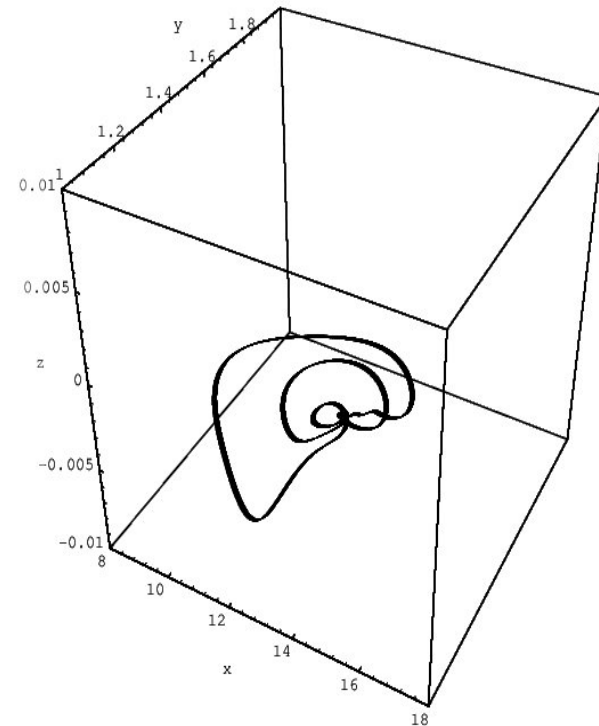


Fig. 3:

Projected three-dimensional attractor for $N = 100.000$ system, $x = \log \rho'_c$, $y = \log \sigma'_c$, $z = \xi$.

Follow-Up of Angeletti & Giannone and Larson

DRAGON Simulation

<http://silkroad.bao.ac.cn/dragon/>

One million stars direct simulation,

biggest and most realistic direct N-Body simulation of globular star clusters.

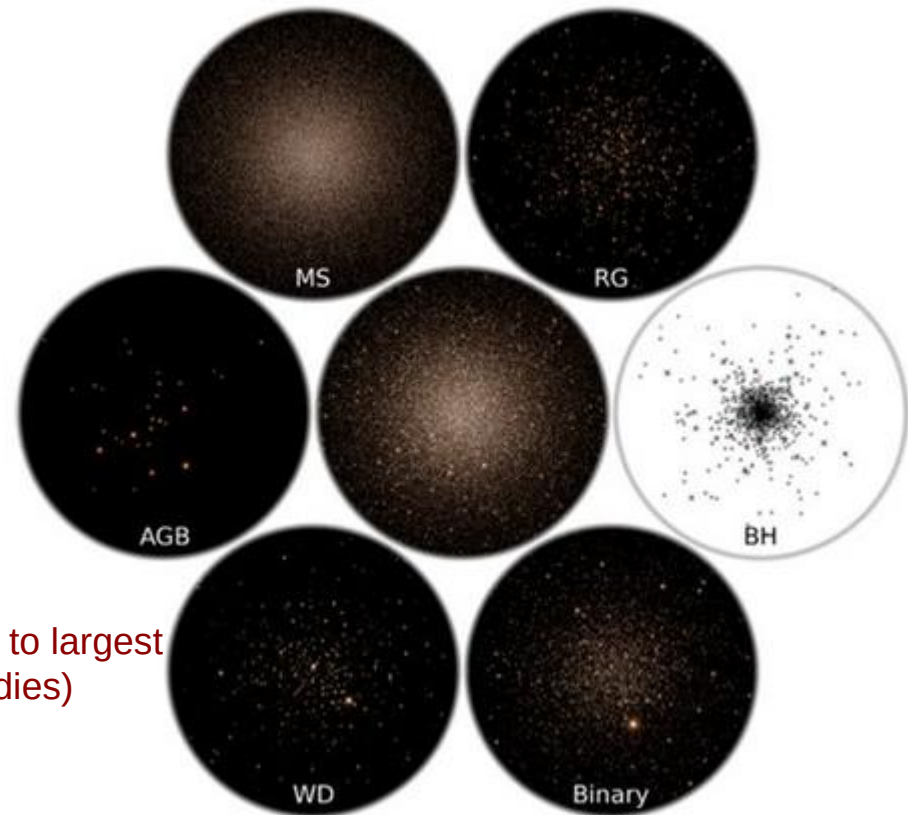
With stellar mass function, single and binary stellar evolution, regularization of close encounters, tidal field (NBODY6++GPU).

(NAOC/Silk Road/MPA collaboration).

Wang, Spurzem, Aarseth, Naab et al.
MNRAS, 2015

Wang, Spurzem, Aarseth Naab, et al.
MNRAS 2016

Number of Floating Point Operations (~1M bodies) similar to largest Cosmological simulations (Millennium, Illustris, ~100M bodies)



THE INITIAL CONDITIONS

DRAGON Simulations

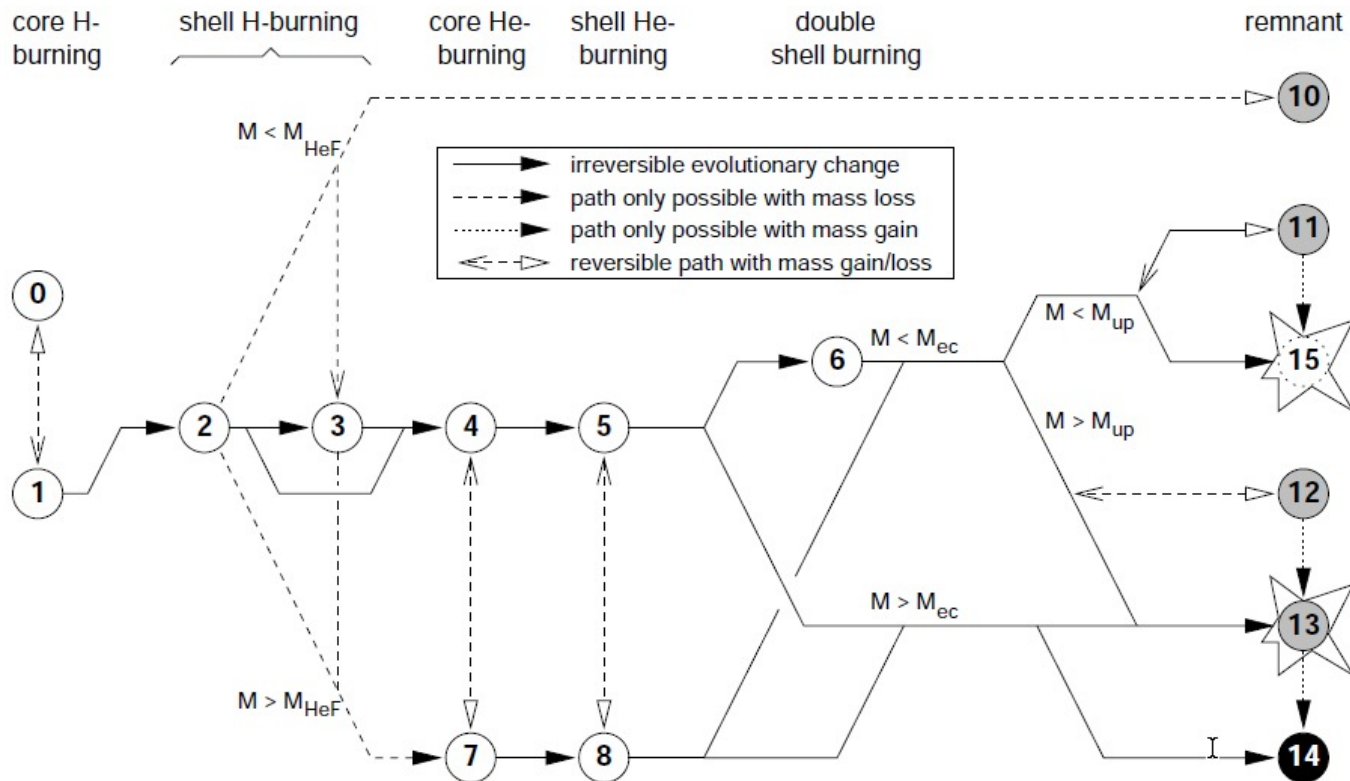
- $N_{\text{single}} = 950\text{K}; N_{\text{binary}} = 50\text{K}$
- **Plummer** + point mass potential (MakeHalo, Dehnen 2005) (XX)
- **IMF**: Kroupa, 2001; $0.08 - 100 M_{\odot}$ Or KTG 1993
- $$M_{\text{tot}} = 0.574 \times 10^8 M_{\odot} = 10 M_{\text{smbh}} \text{ (XX)}$$
- SSE/BSE: High Mass Loss, Common Envelope: $\alpha = 1$
- **Binaries**:
 - Uniform in $\log(a)$
 - Thermal eccentricity distribution $f(e) = 2e$
 - Mass ratios: $f(q) \propto q^{-0.4}$ (Kouwenhoven+2007)
- **Kick**: 265 km/s (Hobbs+2005)

(XX) Only in case of central SMBH

Original Slide by
Taras Panamarev

Most NBODY Codes ...

Hurley,
Ph.D. thesis



0 = main sequence $M < 0.7 M_{\odot}$

1 = main sequence $M > 0.7 M_{\odot}$

2 = Hertzsprung gap / subgiant

3 = first-ascent red giant

4 = horizontal branch / helium-burning giant

5 = early asymptotic giant / red supergiant

6 = thermally pulsating asymptotic giant

7 = naked helium main sequence

8 = naked helium (sub) giant

10 = helium white dwarf

11 = carbon/oxygen white dwarf

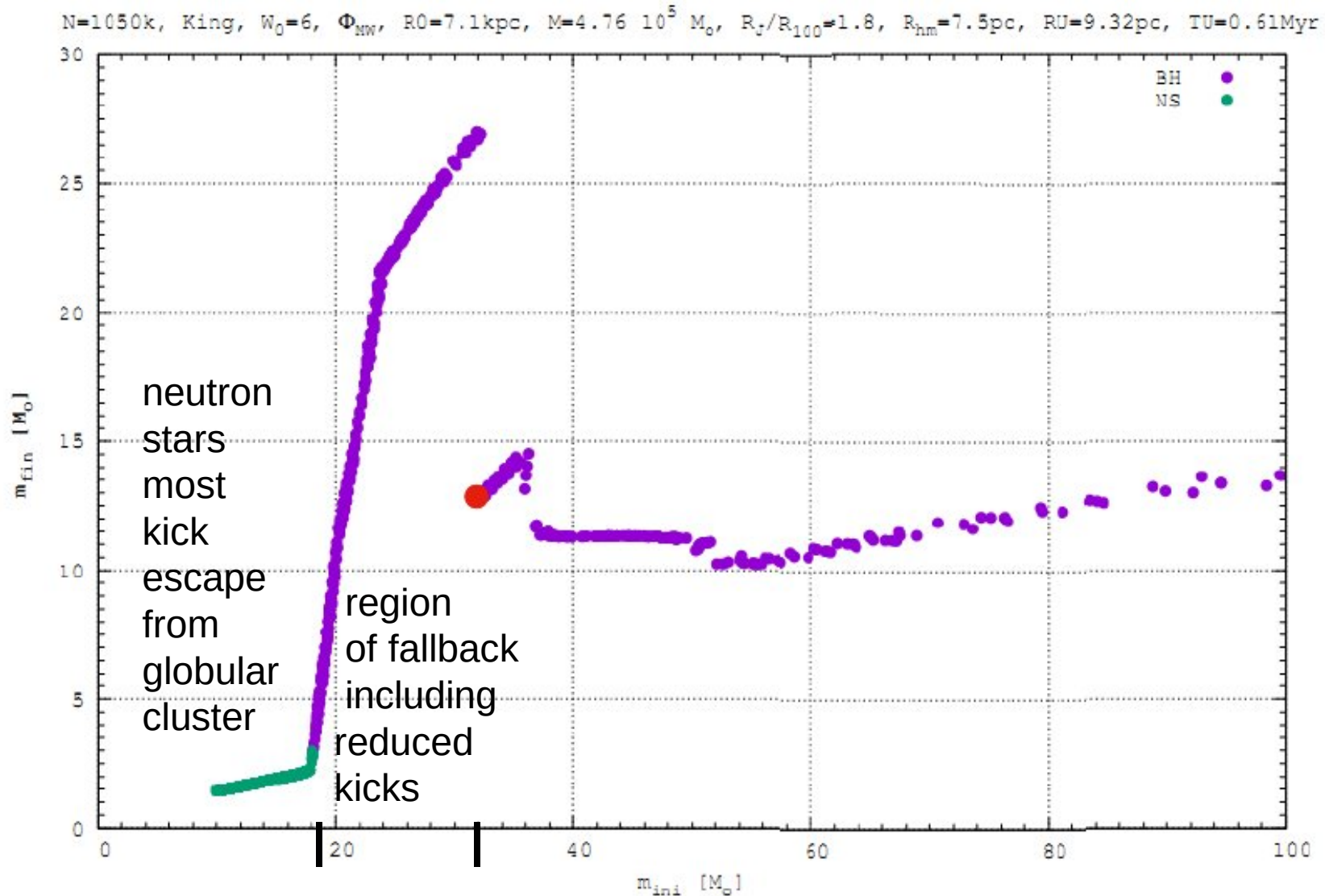
12 = oxygen/neon white dwarf

13 = neutron star

14 = black hole

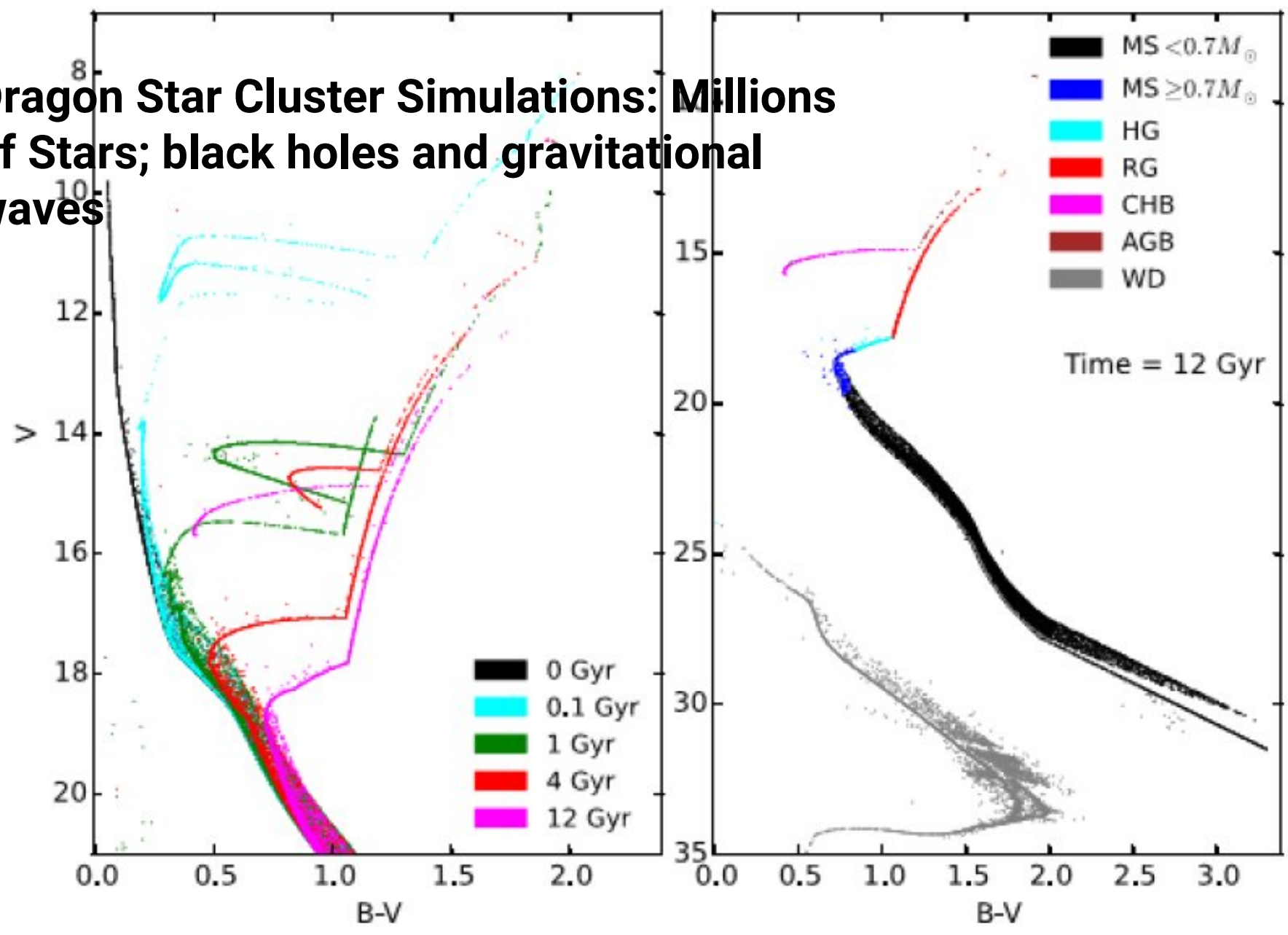
15 = no stellar remnant

Initial – Final Mass Relation in simulations for neutr. stars/black holes

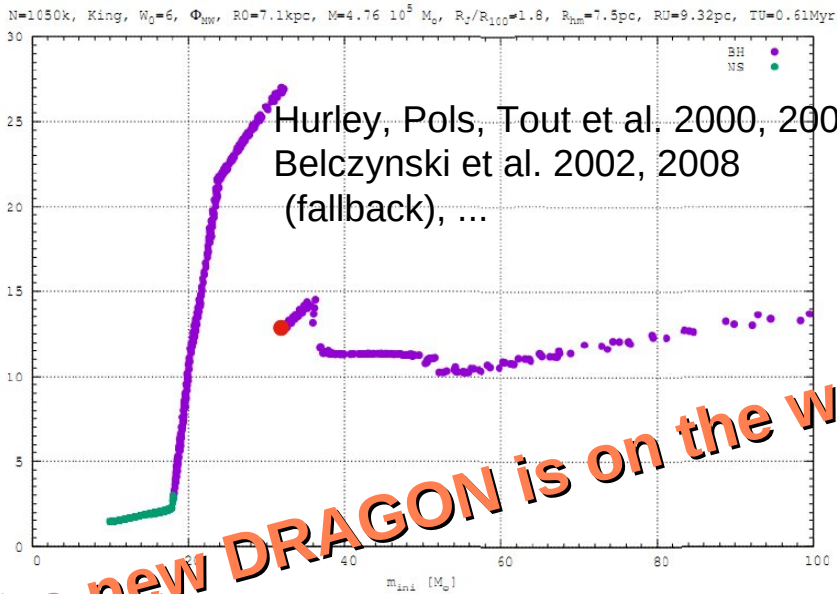


Hurley, Pols, Tout et al. 2000, 2002; Belczynski et al. 2002, 2008 (fallback), ...

Dragon Star Cluster Simulations: Millions of Stars; black holes and gravitational waves

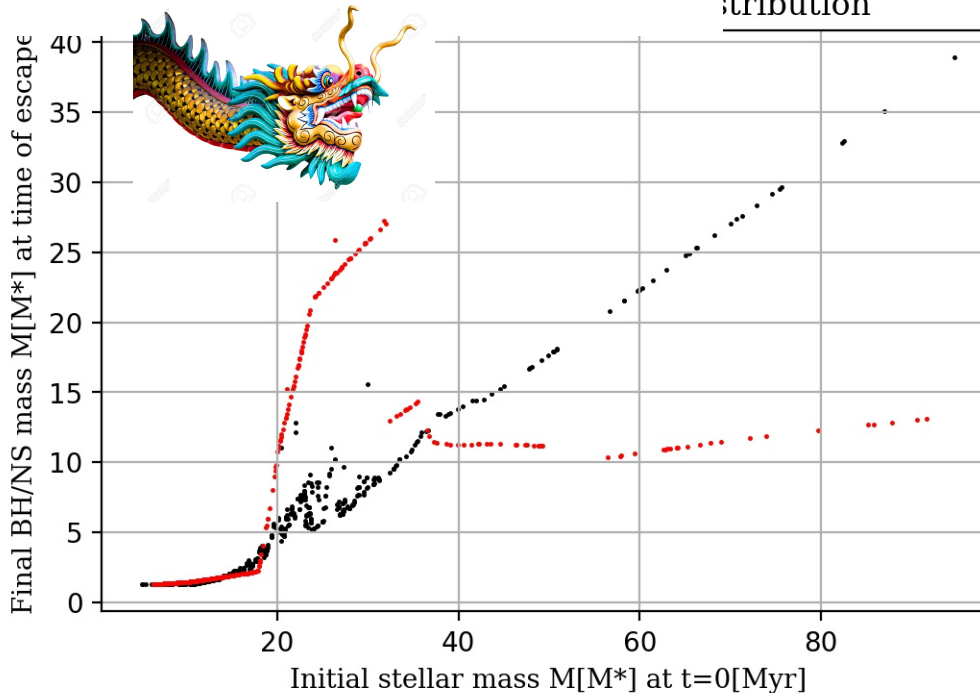


Initial – Final Mass Relation in simulations for neutron stars and black holes
 Old DRAGON vs. New DRAGON
 (see also Belczynski et al. 2019)



The new DRAGON is on the way...

mass and the explosion
 for 6.634 Gyr
 distribution

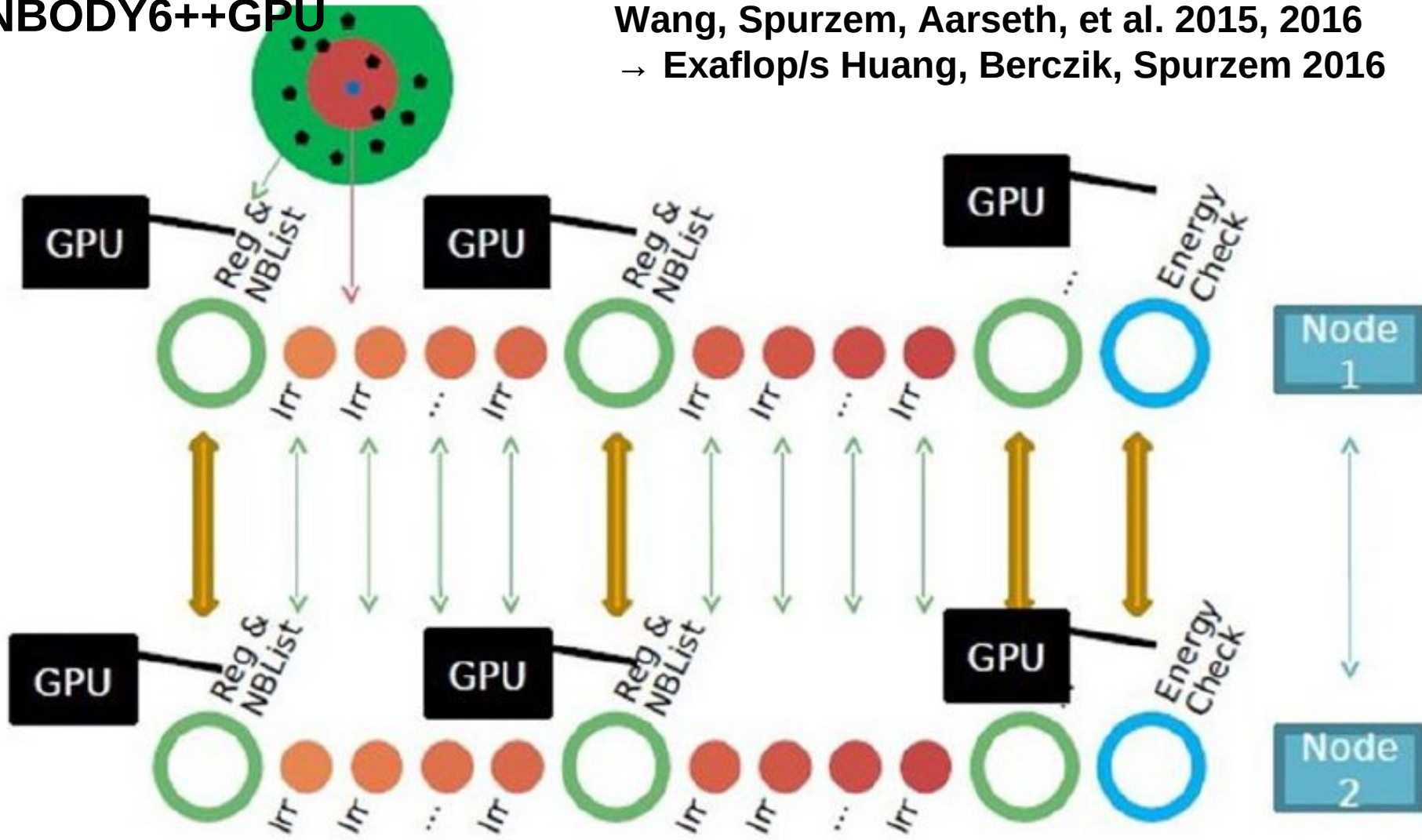


- NGC 3201 - Nbody6++GPU-Oct2019
 #NS = 389, #BH = 371
 Runtime = 6.634 Gyr
- Bhusan - Nbody6++GPU-Feb2019
 #NS = 668, #BH = 157
 Runtime = 2.349 Gyr

Our CPU/GPU N-body (AC) code

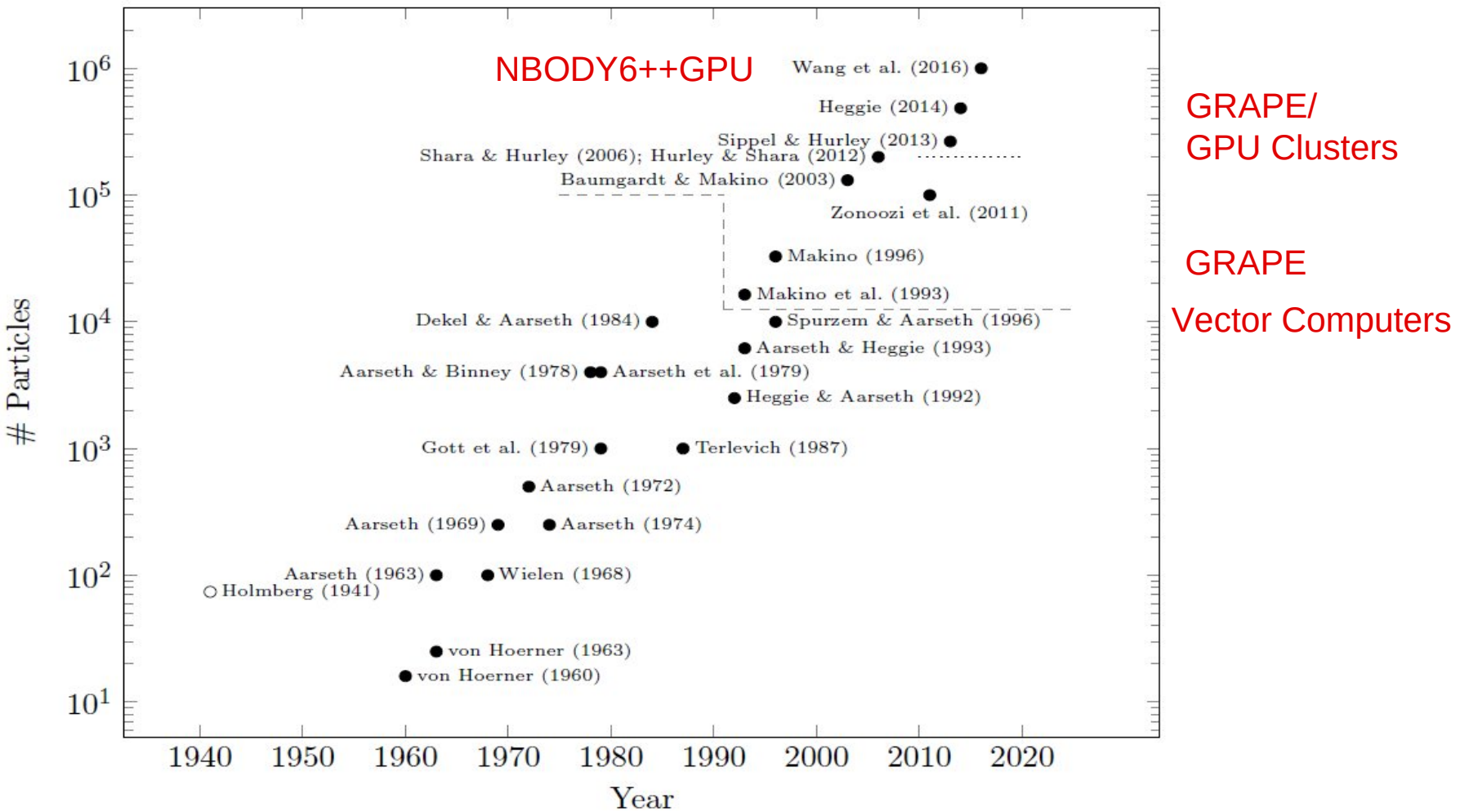
NBODY6++GPU

Wang, Spurzem, Aarseth, et al. 2015, 2016
→ Exaflop/s Huang, Berczik, Spurzem 2016



<https://github.com/lwang-astro/betanb6pp>

“Moore's” Law for Direct N-Body

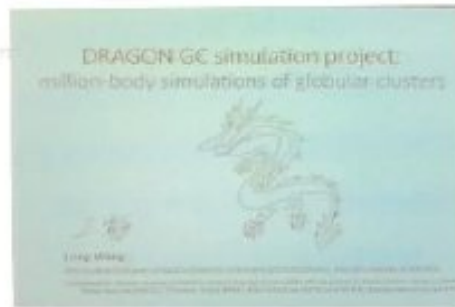


by D.C. Heggie Via added new cits. Sippel

CPU/GPU **N-body6++**

Long Wang, Ph.D. Peking University 2016:
Million-Body Award by MODEST community
And IAU Ph.D. prize

The million-body problem at last!



The bottle of whisky is awarded to
Long Wang (Beijing)

Key Question 1. When will we see the first star-by-star N -body model of a globular cluster?

- Honest N -body simulation
- Reasonable mass at 12 Gyr ($\sim 5 \times 10^4 M_{\odot}$)
- Reasonable tide (circular galactic orbit will do)
- Reasonable IMF (e.g. Kroupa)
- Reasonable binary fraction (a few percent)
- Any initial model you like (Plummer will do)
- A submitted paper (astro-ph will do)

An inducement: a bottle of single malt Scotch whisky worth €50



- 1) Star Cluster Dynamics
- 2) Post-Newtonian Theory
- 3) Black Hole Binaries – Grav. Waves
- 4) Supermassive Black Hole Binaries
- 5) Computational Instruments

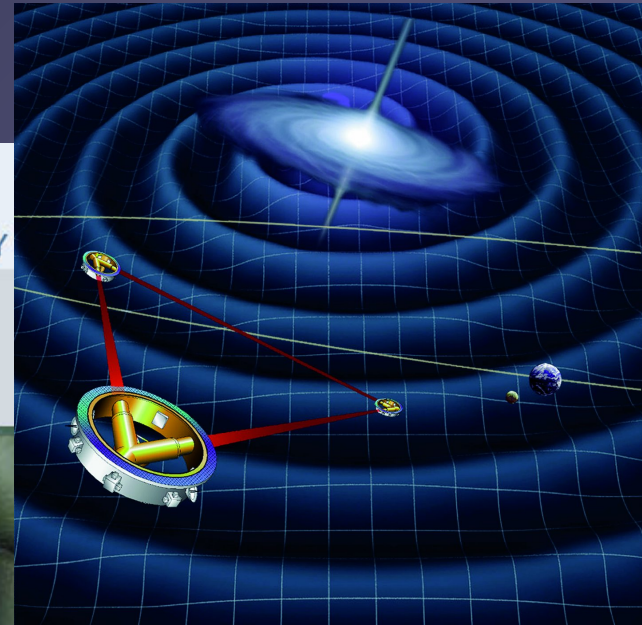
EUROPEAN GRAVITATIONAL OBSERVATORY

EGO



Consortium of

VIRGO Detector in Cascina near Pisa, Italy



LISA =
Laser Space
Interferometer Antenna



Post-Newtonian Dynamics

$\mathbf{r}; \mathbf{v}$: relative distance, velocity

$\mu = m_1 m_2 / M$: reduced mass ($M = m_1 + m_2$)

$\nu = \mu / M$: mass ratio

$\mathbf{n} = \mathbf{r} / r$: unit vector in radial direction

$$\frac{dv^i}{dt} = -\frac{Gm}{r^2} [(1 + \mathcal{A}) n^i + \mathcal{B} v^i] + \mathcal{O}\left(\frac{1}{c^8}\right), \quad (181)$$

and find [43] that the coefficients \mathcal{A} and \mathcal{B} are

$$\begin{aligned} \mathcal{A} = & \frac{1}{c^2} \left\{ -\frac{3\dot{r}^2 \nu}{2} + v^2 + 3\nu v^2 - \frac{Gm}{r} (4 + 2\nu) \right\} && \text{Perihel shift} \\ & + \frac{1}{c^4} \left\{ \frac{15\dot{r}^4 \nu}{8} - \frac{45\dot{r}^4 \nu^2}{8} - \frac{9\dot{r}^2 \nu v^2}{2} + 6\dot{r}^2 \nu^2 v^2 + 3\nu v^4 - 4\nu^2 v^4 \right. && \dots \text{ higher order...} \\ & \left. + \frac{Gm}{r} \left(-2\dot{r}^2 - 25\dot{r}^2 \nu - 2\dot{r}^2 \nu^2 - \frac{13\nu v^2}{2} + 2\nu^2 v^2 \right) + \frac{G^2 m^2}{r^2} \left(9 + \frac{87\nu}{4} \right) \right\} \\ & + \frac{1}{c^5} \left\{ -\frac{24\dot{r} \nu v^2}{5} \frac{Gm}{r} - \frac{136\dot{r} \nu}{15} \frac{G^2 m^2}{r^2} \right\} && \text{Grav. Radiation} \end{aligned}$$

Schäfer, Gauge Theor. Grav. 36, 2223 (2004)

Memmesheimer, Gopakumar, Schäfer, Phys. Rev.D 70, 104011 (2004)

Blanchet, Luc; Living Reviews 2002, llr-2002-3

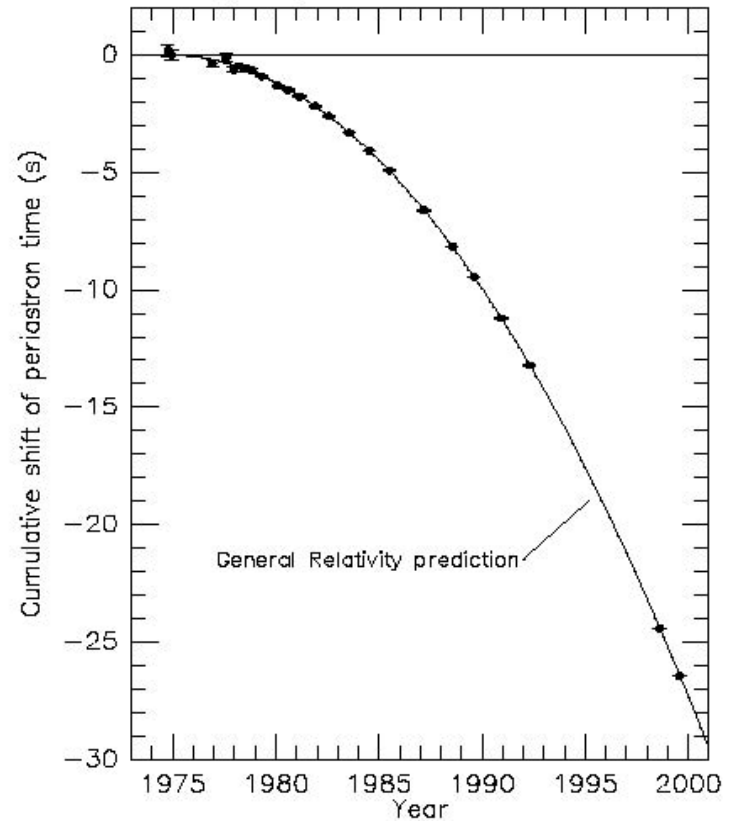
$$\begin{aligned}
& + \frac{1}{c^6} \left\{ -\frac{35\dot{r}^6\nu}{16} + \frac{175\dot{r}^6\nu^2}{16} - \frac{175\dot{r}^6\nu^3}{16} + \frac{15\dot{r}^4\nu v^2}{2} - \frac{135\dot{r}^4\nu^2 v^2}{4} + \frac{255\dot{r}^4\nu^3 v^2}{8} \right. \\
& \quad - \frac{15\dot{r}^2\nu v^4}{2} + \frac{237\dot{r}^2\nu^2 v^4}{8} - \frac{45\dot{r}^2\nu^3 v^4}{2} + \frac{11\nu v^6}{4} - \frac{49\nu^2 v^6}{4} + 13\nu^3 v^6 \\
& \quad + \frac{Gm}{r} \left(79\dot{r}^4\nu - \frac{69\dot{r}^4\nu^2}{2} - 30\dot{r}^4\nu^3 - 121\dot{r}^2\nu v^2 + 16\dot{r}^2\nu^2 v^2 + 20\dot{r}^2\nu^3 v^2 + \frac{75\nu v^4}{4} \right. \\
& \quad \quad \left. + 8\nu^2 v^4 - 10\nu^3 v^4 \right) \\
& \quad + \frac{G^2 m^2}{r^2} \left(\dot{r}^2 + \frac{32573\dot{r}^2\nu}{168} + \frac{11\dot{r}^2\nu^2}{8} - 7\dot{r}^2\nu^3 + \frac{615\dot{r}^2\nu\pi^2}{64} - \frac{26987\nu v^2}{840} + \nu^3 v^2 \right. \\
& \quad \quad \left. - \frac{123\nu\pi^2 v^2}{64} - 110\dot{r}^2\nu \ln\left(\frac{r}{r'_0}\right) + 22\nu v^2 \ln\left(\frac{r}{r'_0}\right) \right) \\
& \quad + \frac{G^3 m^3}{r^3} \left(-16 - \frac{437\nu}{4} - \frac{71\nu^2}{2} + \frac{41\nu\pi^2}{16} \right) \left. \right\} \\
& + \frac{1}{c^7} \left\{ \frac{Gm}{r} \left(\frac{366}{35}\nu v^4 + 12\nu^2 v^4 - 114v^2\nu\dot{r}^2 - 12\nu^2 v^2\dot{r}^2 + 112\nu\dot{r}^4 \right) \right. \\
& \quad + \frac{G^2 m^2}{r^2} \left(\frac{692}{35}\nu v^2 - \frac{724}{15}v^2\nu^2 + \frac{294}{5}\nu\dot{r}^2 + \frac{376}{5}\nu^2\dot{r}^2 \right) \\
& \quad \left. + \frac{G^3 m^3}{r^3} \left(\frac{3956}{35}\nu + \frac{184}{5}\nu^2 \right) \right\}, \tag{182}
\end{aligned}$$

$$\begin{aligned}
\mathcal{B} = & \frac{1}{c^2} \{-4\dot{r} + 2\dot{r}\nu\} \\
& + \frac{1}{c^4} \left\{ \frac{9\dot{r}^3\nu}{2} + 3\dot{r}^3\nu^2 - \frac{15\dot{r}\nu v^2}{2} - 2\dot{r}\nu^2 v^2 + \frac{Gm}{r} \left(2\dot{r} + \frac{41\dot{r}\nu}{2} + 4\dot{r}\nu^2 \right) \right\} \\
& + \frac{1}{c^5} \left\{ \frac{8\nu v^2 Gm}{5r} + \frac{24\nu G^2 m^2}{5r^2} \right\} \\
& + \frac{1}{c^6} \left\{ -\frac{45\dot{r}^5\nu}{8} + 15\dot{r}^5\nu^2 + \frac{15\dot{r}^5\nu^3}{4} + 12\dot{r}^3\nu v^2 - \frac{111\dot{r}^3\nu^2 v^2}{4} - 12\dot{r}^3\nu^3 v^2 - \frac{65\dot{r}\nu v^4}{8} \right. \\
& \quad + 19\dot{r}\nu^2 v^4 + 6\dot{r}\nu^3 v^4 \\
& \quad + \frac{Gm}{r} \left(\frac{329\dot{r}^3\nu}{6} + \frac{59\dot{r}^3\nu^2}{2} + 18\dot{r}^3\nu^3 - 15\dot{r}\nu v^2 - 27\dot{r}\nu^2 v^2 - 10\dot{r}\nu^3 v^2 \right) \\
& \quad \left. + \frac{G^2 m^2}{r^2} \left(-4\dot{r} - \frac{18169\dot{r}\nu}{840} + 25\dot{r}\nu^2 + 8\dot{r}\nu^3 - \frac{123\dot{r}\nu\pi^2}{32} + 44\dot{r}\nu \ln \left(\frac{r}{r_0'} \right) \right) \right\} \\
& + \frac{1}{c^7} \left\{ \frac{Gm}{r} \left(-\frac{626}{35}\nu v^4 - \frac{12}{5}\nu^2 v^4 + \frac{678}{5}\nu v^2 \dot{r}^2 + \frac{12}{5}\nu^2 v^2 \dot{r}^2 - 120\nu \dot{r}^4 \right) \right. \\
& \quad + \frac{G^2 m^2}{r^2} \left(\frac{164}{21}\nu v^2 + \frac{148}{5}\nu^2 v^2 - \frac{82}{3}\nu \dot{r}^2 - \frac{848}{15}\nu^2 \dot{r}^2 \right) \\
& \quad \left. + \frac{G^3 m^3}{r^3} \left(-\frac{1060}{21}\nu - \frac{104}{5}\nu^2 \right) \right\}.
\end{aligned} \tag{183}$$

Indirect Proof by Hulse and Taylor, binary pulsar (Nobel prize 1993)



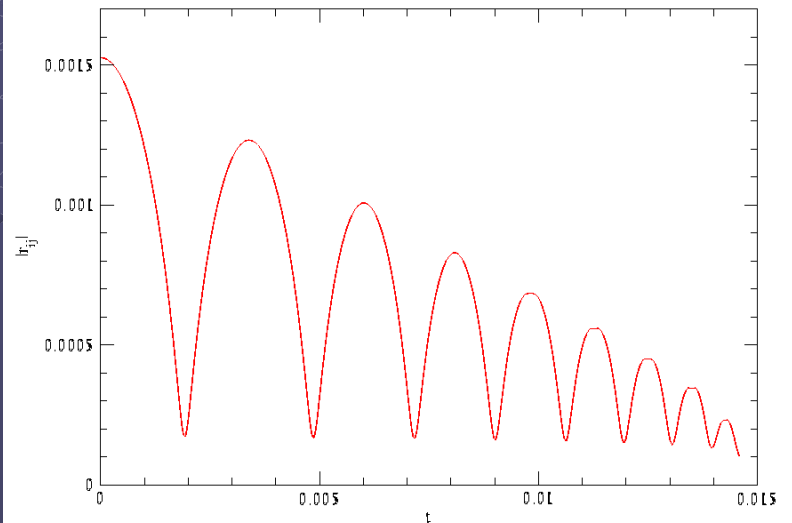
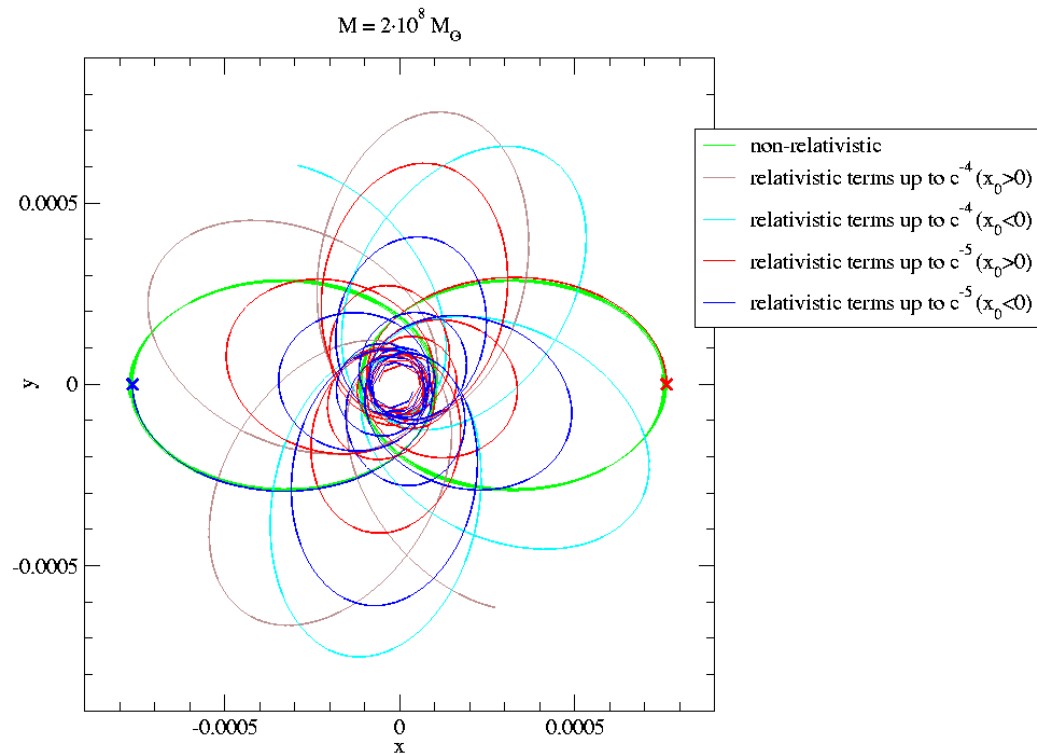
Comparison between observations of the binary pulsar PSR1913+16, and the prediction of general relativity based on loss of orbital energy via gravitational waves



From J. H. Taylor and J. M. Weisberg, unpublished (2000)

Gravitational Waves

What happens afterwards? Post-Newton Order „2.5“ ...



Kupi, Amaro-Seoane & Spurzem 2006

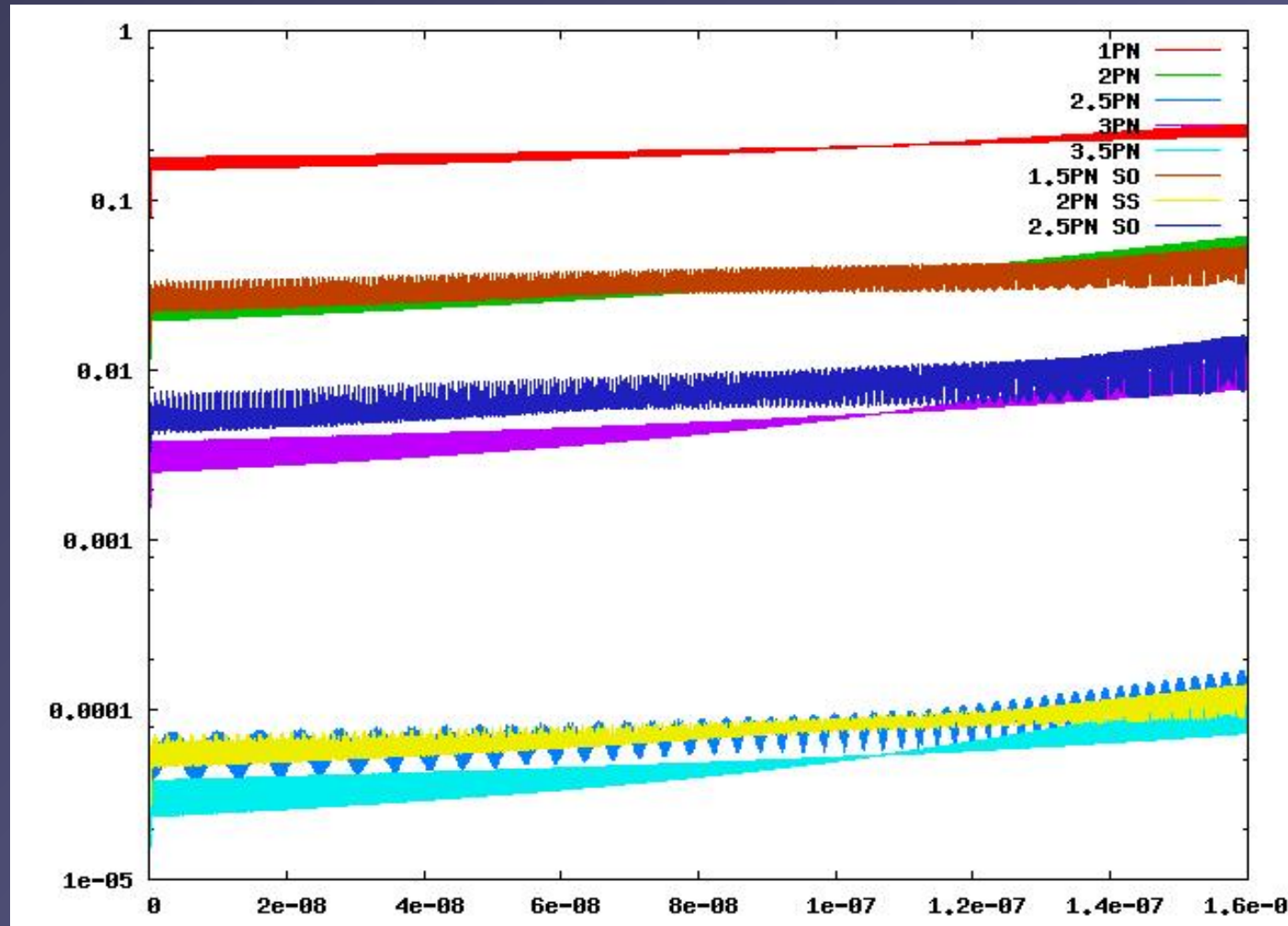
Post-Newtonian Dynamics

Brem, Amaro-Seoane,
Spurzem,
MNRAS 2013

Include
Spin-Orbit
Spin-Spin
PN3, PN3.5
Spin Dynamics

By Patrick Brem
(Diploma Thesis
Univ. Heidelberg)

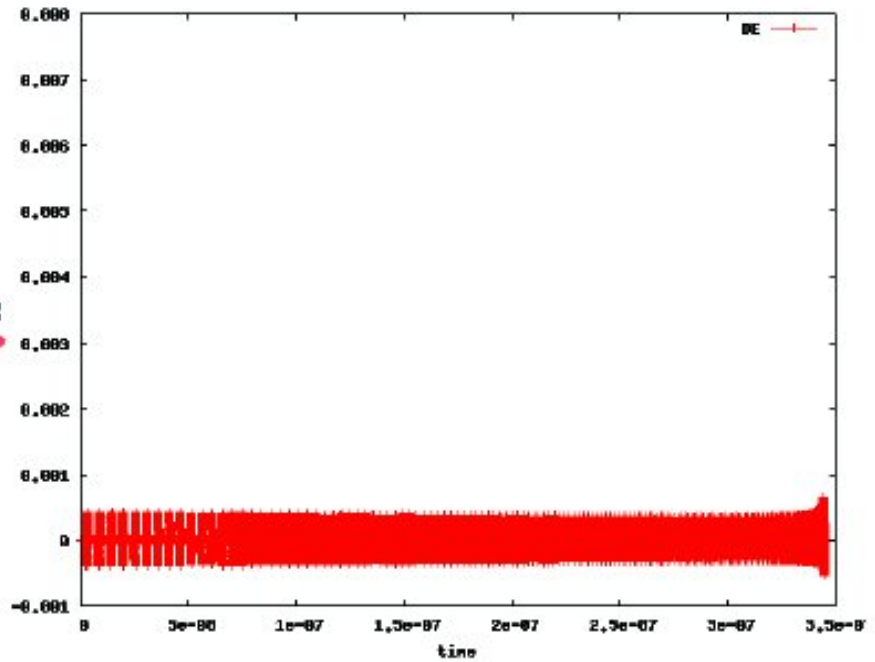
1PN
2PN + 1.5PN SO
3PN + 2.5PN SO
2.5PN + 2PN SS
3.5PN



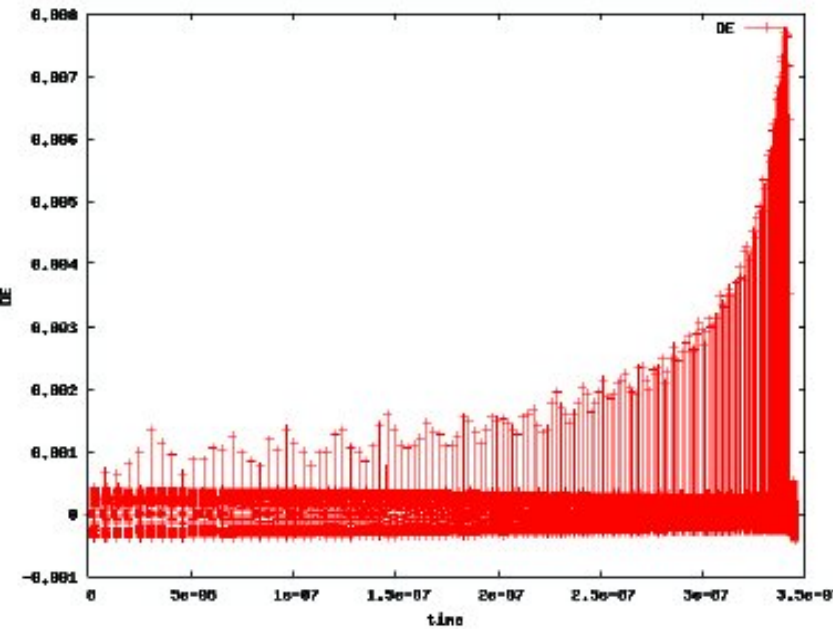
within ksint.f routine:

*Turning on PN routines

Einstein Shift $\Delta\omega = \frac{6\pi M}{c^2 a(1-e^2)}$



v/c

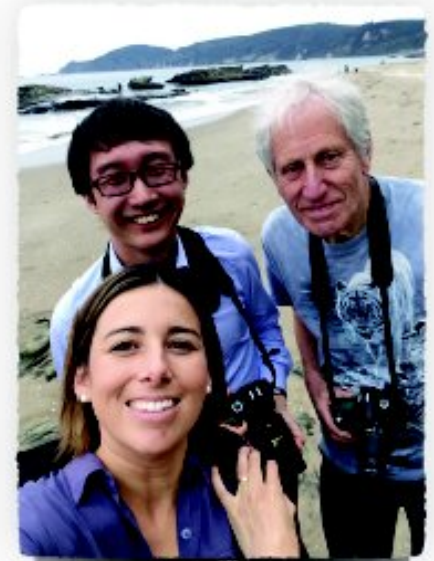


Slide by Paulina Assmann et al. subm. MNRAS 2018

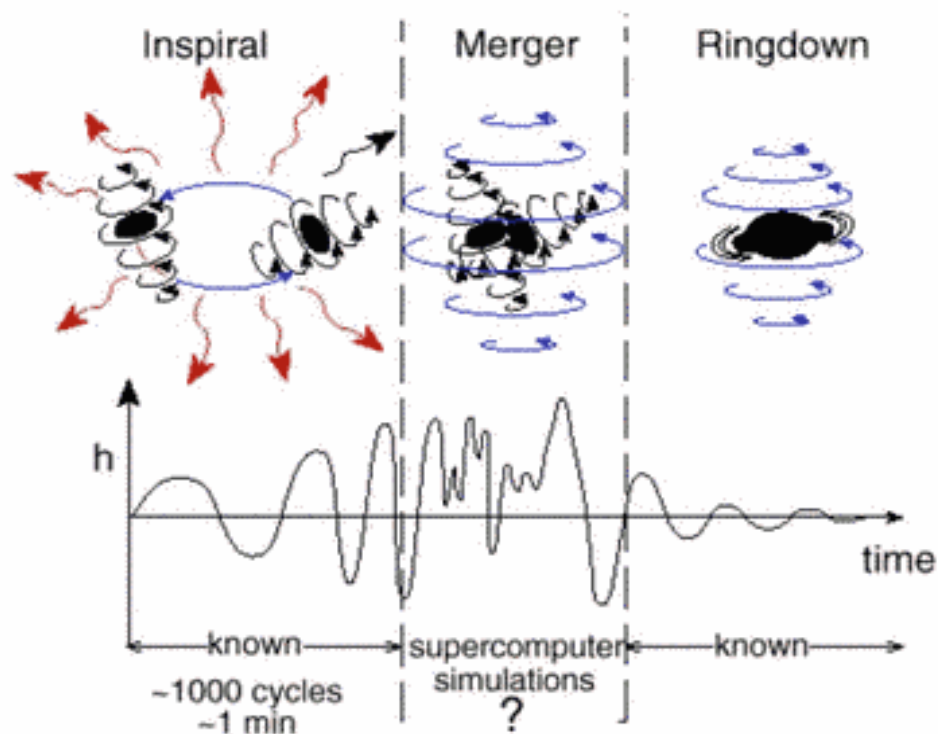
*Merger Criteria

7 * RSCH

~Weak Field



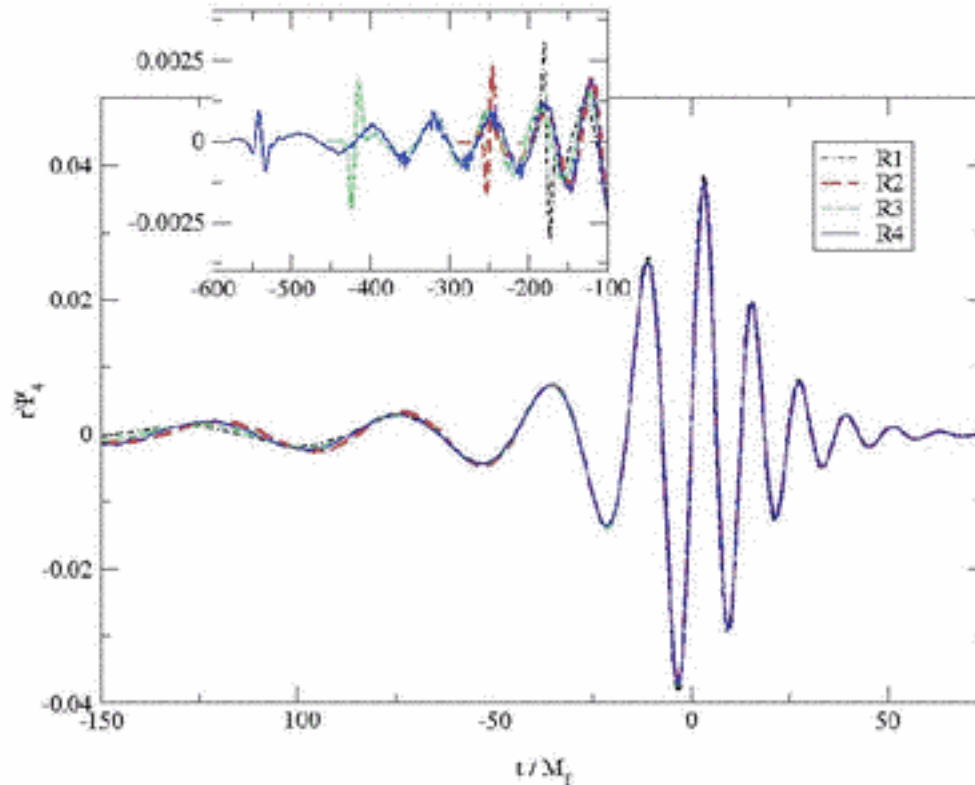
Gravitational Waves: Degree of Complexity



Slide by P. Laguna

Is this the right picture?

So far, it seems not!



Initial separations:

R1 = 6.5 M

R2 = 7.6 M

R3 = 8.5 M

R4 = 9.6 M

NASA-GSFC
Baker, Centrella, Choi, Koppitz, van Meter
Phys.Rev. D73 (2006) 104002

Slide by P. Laguna

Post-Newtonian Dynamics

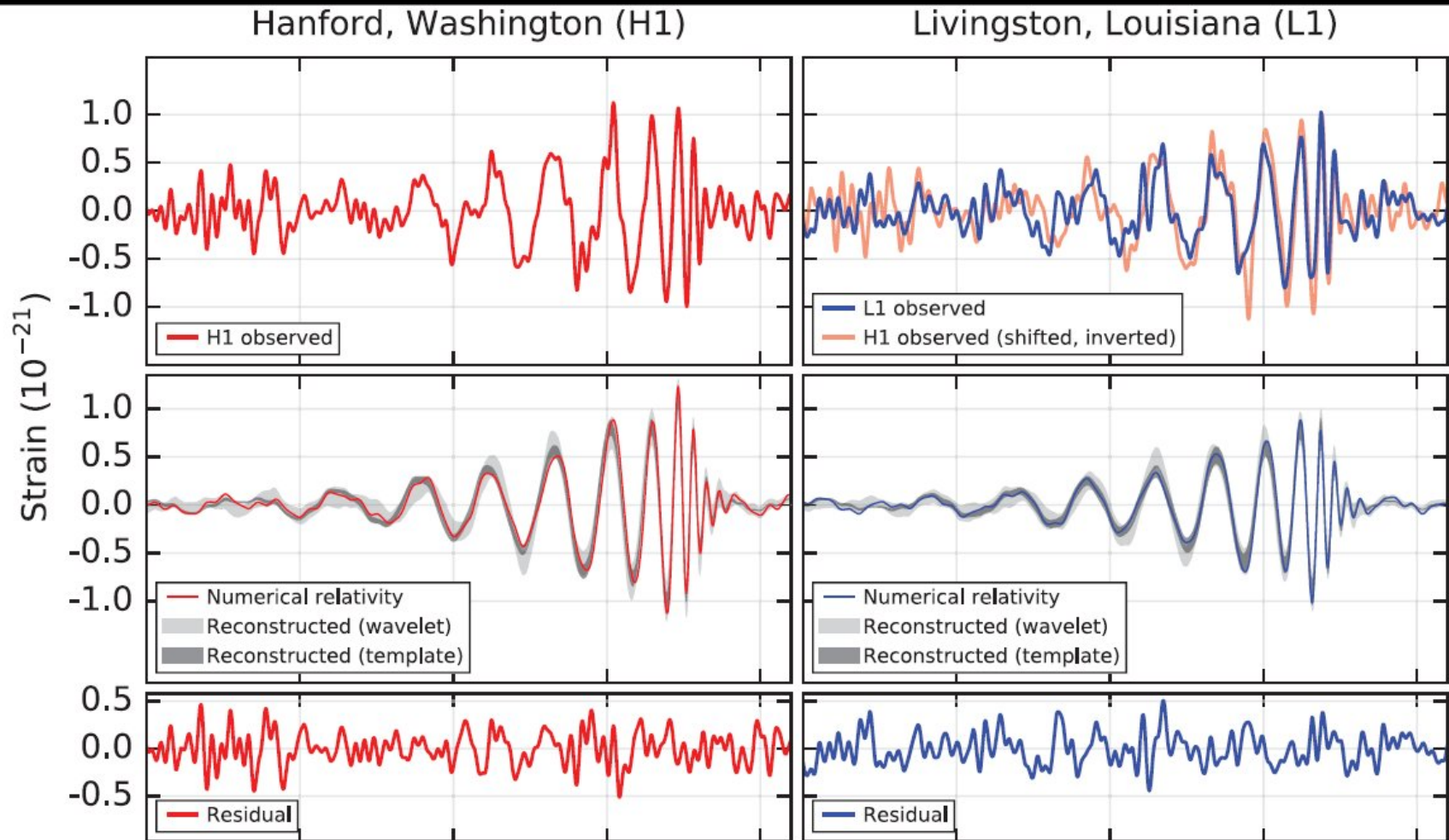
Spin-Orbit Interaction S / Spin-Spin SS

$$\begin{aligned} \frac{d\mathbf{v}_1}{dt} = & \mathbf{A}_N + \frac{1}{c^2} \mathbf{A}_{1\text{PN}} + \frac{1}{c^3} \mathbf{A}_S^{1.5\text{PN}} + \frac{1}{c^4} [\mathbf{A}_{2\text{PN}} + \mathbf{A}_{\text{SS}}^{2\text{PN}}] \\ & + \frac{1}{c^5} [\mathbf{A}_{2.5\text{PN}} + \mathbf{A}_S^{2.5\text{PN}}] + \mathcal{O}\left(\frac{1}{c^6}\right). \end{aligned} \quad (5.1)$$

Faye, Blanchet, Buonanno 2006

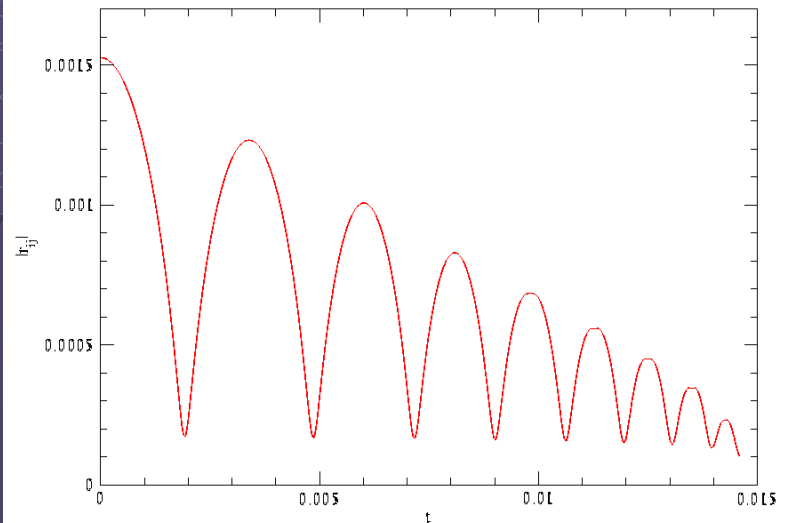
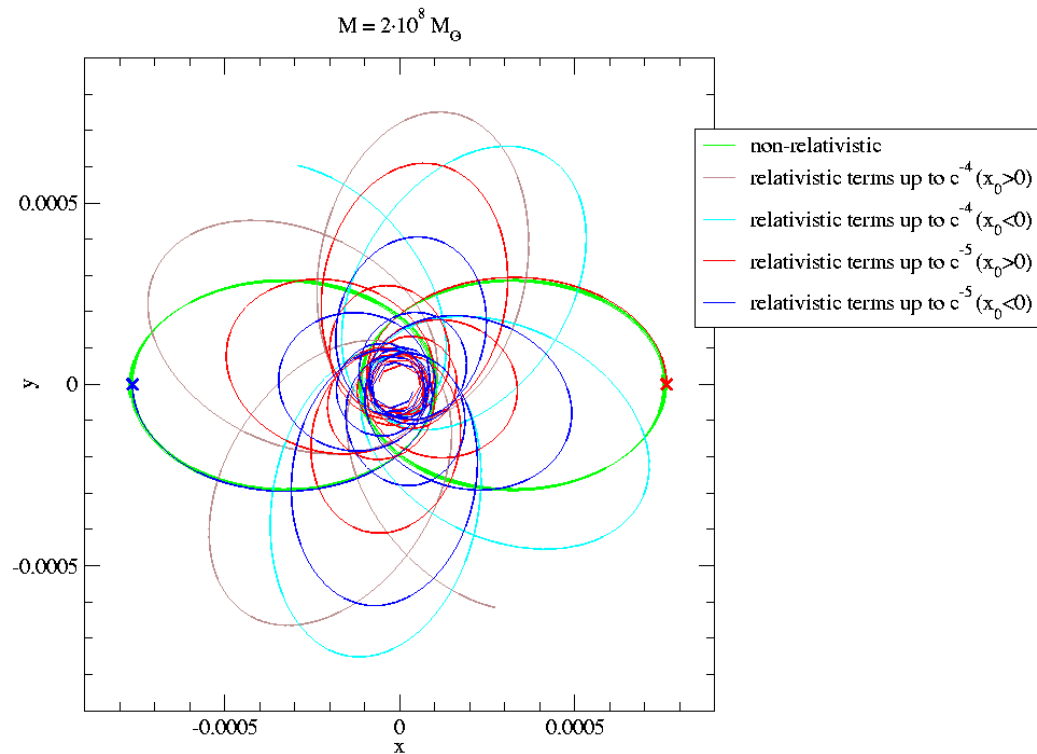
$$\begin{aligned} \mathbf{A}_S^{1.5\text{PN}} = & \frac{Gm_2}{r_{12}^3} \left\{ \left[6 \frac{(\mathbf{S}_1, \mathbf{n}_{12}, \mathbf{v}_{12})}{m_1} + 6 \frac{(\mathbf{S}_2, \mathbf{n}_{12}, \mathbf{v}_{12})}{m_2} \right] \mathbf{n}_{12} \right. \\ & + 3(n_{12} \mathbf{v}_{12}) \frac{\mathbf{n}_{12} \times \mathbf{S}_1}{m_1} + 6(n_{12} \mathbf{v}_{12}) \frac{\mathbf{n}_{12} \times \mathbf{S}_2}{m_2} \\ & \left. - 3 \frac{\mathbf{v}_{12} \times \mathbf{S}_1}{m_1} - 4 \frac{\mathbf{v}_{12} \times \mathbf{S}_2}{m_2} \right\}. \end{aligned} \quad (5.3a)$$

GW Detection Abbott et al. 2016



Gravitational Waves

What happens afterwards? Post-Newton Order „2.5“ ...



Kupi, Amaro-Seoane & Spurzem 2006

$$|\mathbf{a}_{\text{fin}}| = \frac{1}{(1+q)^2} \left[|\mathbf{a}_1|^2 + |\mathbf{a}_2|^2 q^4 + 2|\mathbf{a}_2||\mathbf{a}_1|q^2 \cos \alpha \right. \\ \left. + 2(|\mathbf{a}_1| \cos \beta + |\mathbf{a}_2| q^2 \cos \gamma) |\mathbf{l}| q + |\mathbf{l}|^2 q^2 \right]^{1/2},$$

where $q = M_2/M_1$ is the mass ratio and the angles are defined as

$$\cos \alpha = \hat{\mathbf{a}}_1 \cdot \hat{\mathbf{a}}_2, \quad \cos \beta = \hat{\mathbf{a}}_1 \cdot \hat{\mathbf{l}}, \quad \cos \gamma = \hat{\mathbf{a}}_2 \cdot \hat{\mathbf{l}}.$$

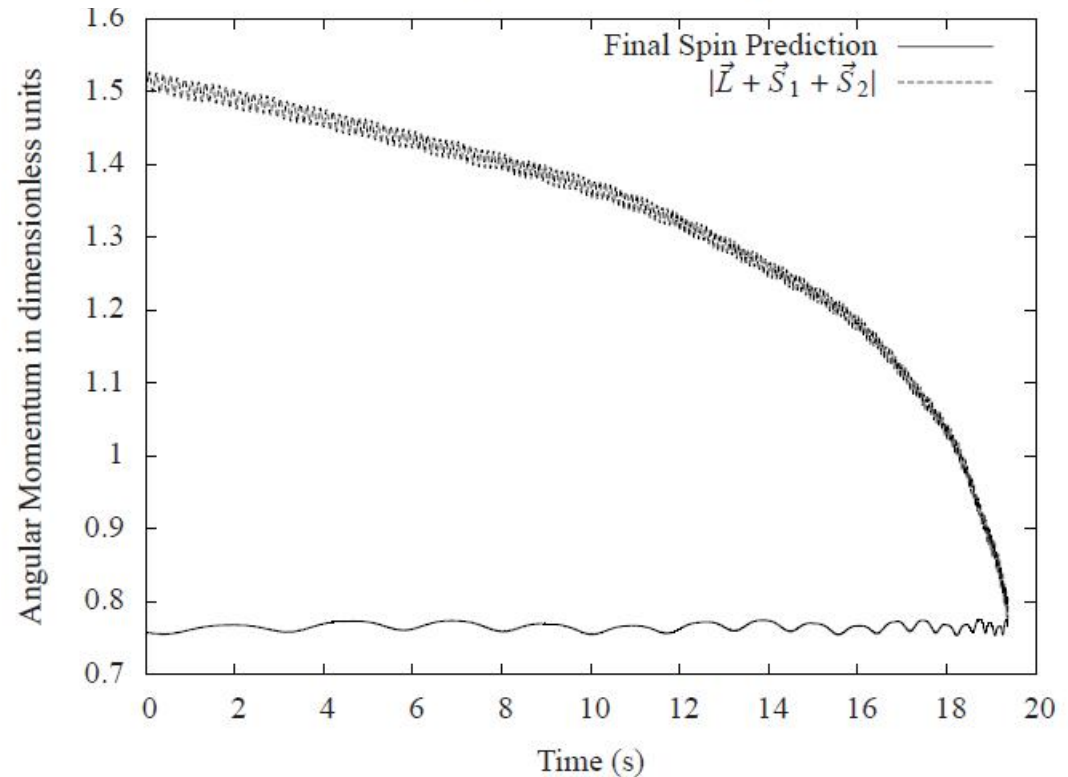
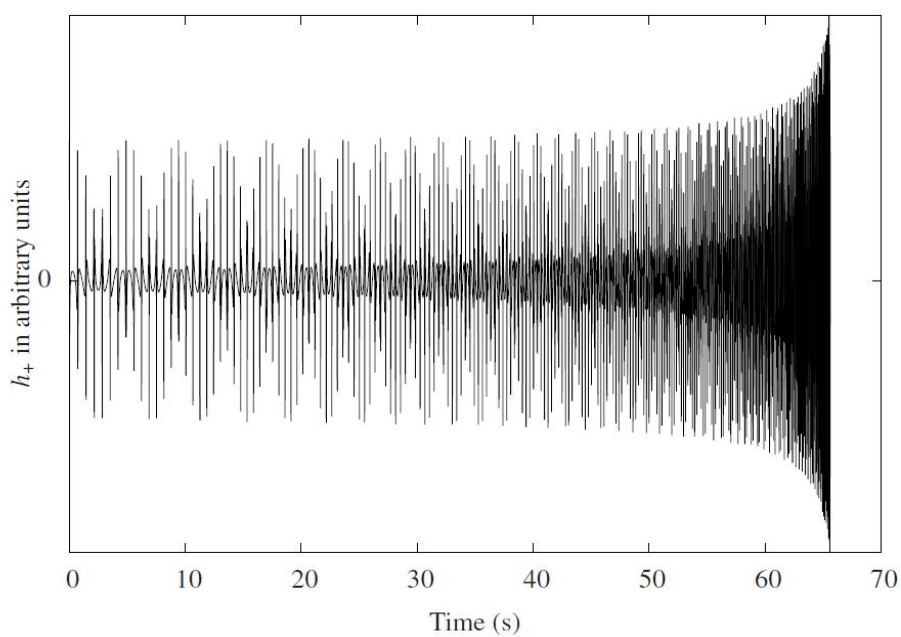


Figure 3.7: Comparison between the current final spin prediction and the actual total angular momentum of the binary system.



Post-Newtonian Dynamics Gravitational Wave Templates

Figure 3.11: Waveform for two equal mass objects on a an orbit with $e = 0.5$.

Handle spin-orbit and
spin-spin coupling
(P.Brem, R. Spurzem,
Univ. Heidelberg)

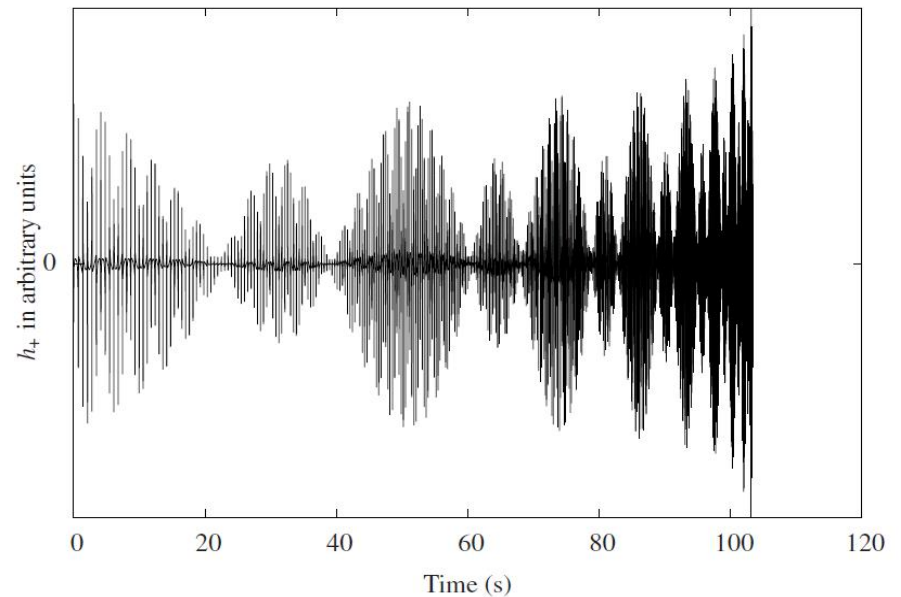


Figure 3.12: Waveform for two objects with a mass ratio of $q = 1/10$ on an orbit with $e = 0.5$ and spins $a_{1,x} = 1.0$, $a_{2,y} = 1.0$.

- 1) Star Cluster Dynamics
- 2) Post-Newtonian Theory
- 3) Black Hole Binaries – Grav. Waves**
- 4) Supermassive Black Hole Binaries
- 5) Computational Instruments

Kupi, G., Amaro-Seoane, P., Spurzem, R., Dynamics of compact object clusters: a post-Newtonian study, 2006, MNRAS 371, L45

Berentzen, I., Preto, M., Berczik, P., Merritt, D., Spurzem, R., Binary Black Hole Merger in Galactic Nuclei: Post-Newtonian Simulations, 2009, ApJ 695, 455



Super-Rechner spürt Schwarzen Löchern nach

Astronomisches Rechen-Institut stellte mit „Grace“ einen der schnellsten Rechnern der Welt vor – 3200 Milliarden Rechenoperationen pro Sekunde

Von Harald Berlinghof

Schon ein ganz durchschnittliches dieser gefräßigen, schwarzen Ungeheuer des Universums, die oft in den Zentren der Galaxien hausen, wäre ein furchteinflößendes Etwas, könnten wir ihm je begegnen. Sie sind zwar dunkle Mysterien des Kosmos, doch unnahbar sind sie nicht. Vielmehr zerren sie sogar gerne alles an sich, um es sich einzuverleiben. Schwarze Löcher sind ausgenutzte, kollabierte Sterne, deren Brennstoff nicht mehr ausreicht, um sie strahlen zu lassen. Unter ihrem eigenen Gewicht brechen sie in sich zusammen und bilden eine gewaltige Masse, die solche Gravitationskräfte ausübt, dass nichts, was einmal den sogenannten Ereignishorizont überschritten hat, je wieder zurück kehren kann – noch nicht einmal Licht.

Wie gesagt, dies gilt für ganz normale Schwarze Löcher. Im Astronomischen Rechen-Institut (ARI) der Universität Heidelberg wagt man sich aber inzwischen sogar an sogenannte „supermassive Schwarze Löcher“ heran – rein rechnerisch natürlich. „Das sind Schwarze Löcher mit einer Masse vom mindestens einer Million Sonnenmassen und der Größe unseres gesamten Sonnensystems“, erklärt Professor Rainer Spurzem vom ARI.

In Computersimulationen wird berechnet, was passiert, wenn zwei Galaxien, die solche supermassiven Schwarzen Löcher in sich tragen, miteinander kollidieren. Millionen von



Am Astronomischen Recheninstitut stellten Mitarbeiter ihren neuen schnellen Rechner vor, der auf der Suche nach den Gravitationswellen helfen soll. Von der Rechenkraft gehört er in die Top 50 der schnellsten Rechner auf der Welt, obwohl er nur aus einfachen PCs zusammengebaut ist.

Foto: Kresin

Sonnen und Planetensystemen kommen sich dann so nahe, dass die gegenseitigen Anziehungskräfte die jeweiligen Bahnen der Sonnen verändern und beide Galaxien in starke Drehbewegungen und rotierende Verwirbelungen versetzen. Aus den beiden kollidierenden Spiralgalaxien entstehen kurzzeitig – für wenige Millionen Jahre – sogenannte Antennengalaxien – so bezeichnet wegen ihrer Form.

Berechnen muss man solche hochkomplexen Ereignisse freilich mit einem Superrechner. Und im Astronomischen Rechen-Institut hat man mit der finanziellen Hilfe der Volkswagenstiftung, der Deutschen Forschungsgemeinschaft und dem Land Baden-Württemberg

berg sowie des Hardware-Know-Hows der Informatik der Mannheimer Universität am Lehrstuhl von Professor Reinhard Männer aus 32 Hochleistungs-PCs einen Top-50-Rechner namens „Grace“ konstruiert, der zu den schnellsten Rechnern der Welt zählt.

So richtig schnell machen ihn spezielle Grafikkarten namens „Grape“ aus Japan und solche aus Mannheim mit Namen „MPRace“. 3200 Milliarden Rechenoperationen in der Sekunde sind die Folge. „Ein Rechner für 20 Millionen Euro bringt auch nicht mehr“, so Spurzem. Allerdings schafft es Grace nicht in die Weltrangliste der schnellsten Rechner, weil er ein Spezialist ist, der nur auf dem Problem der Gravitationsberechnung funktioniert. In anderen Bereichen würde er kläglich versagen.

Im Jahr 1937, also bevor Computersimulationen möglich waren, weil Konrad Zuse den Computer erst später erdachte, hatte der Forscher Erk Holmberg die Entstehung der „Antennengalaxien“ beim Zusammenstoß zweier Spiralgalaxien bereits aufgezeigt. Seine mechanische Methode brachte ein ähnliches Ergebnis hervor wie der Rechner „Grace“. Doch „Grace“ hat noch etwas anderes berechnet.

Der Zusammenschluss zweier supermassiver Schwarzer Löcher erfolgt viel schneller als bisher vermutet – sie benötigen nur rund 100 Millionen Jahre, um zu verschmelzen und dabei starke Gravitationswellen auszusenden. Könnte man die Gravitationswellen nachweisen, wäre der letzte große Lückenschluss in Einsteins Relativitätstheorie gelungen.

Maybe he detects gravitational waves with this?

VolkswagenStiftung

Miro „schnappt“ zwei Einbrecher

Der Polizeihund erschnüffelte in Wieblingen die Männer, die sich im Keller versteckt hatten

POLIZEIBERICHT

Zwei verletzt

Black Holes were retained in globular clusters:

- Before Strader et al. detection
- Before Breen & Heggie
- Before LIGO detection

Downing 2012, Downing, Benacquista, Giersz & Spurzem, 2010, 2011:
(see also Banerjee, Baumgardt & Kroupa 2010 but ...)



Compact Binaries in Star Clusters I - Black Hole Binaries Inside Globular Clusters

J. M. B. Downing^{3*}, M. Benacquista⁴, R. Spurzem^{1,2,3}, and M. Giersz⁵

¹National Astronomical Observatories, Chinese Academy of Sciences, 20A Datun Ln, Chaoyang District, 100012, China

²Kavli Institute of Astronomy and Astrophysics, Peking University, Beijing, China

³Astronomisches Rechen-Institut, Zentrum für Astronomie der Universität Heidelberg, Mönchhofstraße 12-14, D-69120 Heidelberg, Germany

⁴Center for Gravitational Wave Astronomy, University of Texas at Brownsville, Brownsville, TX 78520, USA

⁵Nicolaus Copernicus Astronomical Center, Polish Academy of Sciences, ul. Bartycka 18, 00-716 Warsaw, Poland

Compact Binaries in Star Clusters II - Escapers and Detection Rates

J. M. B. Downing^{1,2*}, M. J. Benacquista³, M. Giersz⁴, and R. Spurzem^{5,6,1}

¹Astronomisches Rechen-Institut, Zentrum für Astronomie der Universität Heidelberg, Mönchhofstraße 12-14, D-69120 Heidelberg, Germany

²Fellow of the International Max-Planck Research School for Astronomy and Cosmic Physics at the University of Heidelberg, Heidelberg, Germany

³Center for Gravitational Wave Astronomy, University of Texas at Brownsville, Brownsville, TX 78520, USA

⁴Nicolaus Copernicus Astronomical Center, Polish Academy of Sciences, ul. Bartycka 18, 00-716 Warsaw, Poland

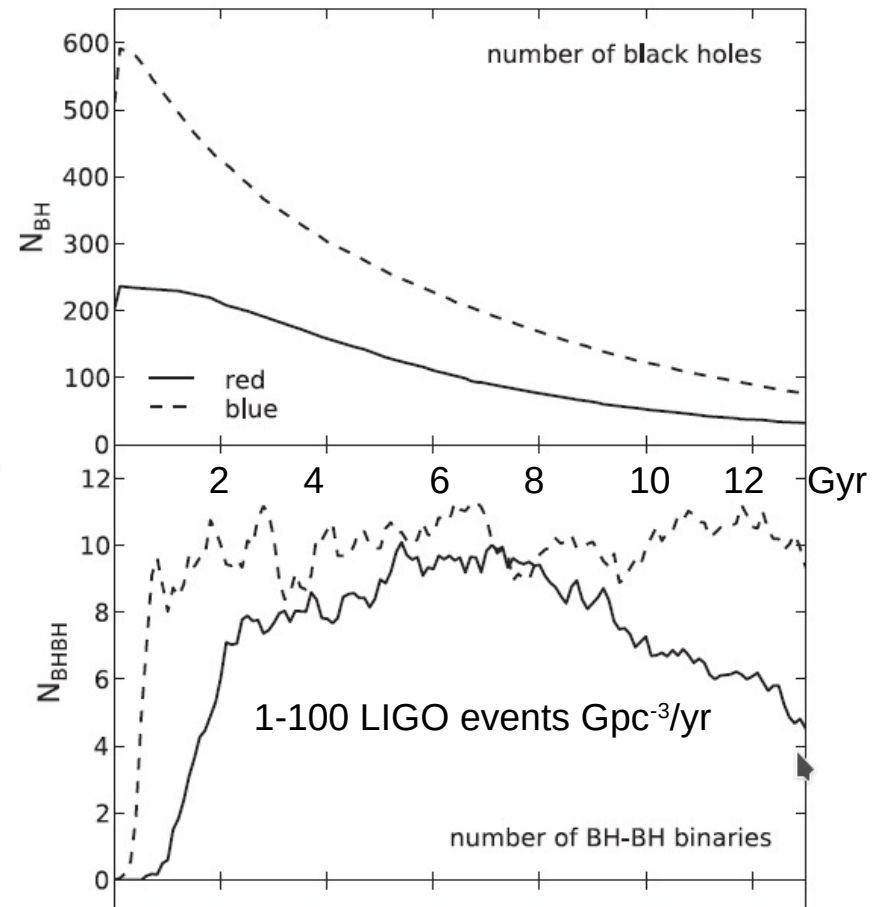
⁵National Astronomical Observatories, Chinese Academy of Sciences, 20A Datun Rd., Chaoyang District, 100012, China

⁶Kavli Institute of Astronomy and Astrophysics, Peking University, Beijing, China

Is there a size difference between red and blue globular clusters?

J. M. B. Downing^{*}

Astronomisches Rechen-Institut, Zentrum für Astronomie der Universität Heidelberg, Mönchhofstraße 12-14, D-69120 Heidelberg, Germany



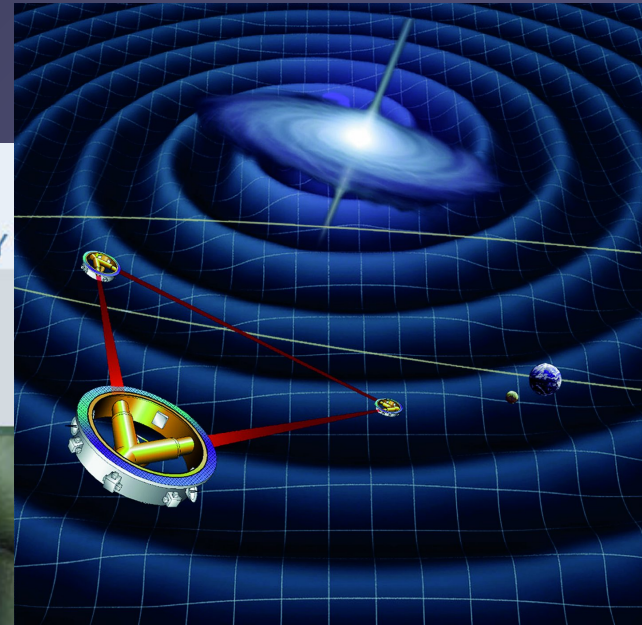
EUROPEAN GRAVITATIONAL OBSERVATORY

EGO



Consortium of

VIRGO Detector in Cascina near Pisa, Italy

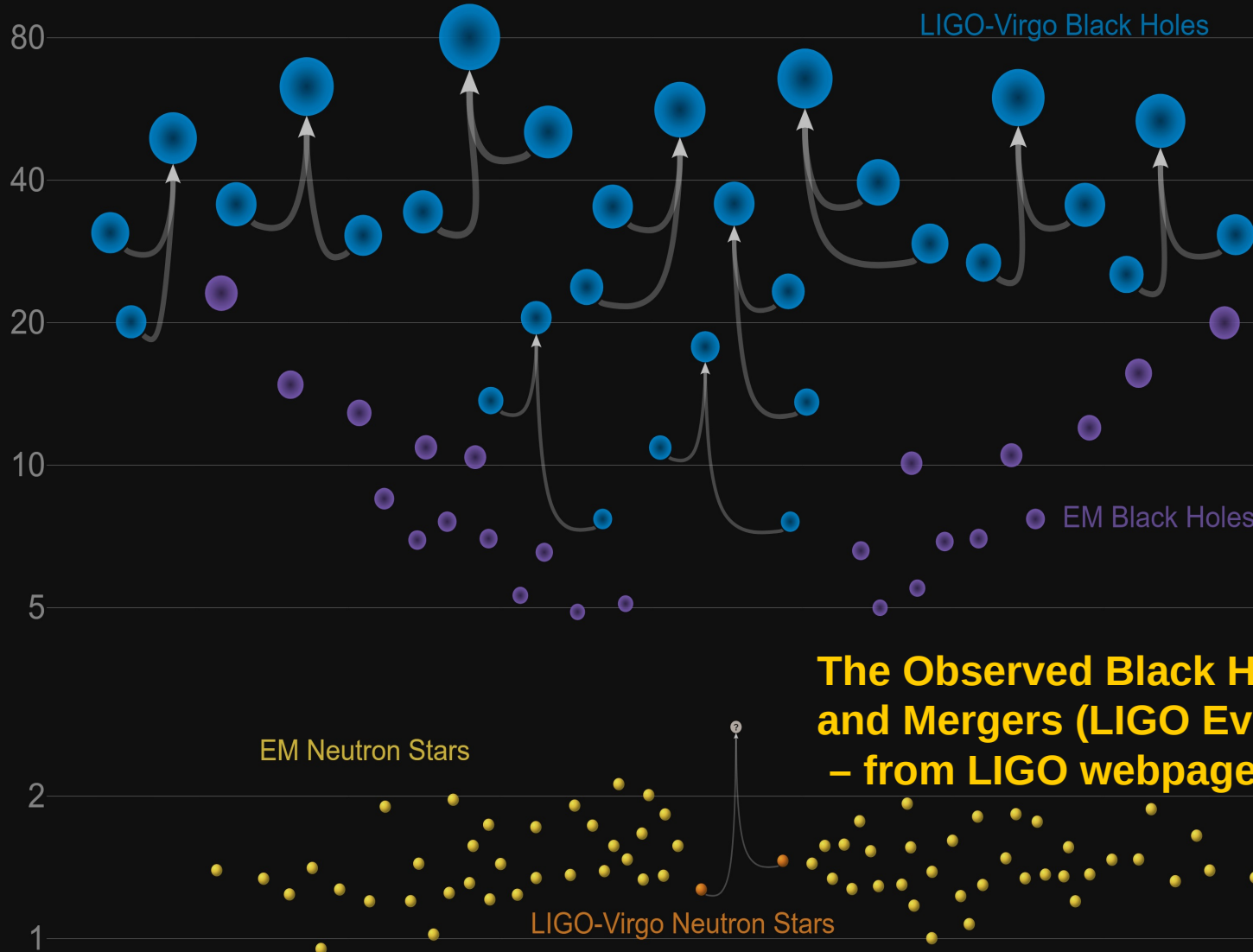


LISA =
Laser Space
Interferometer Antenna



Masses in the Stellar Graveyard

in Solar Masses



The Observed Black Holes and Mergers (LIGO Events) – from LIGO webpage...

Not so surprising in star Cluster dynamics...

Rodriguez et al. 2016, Monte Carlo Simulations Dynamical Formation of the GW150914 Binary Black Hole

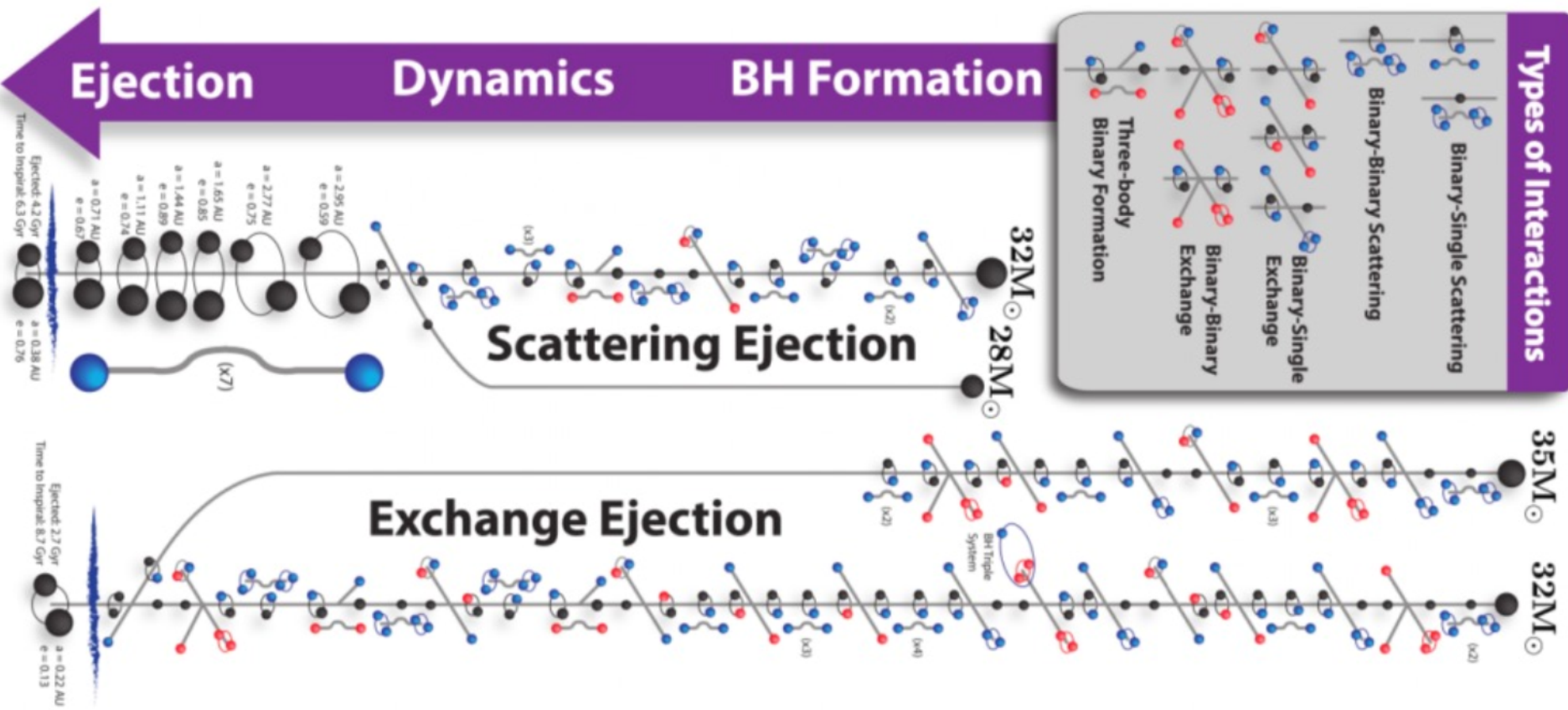


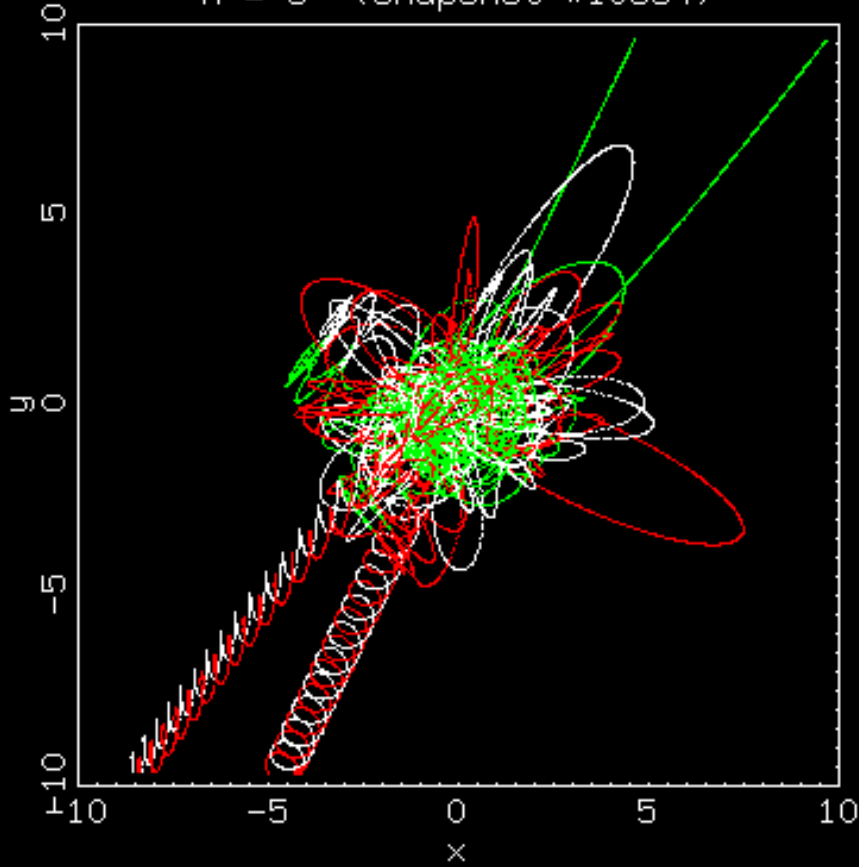
Figure 1. Interaction diagram showing the formation history for two GW150914 progenitors in a single GC model. From top to bottom, the history of each individual BH that will eventually comprise a GW150914-like binary is illustrated, including all binary interactions. The legend shows the various types of gravitational encounters included in our GC models (with the exception of two-body relaxation). In each interaction, the black sphere represents the GW150914 progenitor BH, while the blue and red spheres represent other BHs (and stars) in the cluster core. (from Rodriguez et al. 2016, Northwestern Group)

Dynamics of Binary Black Holes

StarLab



N = 3 (snapshot #10834)



Unstable 3-body

Encounters Starlab Simulation
(S.L.W. McMillan)

<http://www.physics.drexel.edu/~steve/>

-> Three-Body-Problem

GW Detection Frequency Time Diagram

Top: Our simulation (Wang et al. 2016, Sobolenko et al. In prep.)

Down: Abbott et al. 2016 LIGO measurement

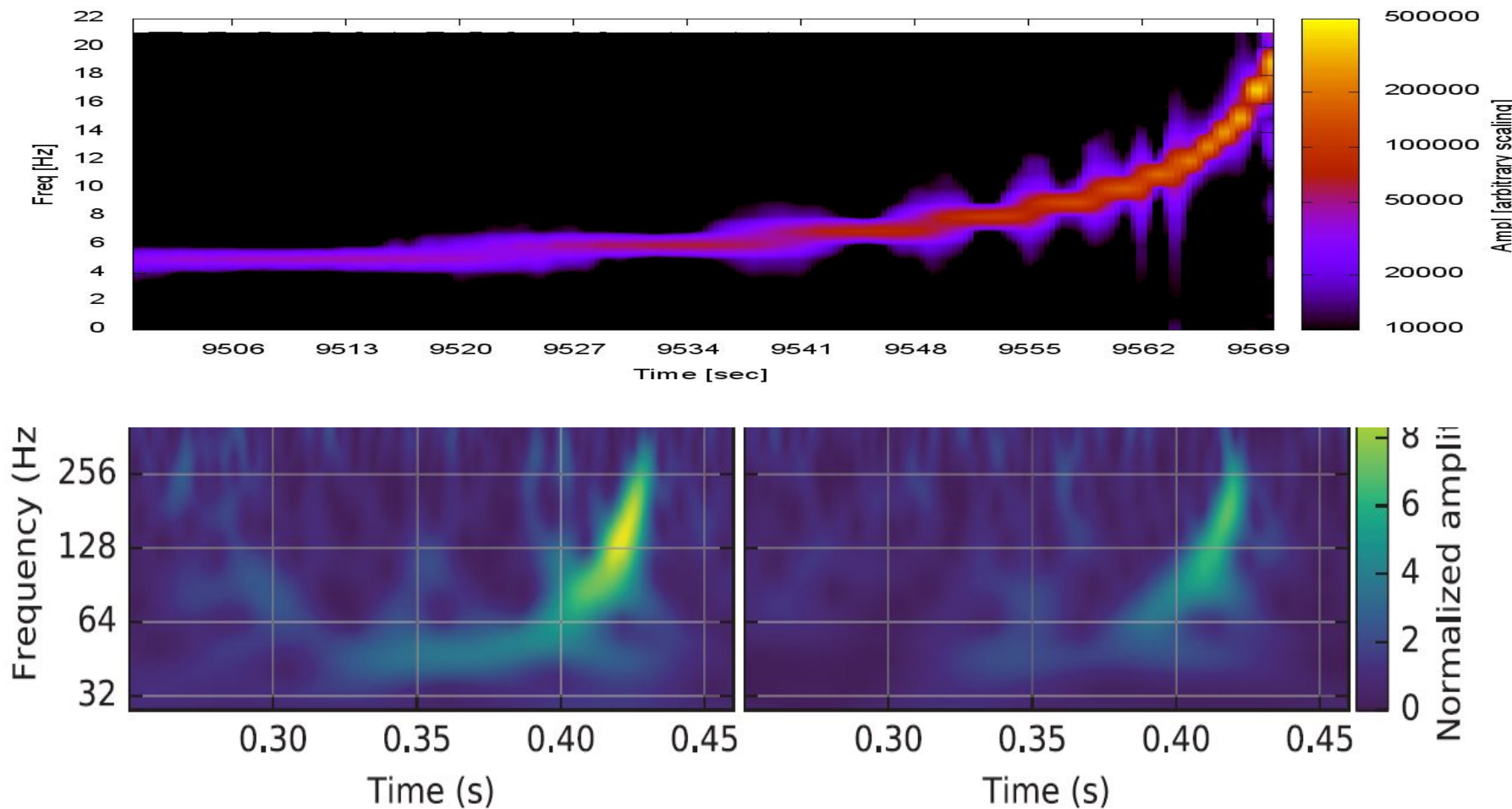
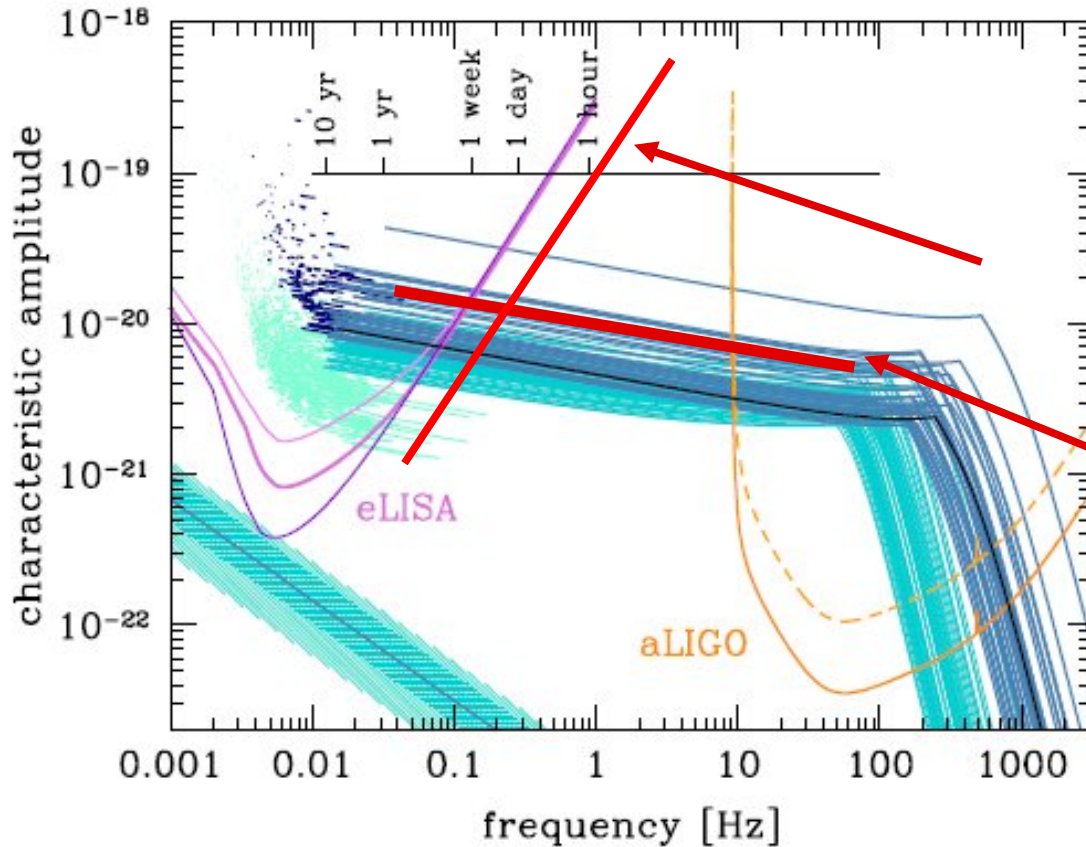


FIG. 1. The gravitational-wave event GW150914 observed by the LIGO Hanford (H1, left column panels) and Livingston (L1, right column panels) detectors. Times are shown relative to September 14, 2015 at 00:50:45 UTC. For visualization, all time series are filtered

Gong, Lau,
... Spurzem ...
2015, 2011
(JphCS, CQGra)



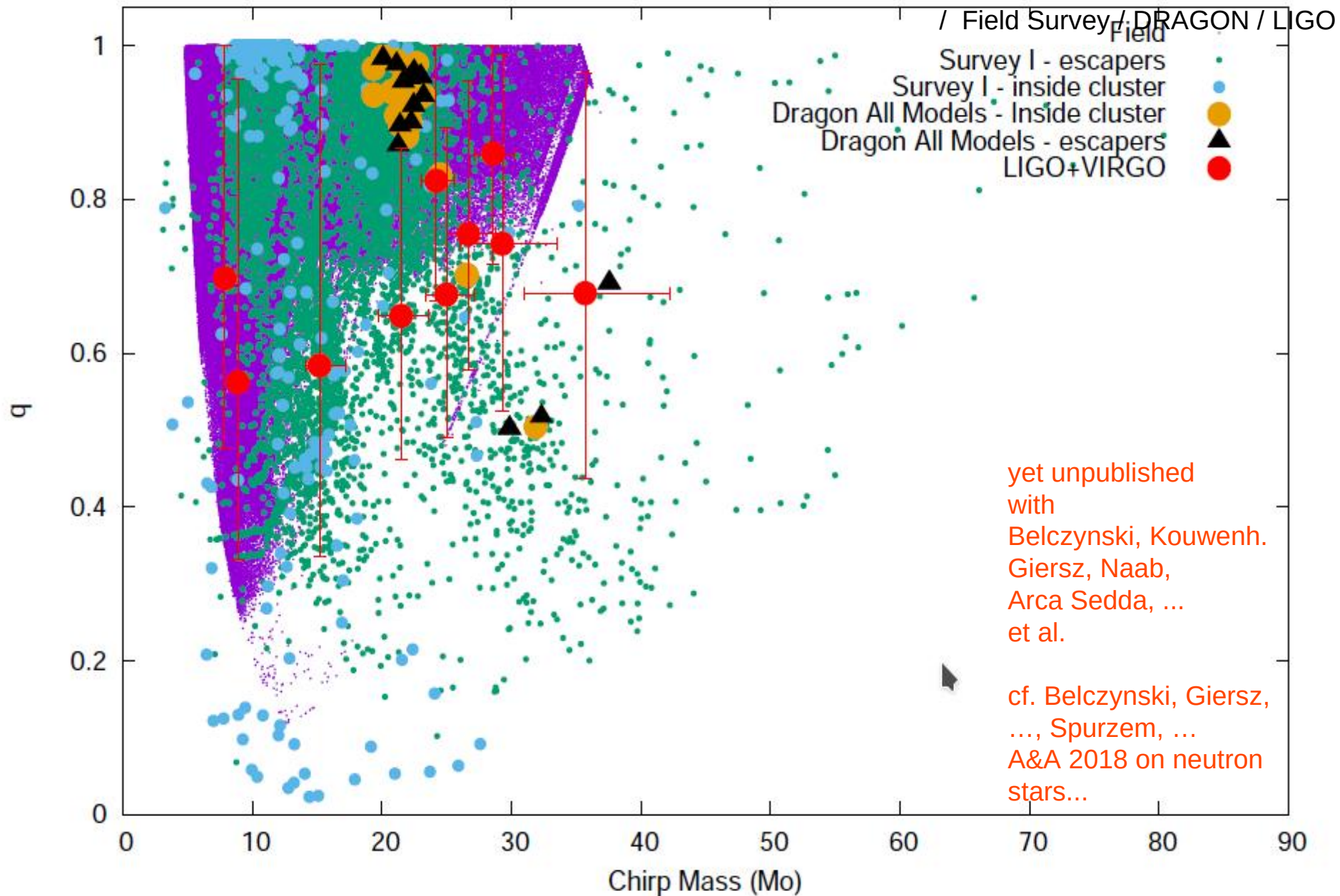
Taiji or
Tianqin
Hand
Drawn
Estimate

“Our”
DRAGON
Black Hole
Binary

Background Plot:
Sesana 2016

FIG. 1: The multi-band GW astronomy concept. The violet lines are the total sensitivity curves (assuming two Michelson) of three eLISA configurations; from top to bottom N2A1, N2A2, N2A5 (from [11]). The orange lines are the current (dashed) and design (solid) aLIGO sensitivity curves. The lines in different blue flavours represent characteristic amplitude tracks of BHB sources for a realization of the *flat* population model (see main text) seen with $S/N > 1$ in the N2A2 configuration (highlighted as the thick eLISA middle curve), integrated assuming a five year mission lifetime. The light turquoise lines clustering around 0.01 Hz are sources seen in eLISA with $S/N < 5$ (for clarity, we down-sampled them by a factor of 20 and we removed sources extending to the aLIGO band); the light and dark blue curves crossing to the aLIGO band are sources with $S/N > 5$ and $S/N > 8$ respectively in eLISA; the dark blue marks in the upper left corner are other sources with $S/N > 8$ in eLISA but not crossing to the aLIGO band within the mission lifetime. For comparison, the characteristic amplitude track completed by GW150914 is shown as a black solid line, and the chart at the top of the figure indicates the frequency progression of this particular source in the last 10 years before coalescence. The shaded area at the bottom left marks the expected confusion noise level produced by the same population model (median, 68% and 95% intervals are shown). The waveforms shown are second order post-Newtonian inspirals phenomenologically adjusted with a Lorentzian function to describe the ringdown.

All BH-BH mergers in the Hubble time



IMBH Formation In Star Cluster

Rizzuto, Spurzem, Naab, Rampp, Wang, Berczik, Kouwenhoven Poster ISC19
... to be published with MOCCA people Giersz, Askar, ...

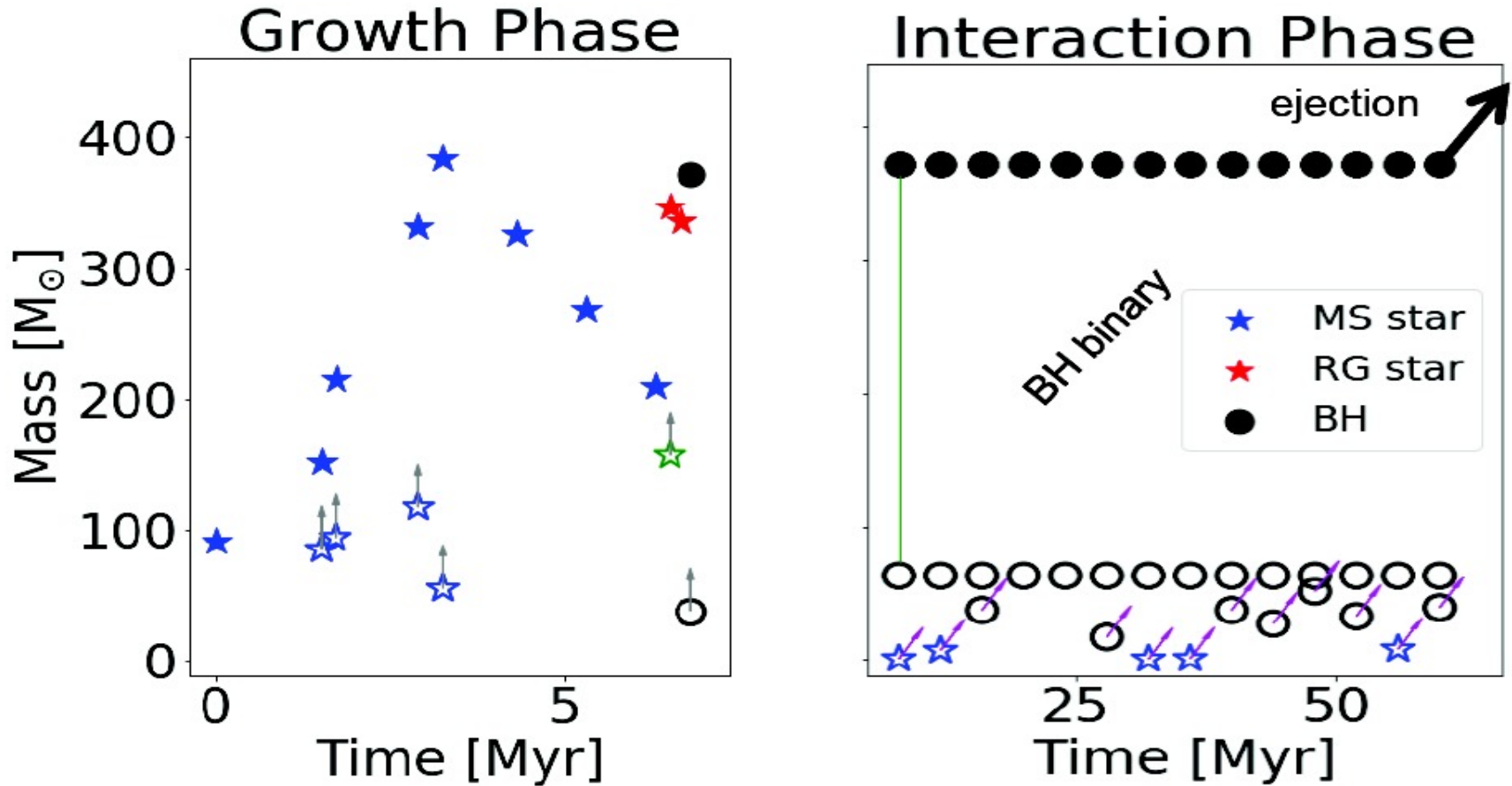


Fig. 3: Evolution of the most massive object (filled symbols) in a GC simulation with 10^5 stars. A massive main sequence star (MS, blue) grows by mergers (upward arrows) with other MS stars and evolves into a red giant (RG, red) and a $\sim 380 M_{\odot}$ IMBH after merging with a $50 M_{\odot}$ BH (left panel). Then the IMBH forms a BH binary (green line) and interacts (diagonal arrows) with other BHs and MS stars. At the end of the interaction phase the BH is kicked out (right panel).

Rodriguez, Chatterjee, Rasio 2016: CMC (Monte Carlo Models) – approximate...
 (compare also work of Giersz, Arca Sedda, Askar ... MOCCA models)
 (Many simulation models, but highly approximate...)

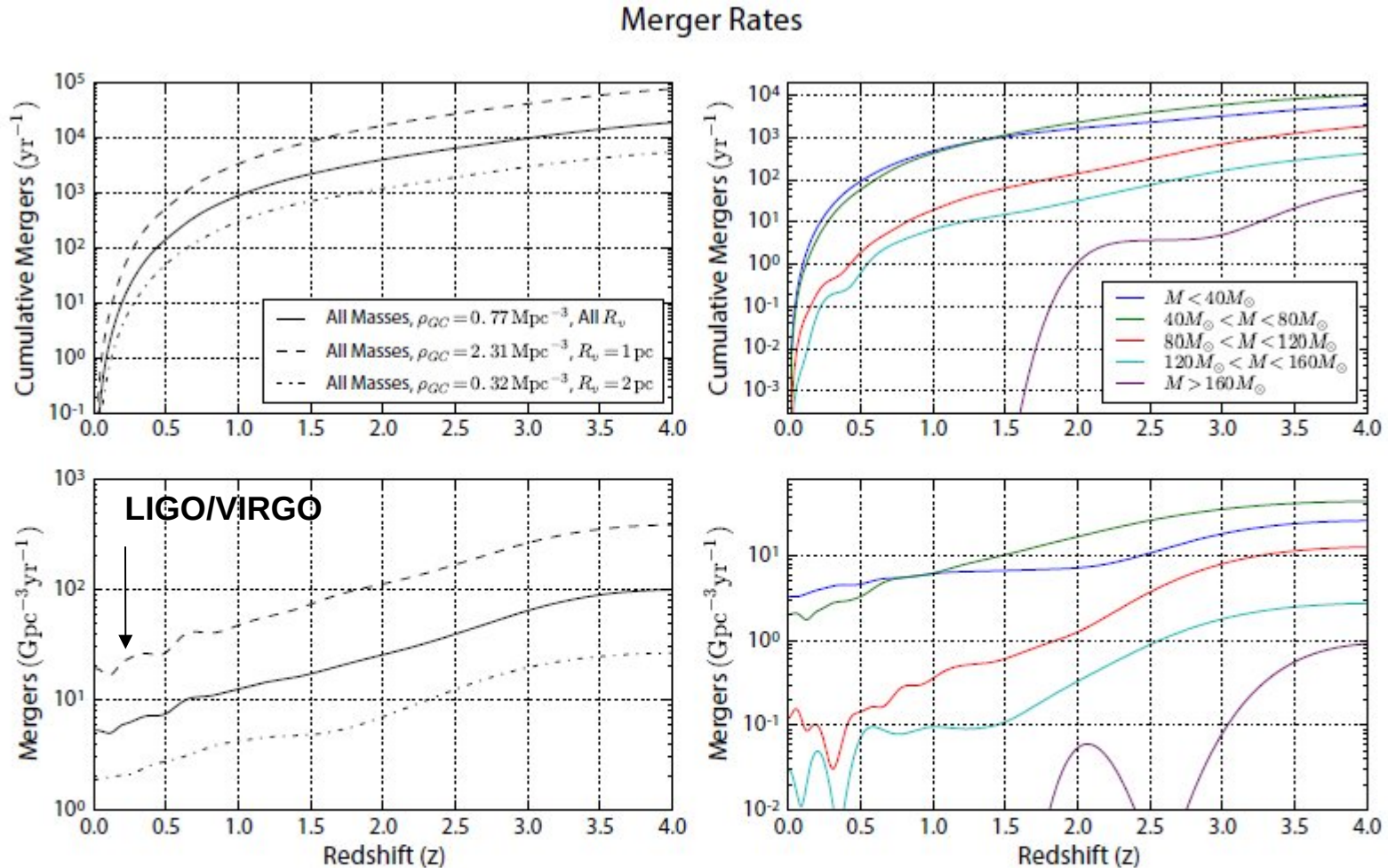


FIG. 12. The BBH merger rates from our models as a function of redshift. The upper panels show the cumulative rate of mergers per year in a volume out to redshift z , with the left panel showing the cumulative merger rate for all binaries, and the right panel showing the cumulative merger rate for binaries with specific total masses. The lower panels show the source merger rate in $\text{Gpc}^{-3} \text{ yr}^{-1}$ at a given redshift for all BBHs (left) and for specific BBH total masses (right). For the total merger rates (the leftmost panels) we illustrate the uncertainties in our models to specific assumptions, showing how the rate varies with the spatial density of GCs and our choice of initial virial radius.

Giacobbo, Mapelli, MNRAS 2018
(classical binaries / gal. field)

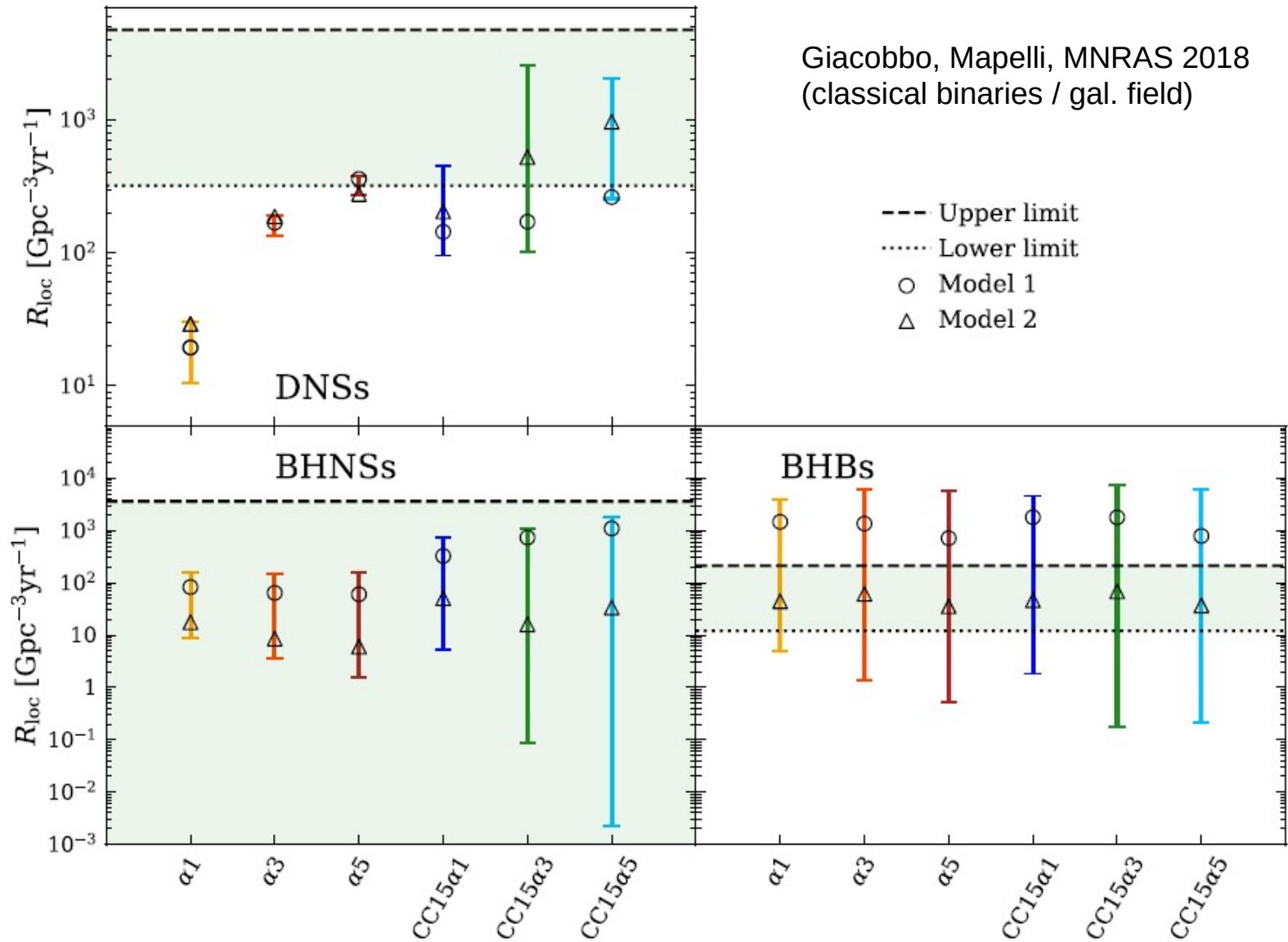


Figure 15. Local merger rate density R_{loc} calculated from equation (10) for each simulation. Top-left: local merger rate density for DNSs. Bottom-left: local merger rate density for BHNSs. Bottom-right: local merger rate density for BHBs. The error bars show the maximum difference between estimates of R_{loc} for different metallicities. Open circles (open triangles) are R_{loc} obtained assuming *model1* (*model2*) for the cosmic evolution of metallicity. Green shaded areas: local merger rate density inferred from LIGO-Virgo observations (from Abbott et al. 2017c, Abbott et al. 2016e and Abbott et al. 2017a for DNSs, BHNSs and BHBs, respectively).

Table 1. Local NS-NS merger rates [yr^{-1}] (< 100 Mpc).

Model	pessimistic	realistic	optimistic
LIGO/Virgo ^a	0.3	1.5	4.7
classical binaries	3×10^{-2}	6×10^{-2}	2×10^{-1}
globular clusters	1×10^{-4}	2×10^{-4}	2×10^{-3}
nuclear clusters	3×10^{-5}	6×10^{-5}	6×10^{-4}
homogeneous evol.	0	unknown	$< 3.8^b$

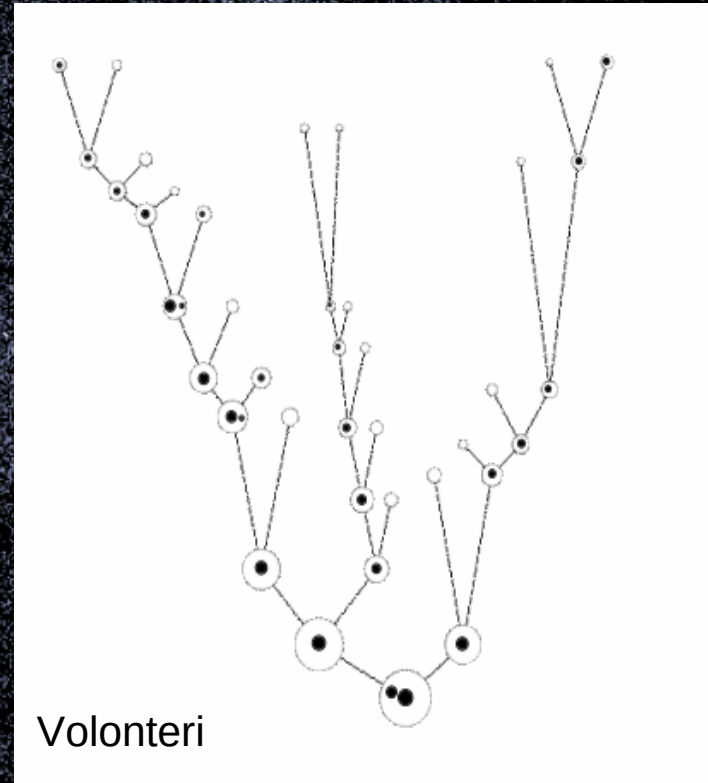
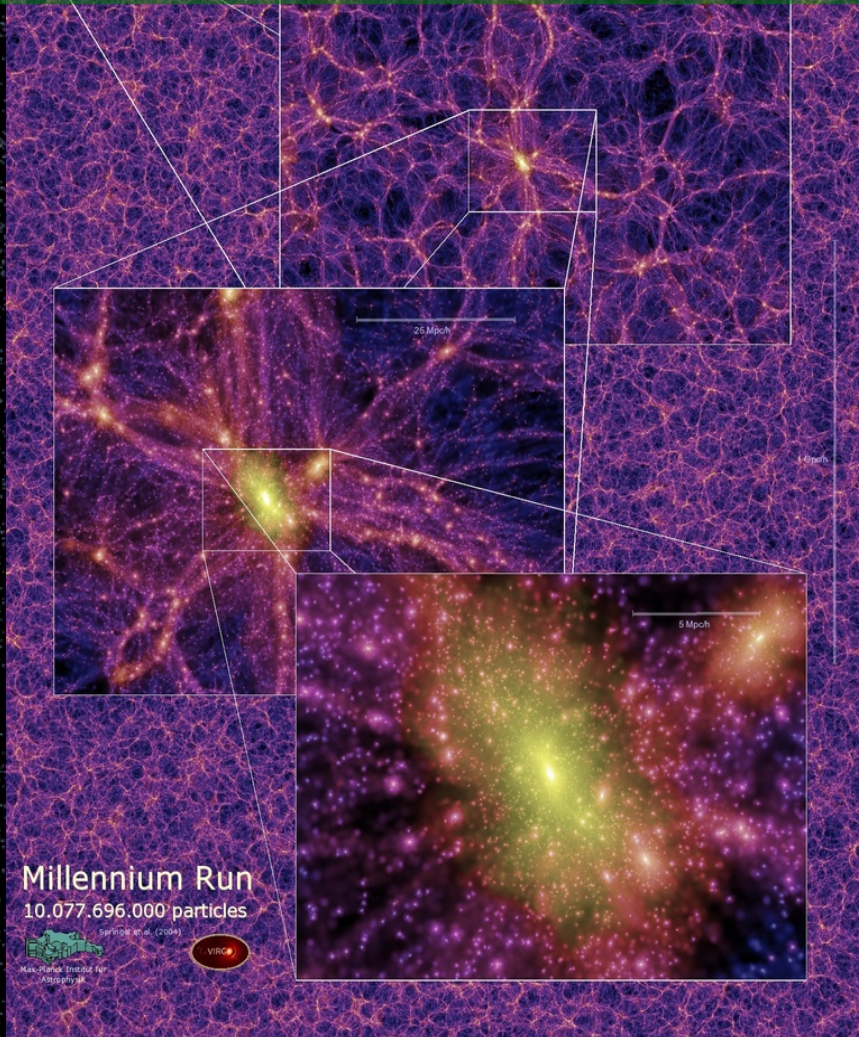
Notes.

^a The LIGO/Virgo estimate of $1540_{-1220}^{+3200} \text{Gpc}^{-3} \text{yr}^{-1}$ is rescaled by factor of 0.001 to change to a merger rate [yr^{-1}] within 100 Mpc.

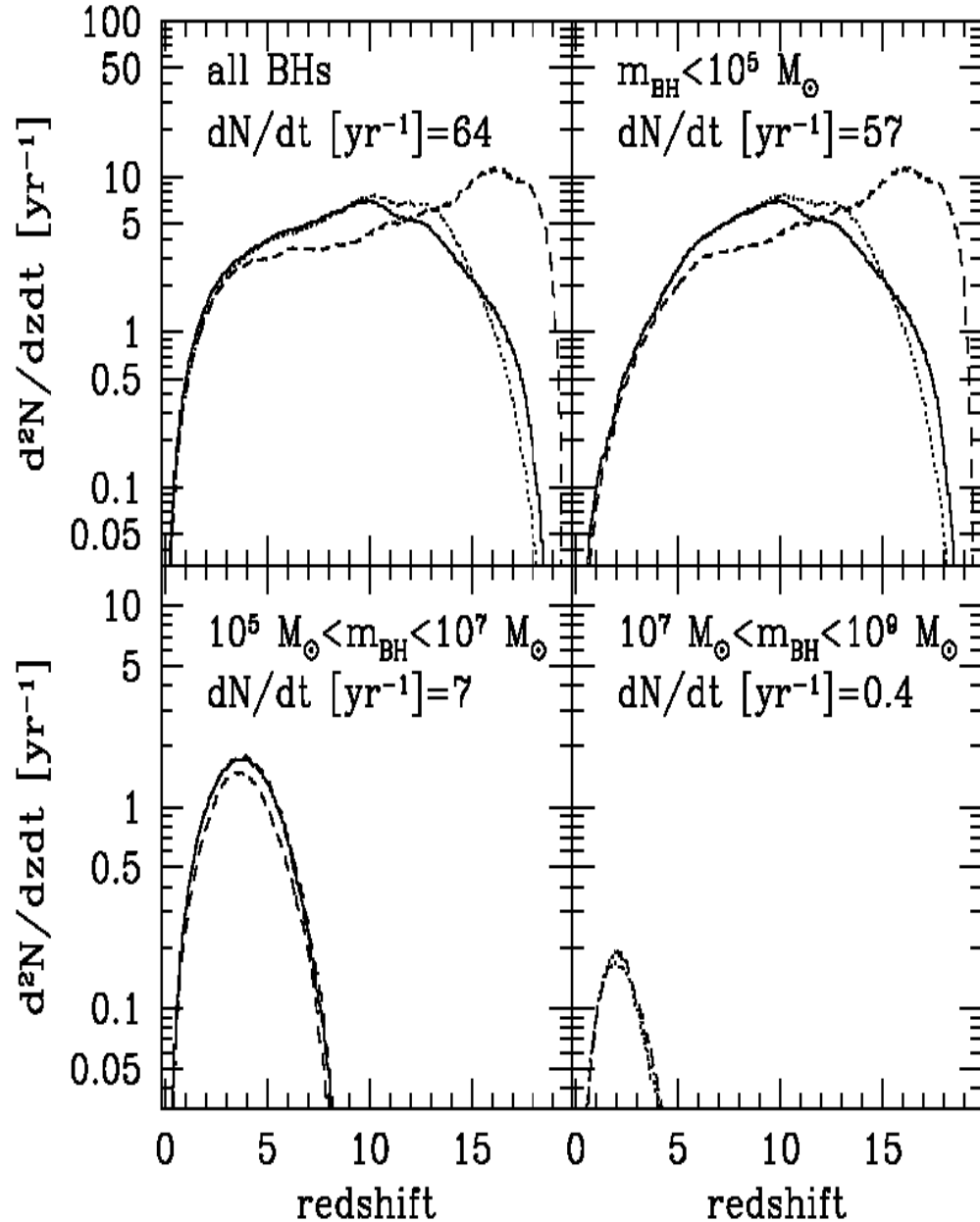
^b This is an upper limit and not actual rate as given for other models.

- 1) Star Cluster Dynamics
- 2) Post-Newtonian Theory
- 3) Black Hole Binaries – Grav. Waves
- 4) Supermassive Black Hole Binaries**
- 5) Computational Instruments

Galaxies merge, hierarchical Structure formation, their centres? Black Holes?



Galactic Nuclei, Black Holes

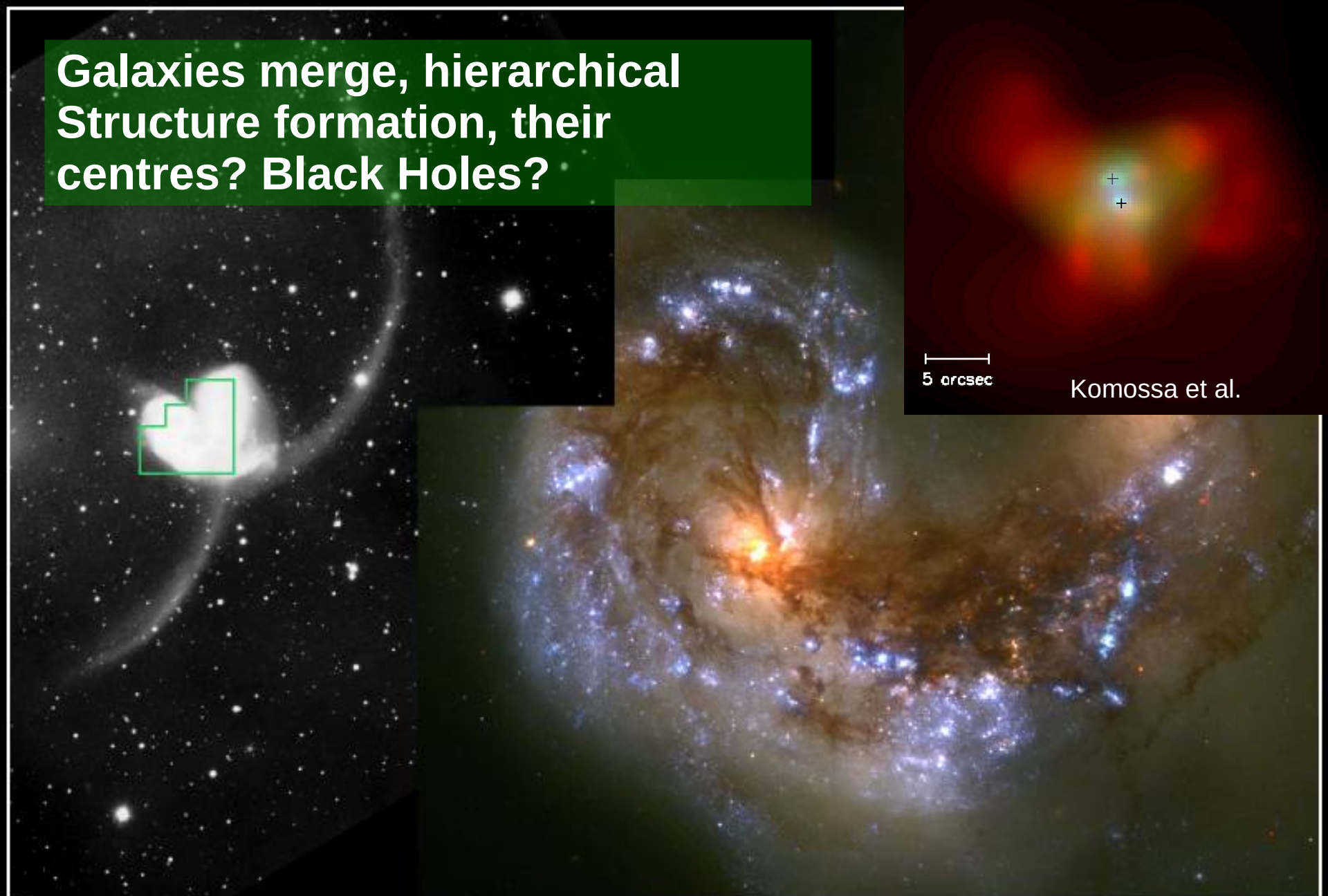


Sesana et al. 2004

Extending study of Volonteri et al. 03: Rate of expected Black Hole Mergers in Galaxies

Number of MBH binary coalescences observed per year at $z=0$, per unit redshift, in different $m_{\text{BH}} = m_1 + m_2$ mass intervals. Each panel also lists the integrated event rate, dN/dt , predicted by our model. The rates (*solid lines*) are compared to a case in which triple black hole interactions are switched off (*dotted lines*). Triple black hole interactions increase the coalescence rate at very high redshifts, while for $10 < z < 15$, the rate is decreased because of the reduced number of surviving binaries. *Dashed lines*: Rates computed assuming binary hardening is instantaneous, i.e., MBHs coalesce after a dynamical friction timescale.

**Galaxies merge, hierarchical
Structure formation, their
centres? Black Holes?**



5 arcsec

Komossa et al.

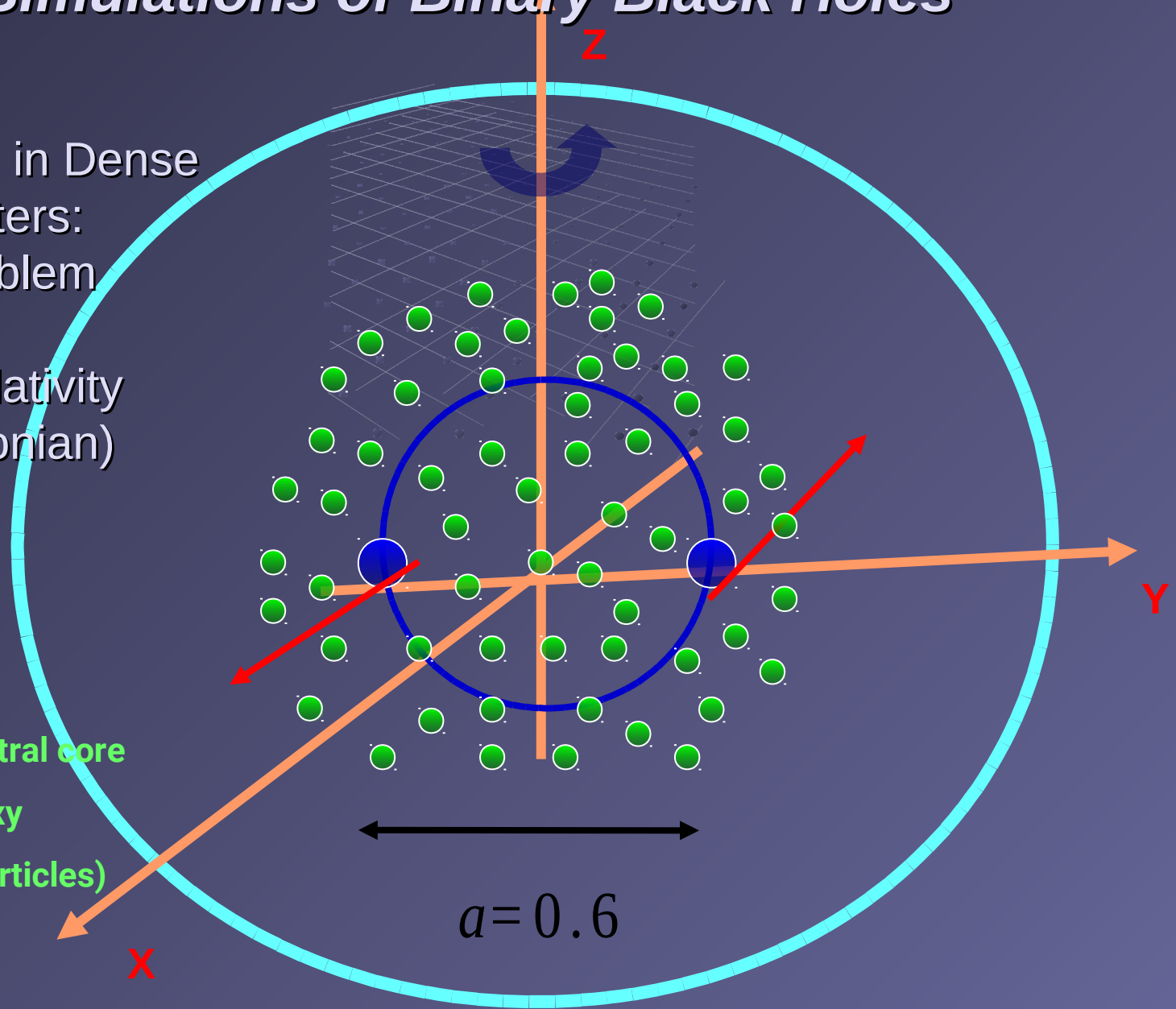
Colliding Galaxies NGC 4038 and NGC 4039

HST • WFPC2

PRC97-34a • ST ScI OPO • October 21, 1997 • B, Whitmore (ST ScI) and NASA

Simulations of Binary Black Holes

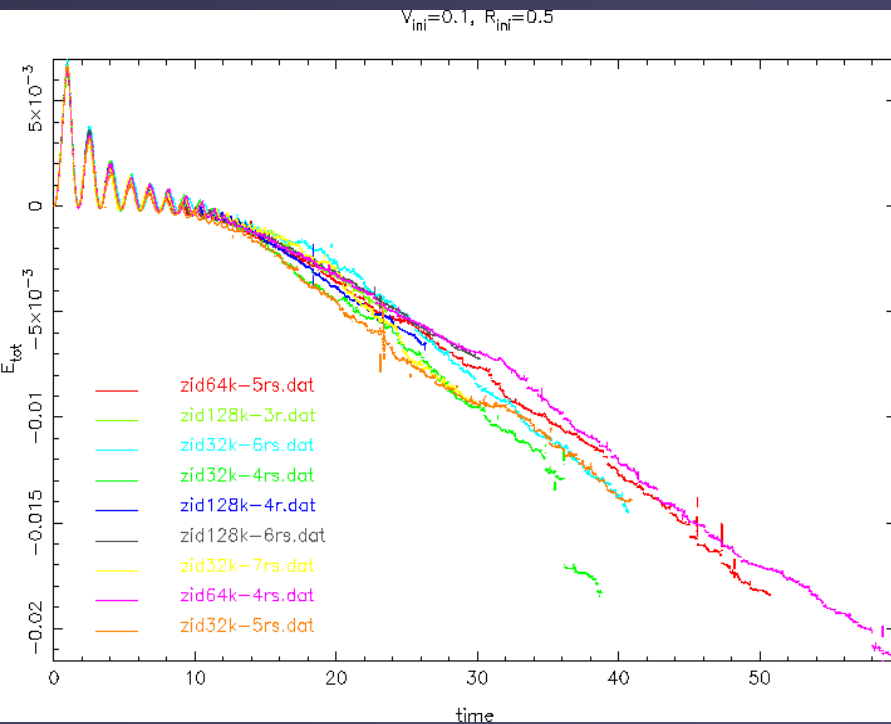
Black Holes in Dense
Stellar Clusters:
N-Body Problem
with
General Relativity
(Post-Newtonian)



Two equal-mass
black holes in central core
of simplified galaxy
(up to 4 million particles)

$$a = 0.6$$

Dynamics of Binary Black Holes in Galactic Nuclei



Stochastic Orbit variations of binary black holes due to superelastic scatterings with stars

Hemsendorf, Sigurdsson, Spurzem,
2002, *Astroph. JI.*

See also:

Ebisuzaki, Makino, (90's)

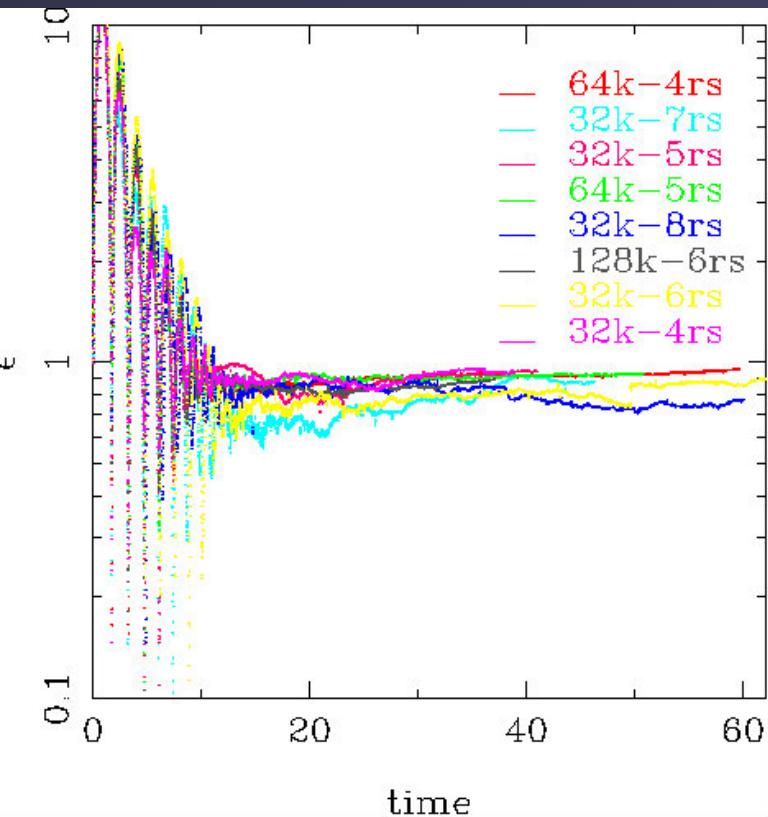
Milos. & Merritt (2001)

Cf. also Aarseth & Mikkola (2003),

Funato & Makino (2005), ...

• Berczik et al. 2005, 2006, ...

Dynamics of Binary Black Holes in Galactic Nuclei



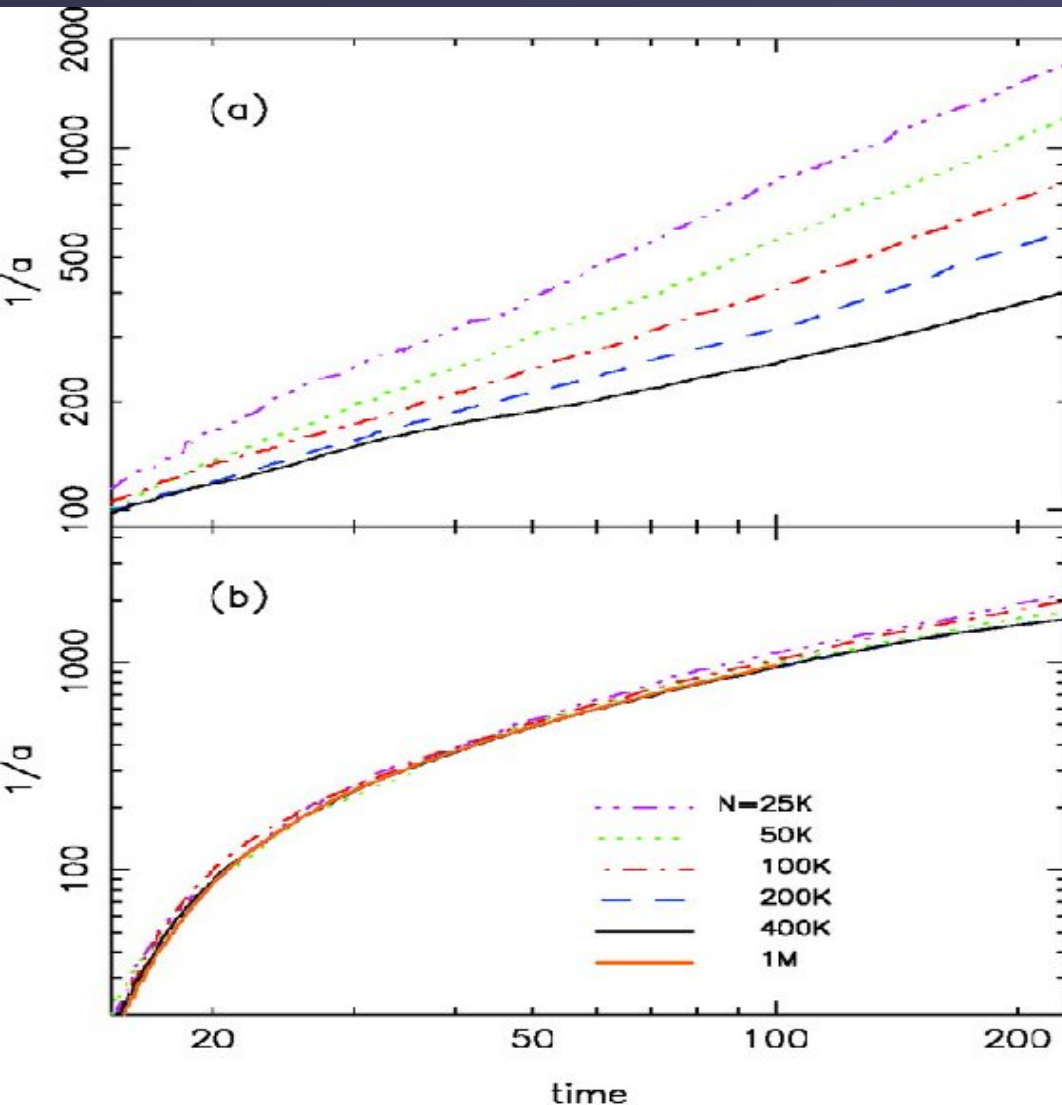
- Hemsendorf, Sigurdsson, Spurzem, 2002 , Astroph. Jl.

- High Eccentricity if loss cone full!

Time Scale for GR merger: $t_{GR} \propto M^{-3}(1 - e^2)^{7/2}$

Important for Background of Ultra-Low GR frequencies (LISA!) 0.01-1 μ Hz

Dynamics of Binary Black Holes in Galactic Nuclei



Spherical Systems:
BH binary stalls with N

**Axisymmetric,
Rotating systems:**
No stalling observed

Berczik, Merritt, Spurzem, 2005, ApJ

Berczik, Merritt, Spurzem, Bischof,
2006, ApJ

Berentzen, Preto, Berczik, Merritt,
Spurzem, 2009, ApJ

Fiestas & Spurzem, 2010,11 MNRAS

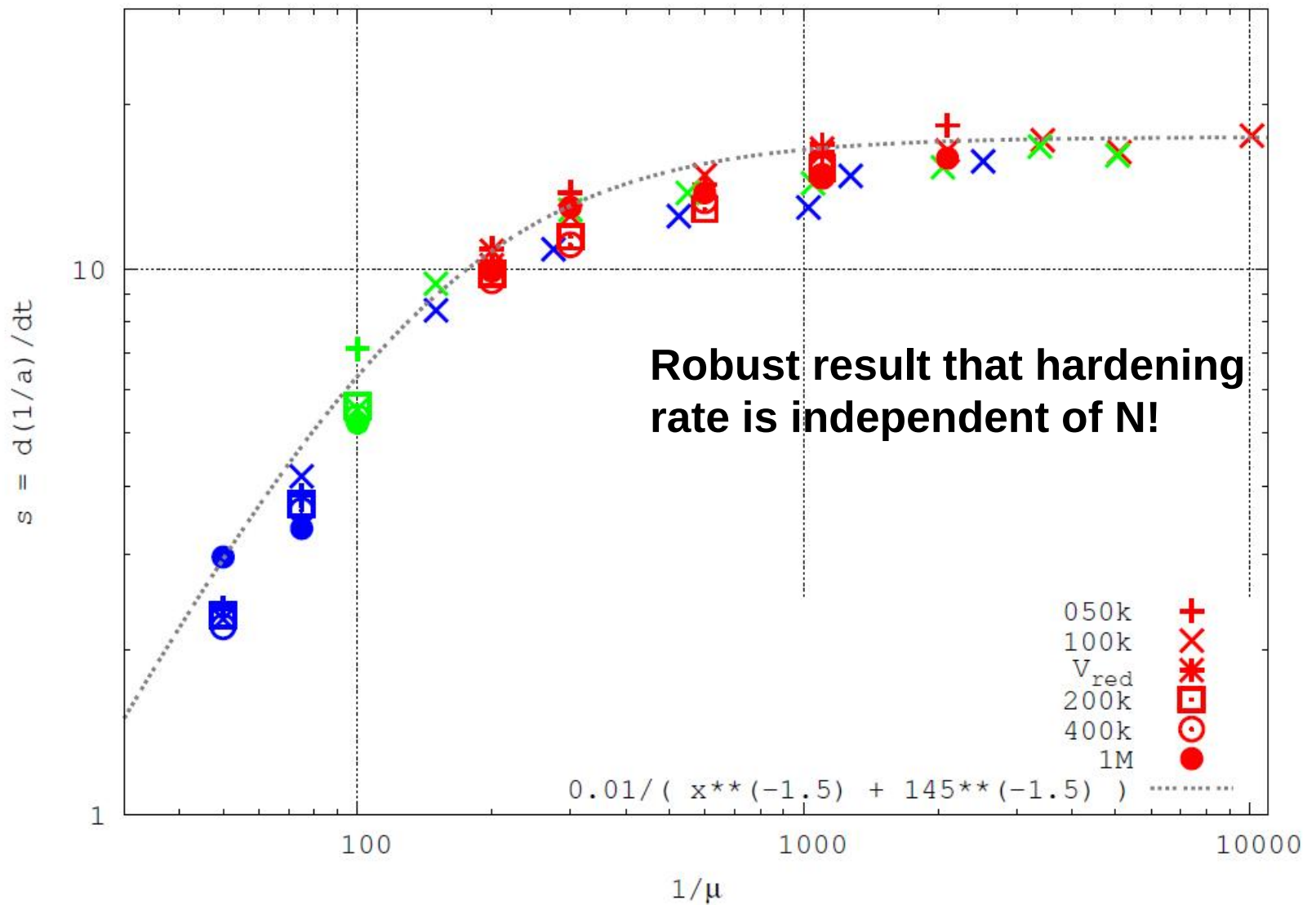
Amaro-Seoane, ..., Sp, MNRAS 2010

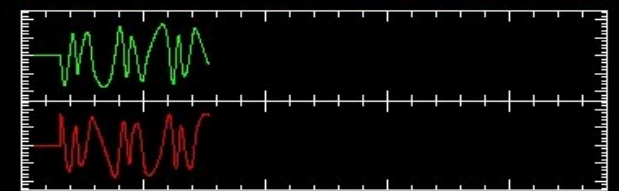
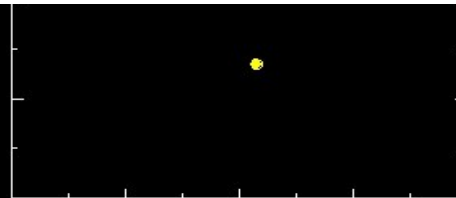
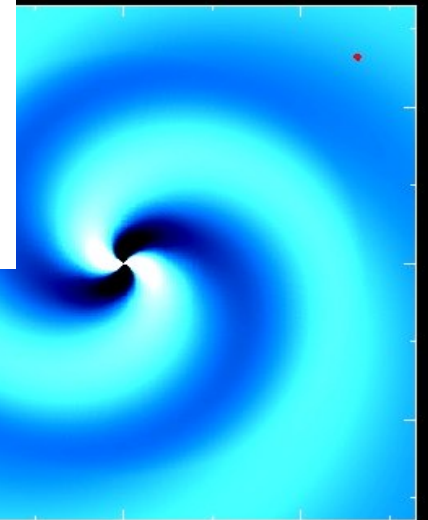
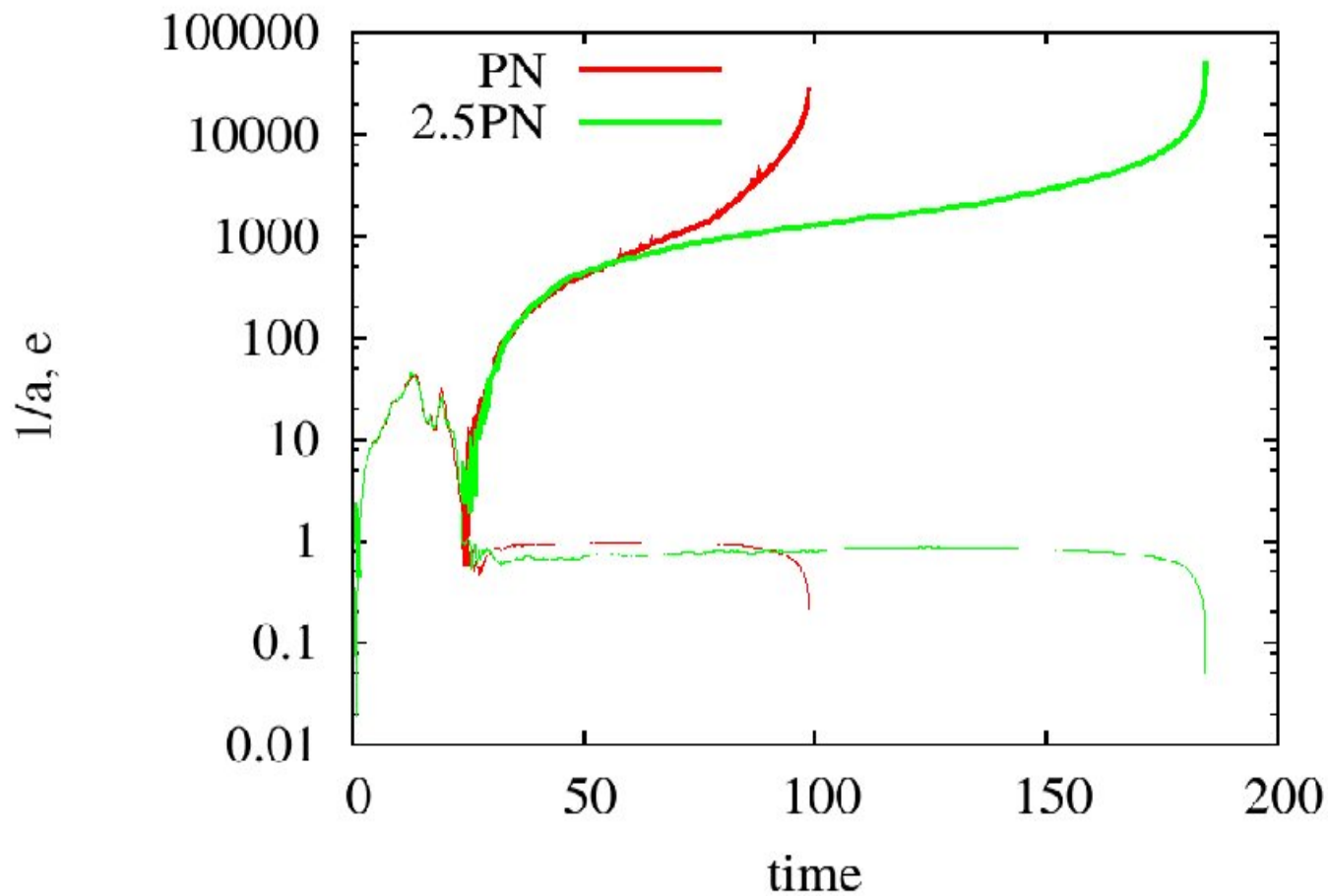
Preto, Berentzen, Berczik,

Spurzem et al. 2011

Khan et al. 2011a, b

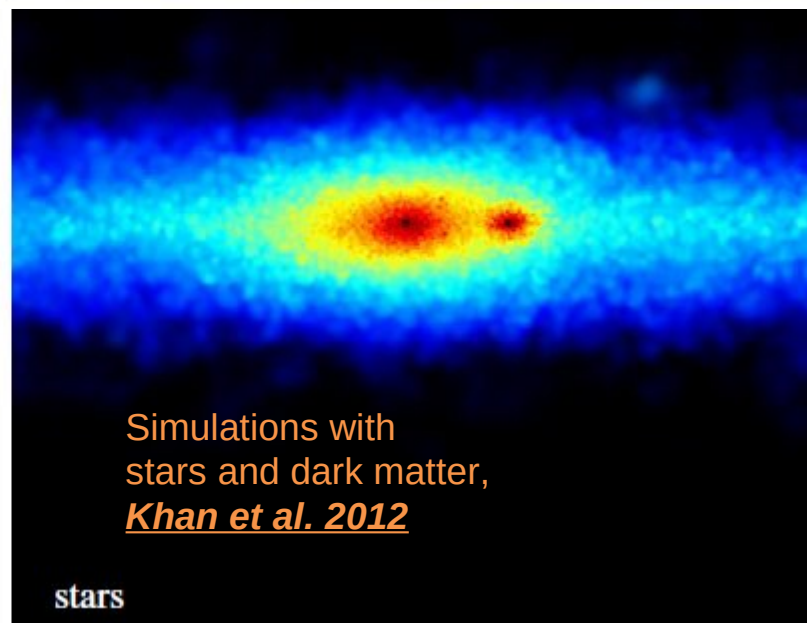
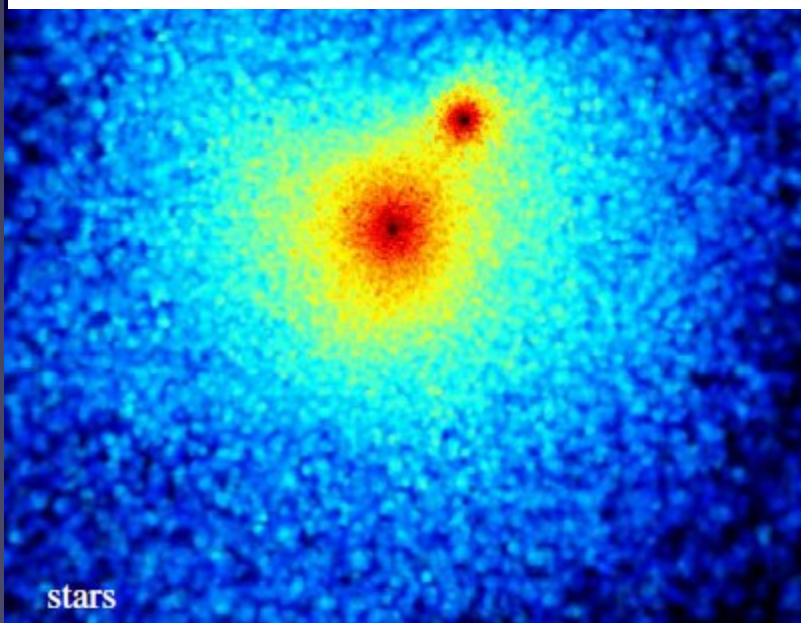
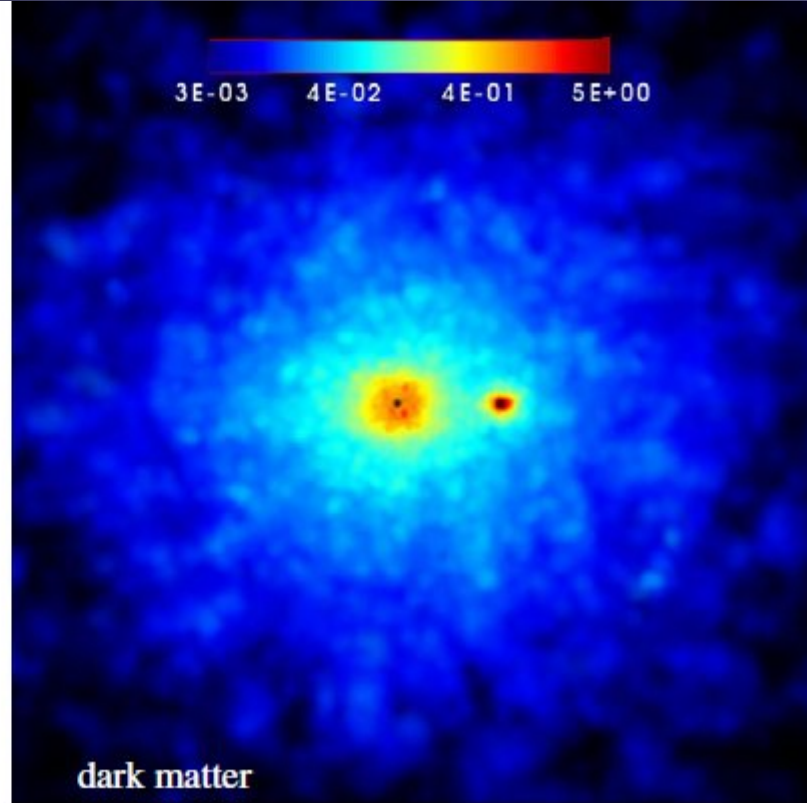
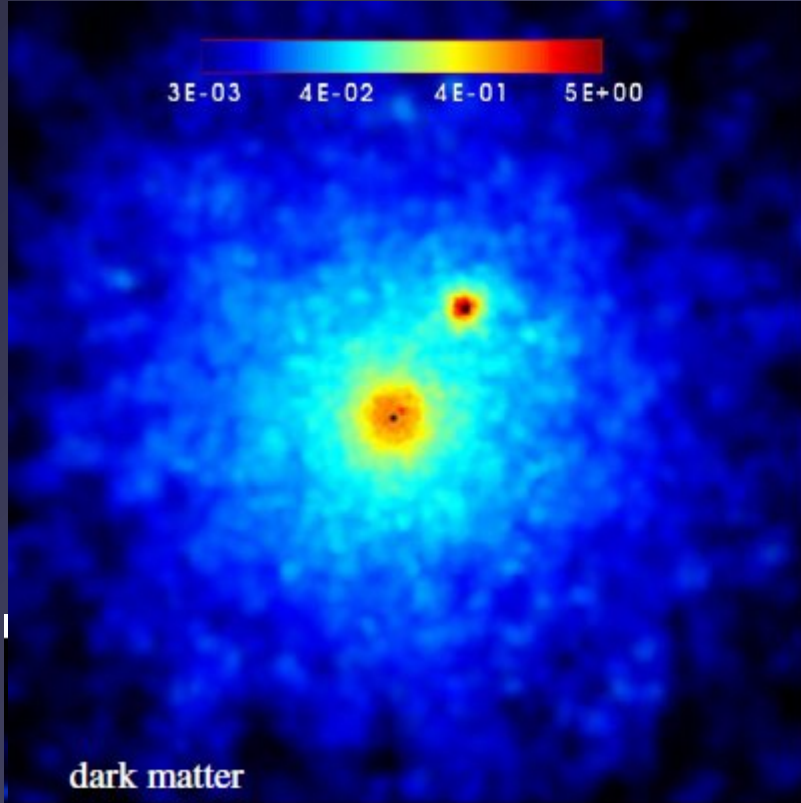
Unequal Mass Black Holes – Preto et al. 2011,
 Khan et al. 2011, 2012... Li et al. 2017, 2019, Berczik et al. 2019



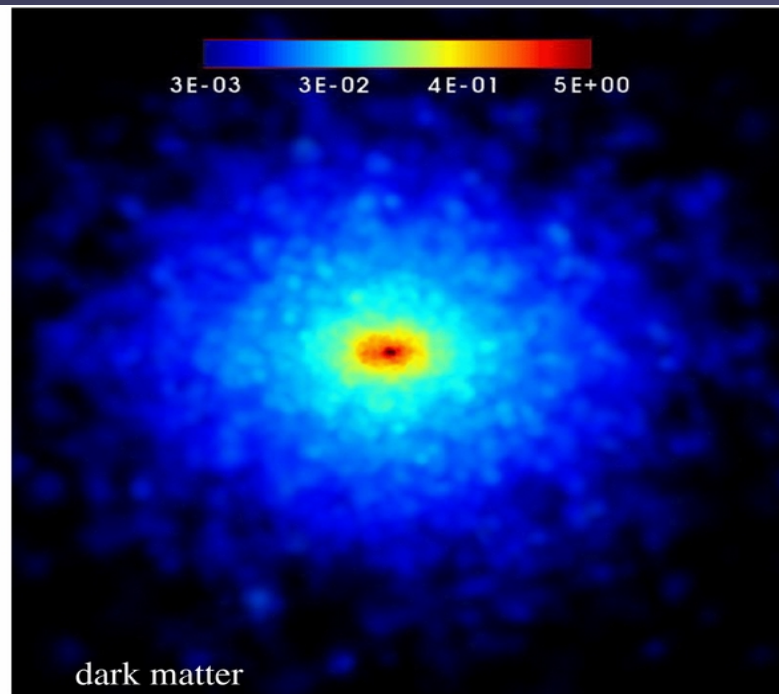
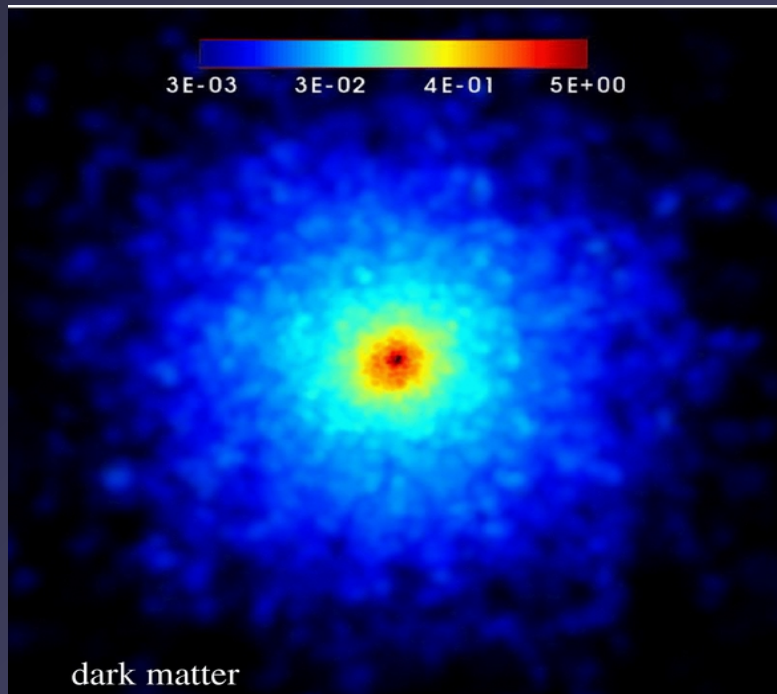


Berentzen, Preto,
 Berczik, Merritt,
 Spurzem,
 2009, ApJ

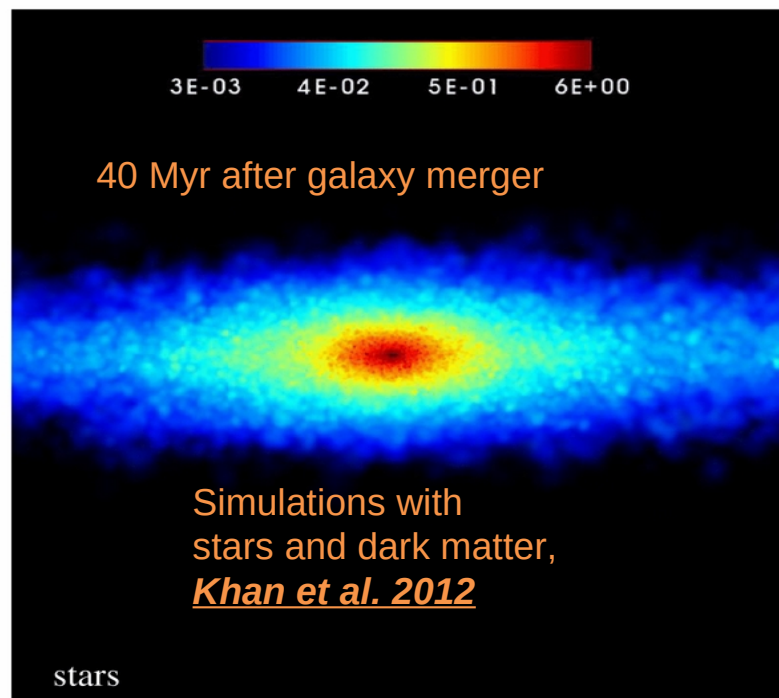
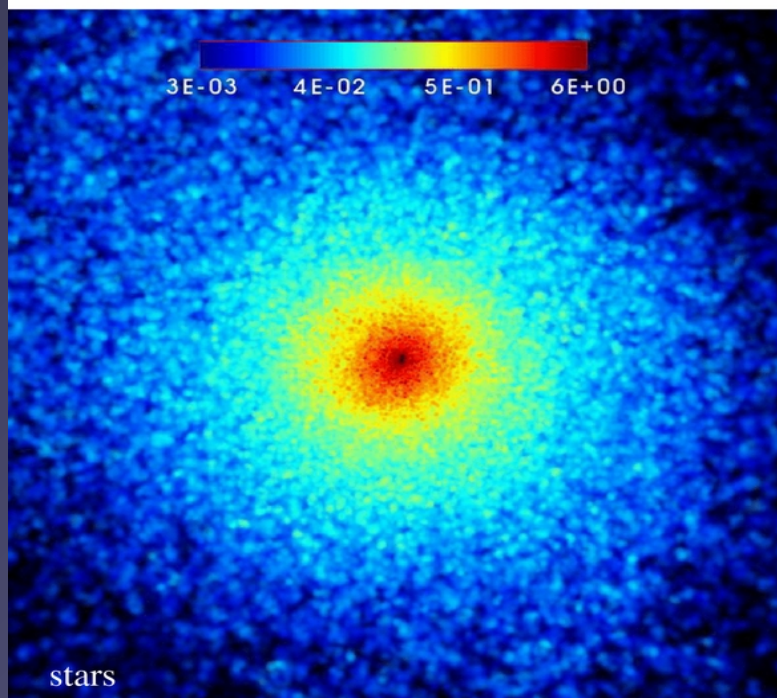
**Post-Newtonian
 Dynamics... and they merge!**



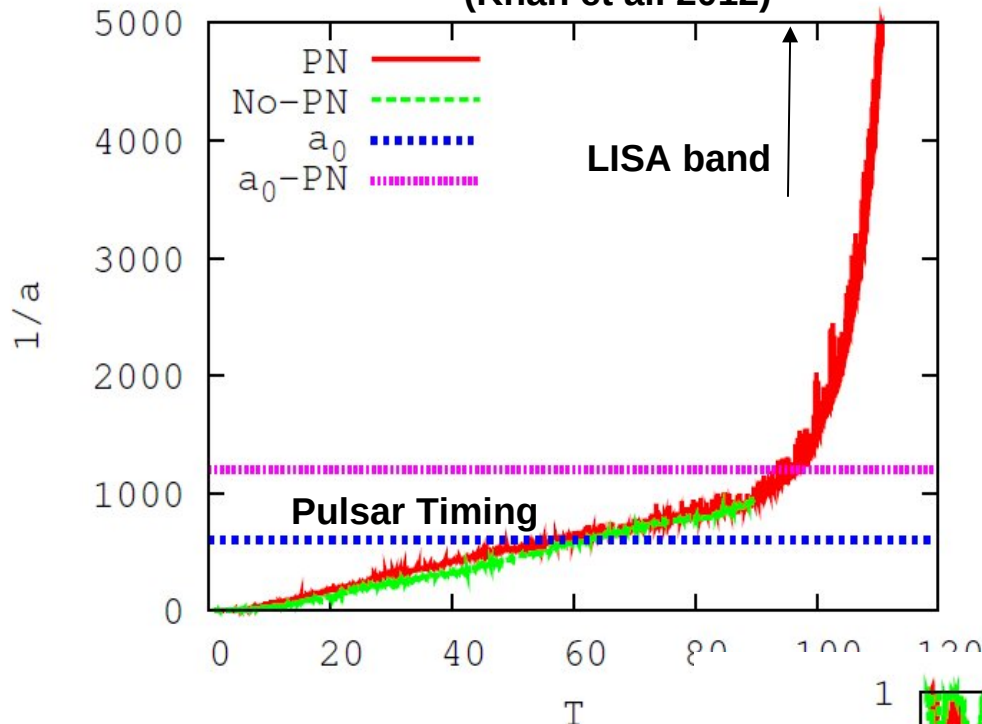
Simulations with stars and dark matter,
Khan et al. 2012



Box
Size
4 kpc



(Khan et al. 2012)



Full Model from Merger
To
SMBH coalescence
6 orders in separation!

*GW Emission from Pulsar Timing to
LISA band modelled*

*Khan et al. 2012, 2013, 2015, 2016
Mirza et al. 2017, Khan et al. 2018,
Berczik et al. 2019*

SMBH Bin. Eccentricity

1 / SMBH Bin. Separation

Also Worked on SMBH Triples!
Amaro-Seoane, Sesana, Benacquista,
... Spurzem MNRAS 2010

!

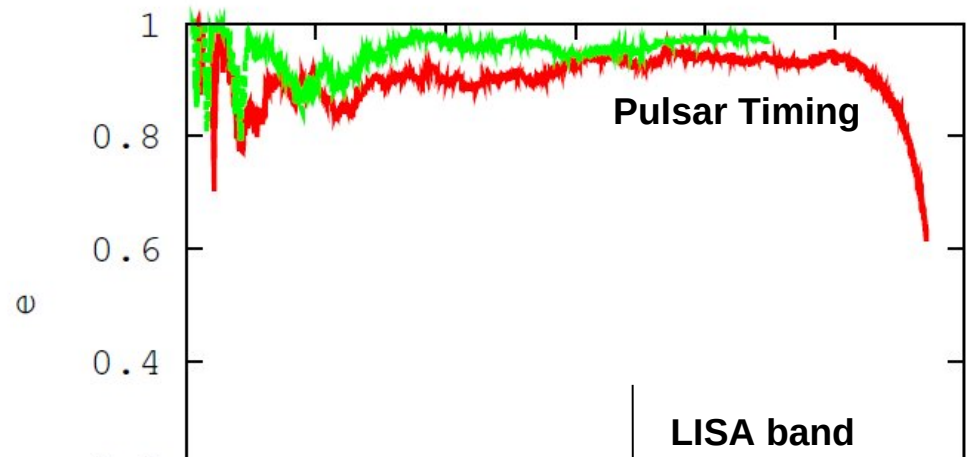
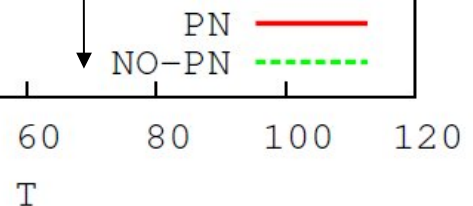
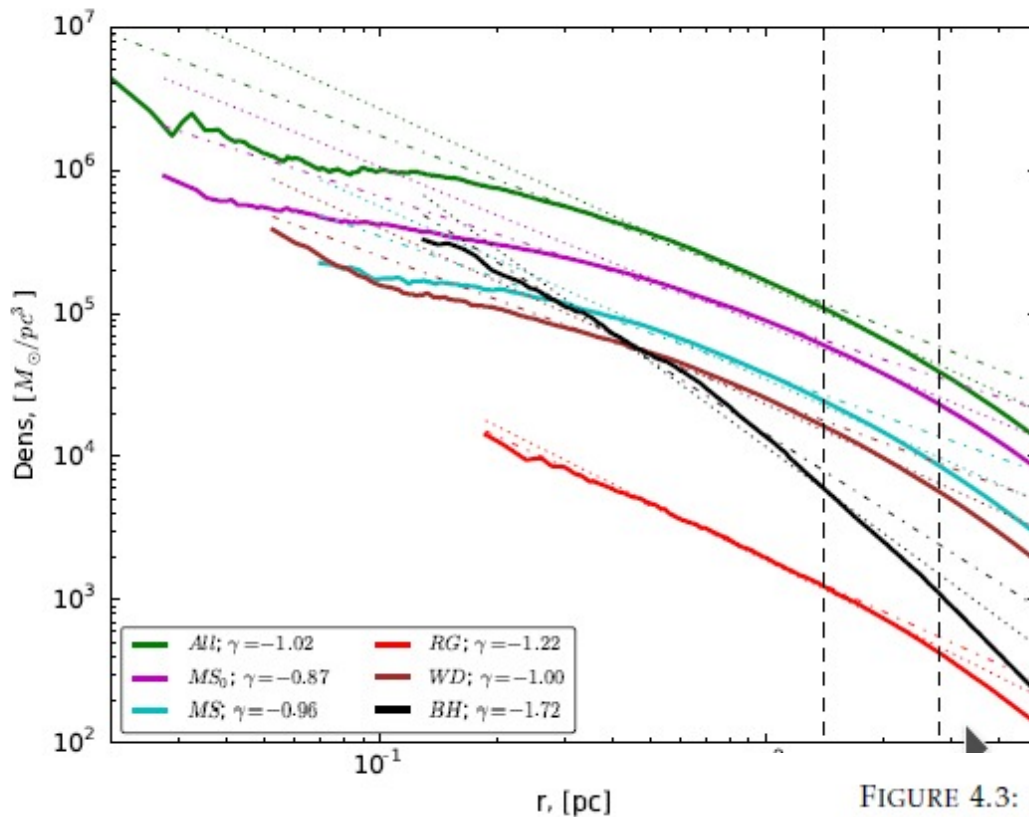


FIG. 7.— Evolution of the inverse semi-major axis $1/a$ (top) and eccentricity e (bottom) for model A2, with and without \mathcal{PN} terms. The horizontal lines represent the estimated semi-major axis of the SMBH binary for which the stellar dynamical hardening becomes equal to the \mathcal{PN} hardening derived from the run without \mathcal{PN} (a_0) and with \mathcal{PN} ($a_0 - \mathcal{PN}$). See main text for further details.



DRAGON Galactic Center Simulations



Density Profiles
of stars and
Black Holes
in the
Galactic Center

FIGURE 4.3: Stellar density profiles at $t = 5$ Gyr for different stellar types. Thick solid lines correspond to: All - all stars, MS_{low} - low mass main sequence stars, MS - main sequence, RG - red giants, WD - white dwarfs, BH - black holes. Corresponding power-law slopes fitted inside the initial and final influence radii of the SMBH are shown as dash-dotted and dotted lines of the same colour. The dashed vertical lines denote the initial influence radius ($r = 1.4$ pc) and the influence radius at $t = 5$ Gyr ($r \sim 2.8$ pc) of the SMBH. The power-law indices fitted inside $r = 1.4$ pc are shown in the legend.

Panamarev, Just, Spurzem, et al. 2019
Panamarev, ..., Just, Spurzem, 2018, MNRAS

Stellar Disk forms inside Gaseous Disk

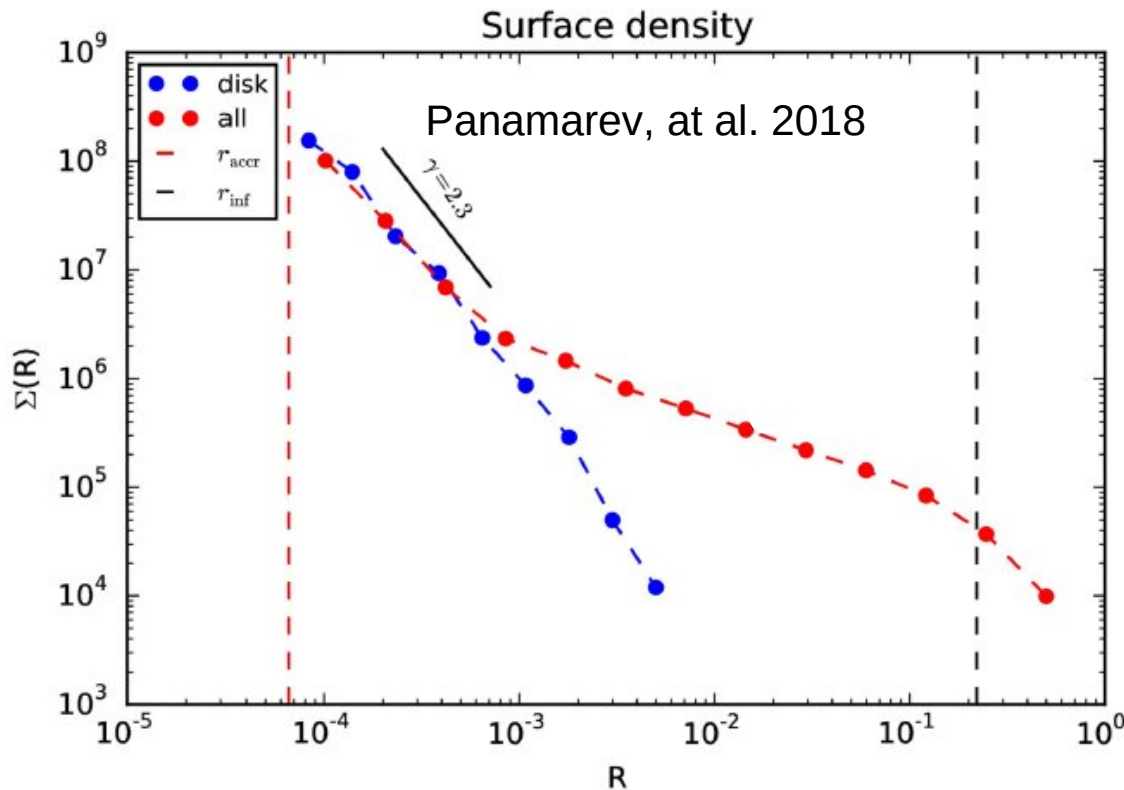


Figure 7. Surface density of the NSD. Red dotted line represents all NSC stars, the blue one shows only the stars that belong to NSD. Dashed red and black vertical lines represent the accretion radius and the influence radius respectively.

**Stellar Disk
Versus
Gaseous Disk**

**Surface
Densities:**

Red: NSC
(nuclear stellar cluster)

Blue: NSD
(nuclear stellar disk)

Vertical dashed line:
Accretion Radius (red)
Influence Radius of
SMBH (black)

- 1) Star Cluster Dynamics
- 2) Post-Newtonian Theory
- 3) Black Hole Binaries – Grav. Waves
- 4) Supermassive Black Hole Binaries
- 5) Computational Instruments

HARDWARE

...before von Neumann...

● Konrad Zuse (1910-1995) Berlin



Invented freely programmable Computer

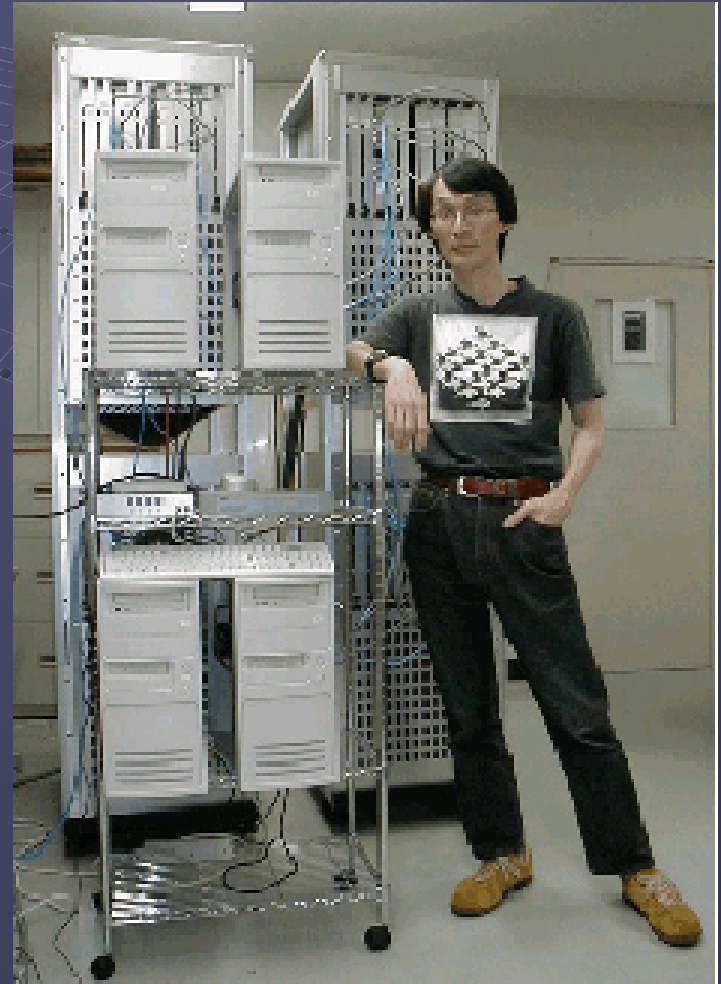


Z1 in parental flat 1936

HARDWARE

GRAPE-6 Gravity/Coulomb Part

- G6 Chip: 0.25μ 2MGate ASIC, 6 Pipelines
- at 90MHz, 31Gflops/chip
- 48Tflops full system (March 2002)
- Plan up to 72Tflops full system (in 2002)
- Installed in Cambridge, Marseille, Drexel, Amsterdam, New York (AMNH), Mitaka (NAO), Tokyo, etc..
New Jersey, Indiana, Heidelberg



Computational Science...

...after von Neumann...

Exaflop/s?

Petaflop/s

Teraflop/s

Gigaflop/s

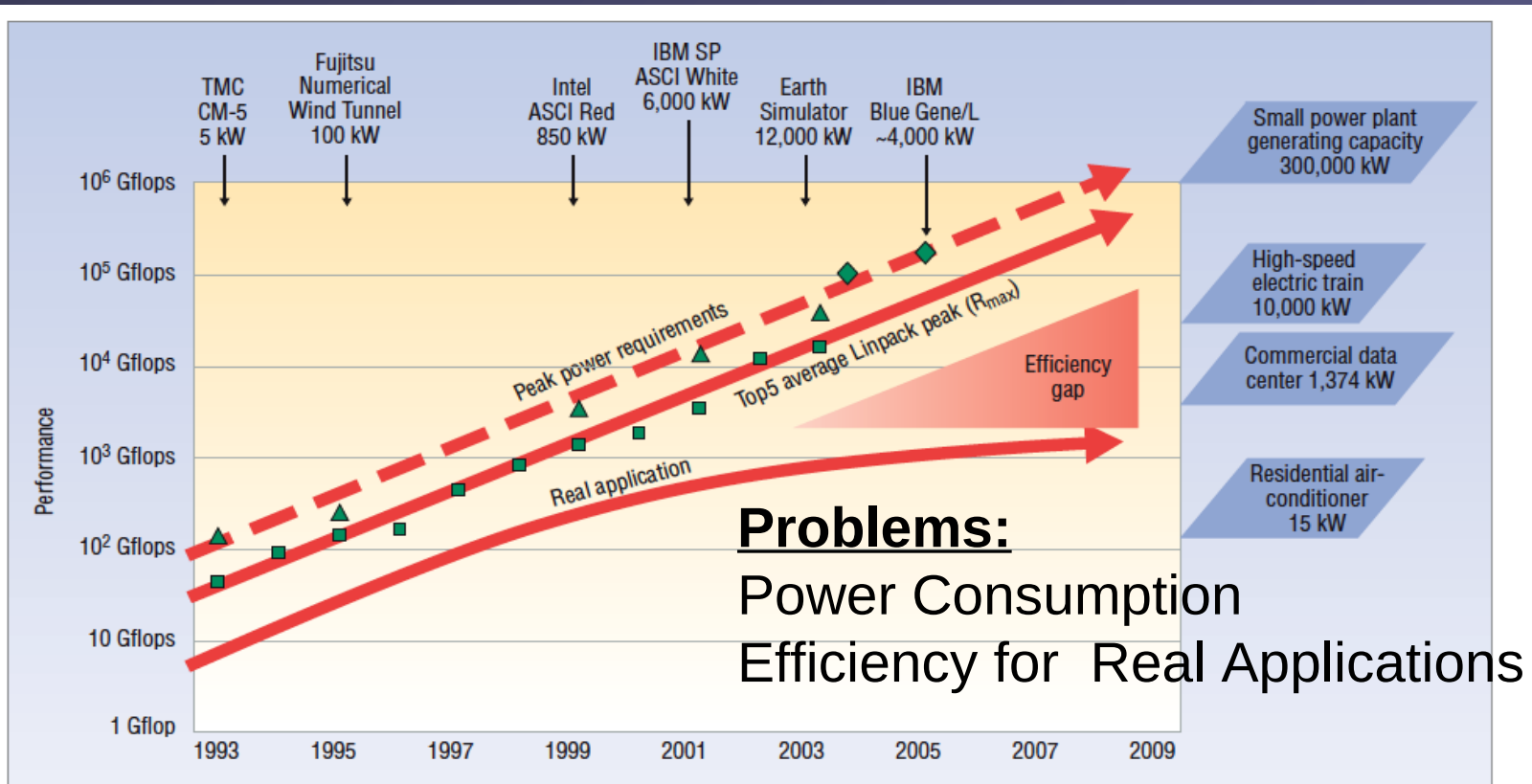


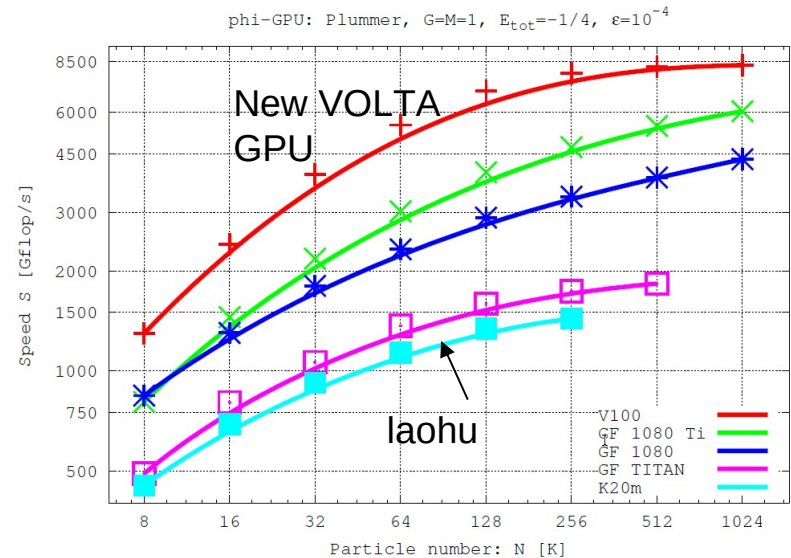
Figure 1. Rising power requirements. Peak power consumption of the top supercomputers has steadily increased over the past 15 years. Thanks to Horst Simon, LBNL/NERSC for this diagram.

NAOC laohu cluster 64 Kepler K20



Laohu: 2009/2015
(Kepler GPU)
100 Tflop/s 150k cores

New GPUs 5-6 times
faster... (see below)





中国科学院国家天文台

National Astronomical Observatories, CAS

the SILK ROAD PROJECT at NAOC

丝绸之路计划

GPU Clusters used:

老虎 Beijing (NAOC/CAS and Silk Road Project)

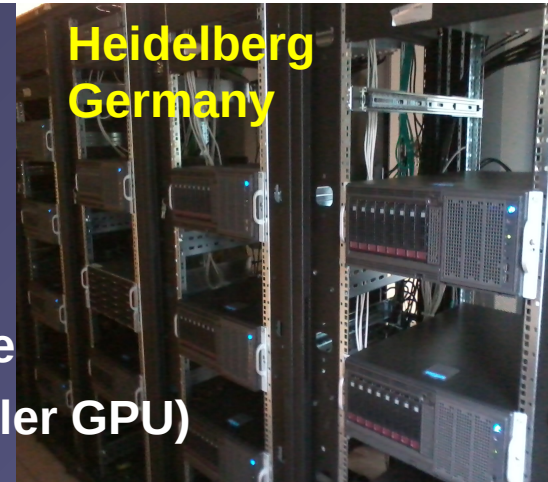
85 Nodes, 64 Kepler K2

JURECA GPU Partition (75x 2x Kepler K80 GPU)

Golowood cluster, Main Astron. Observatory, Kiev, Ukraine

Kepler/bwFor clusters Heidelberg, Germany (12x +18x Kepler GPU)

Max-Planck MPCDF GPU cluster (Kepler K20 GPUs)



Heidelberg
Germany



Kiev,
Ukraine



老虎
NAOC Beijing

2009/11/19



JUWELS Juelich GPU
Cluster Germany

Nr. 1,2 Supercomputer from China: 96/33 Pflop/s Linpack Wuxi/Guangzhou/Tianjin National Supercomputing Center Taihu 10 mill. cores

Tianhe-2 (MilkyWay-2) - TH-IV
E5-2692 12C 2.200GHz, TH Ex
31S1P

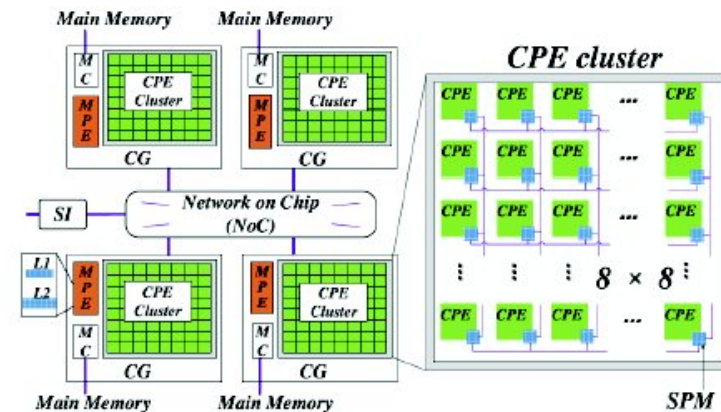


32000 Intel Xeon 12 core,
48000 Intel Phi Accelerators 57 Core

Test of Taihu planned;
But:
Local cluster with new
GPUs at NAOC gives
much more resources.

SUNWAY TAIHULIGHT

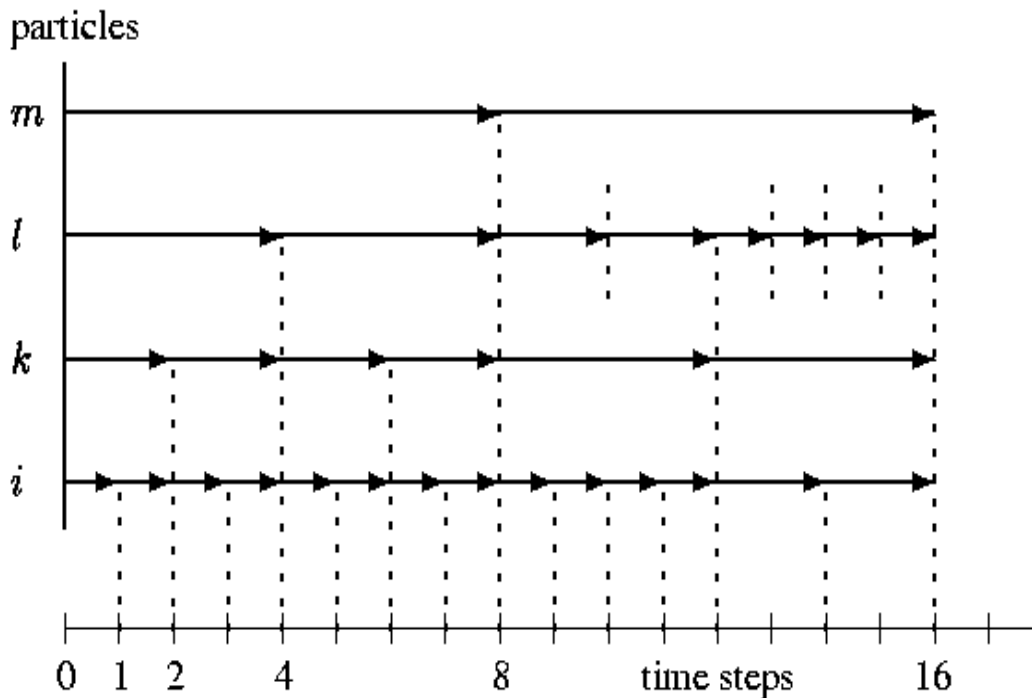
- SW26010 processor (Chinese design, ISA, & fab)
 - 1.45 GHz
 - Node = 260 Cores (1 socket)
 - 4 – core groups
 - 32 GB memory
 - 40,960 nodes in the system
 - 10,649,600 cores total
 - 1.31 PB of primary memory (DDR3).
 - 125.4 Pflop/s theoretical peak
 - 93 Pflop/s HPL, 74% peak
 - 15.3 Mwatts water cooled
 - 3 of the 6 finalists for Gordon Bell Award@SC16
- 6 Gflops/Watt



Presently used GPU (GRAPE) N-body code

Harfst, Berczik, Merritt, Spurzem et al, NewA, 12, 357 (2007)
Spurzem et al., Comp. Science Res. & Dev. 23, 231 (2009)

Hierarchical Individual Block Time Steps



$$\Delta t = \sqrt{\eta \frac{|\vec{a}||\vec{a}^{(2)}| + |\vec{a}|^2}{|\vec{a}||\vec{a}^{(3)}| + |\vec{a}^{(2)}|^2}}$$

4th order Hermite scheme

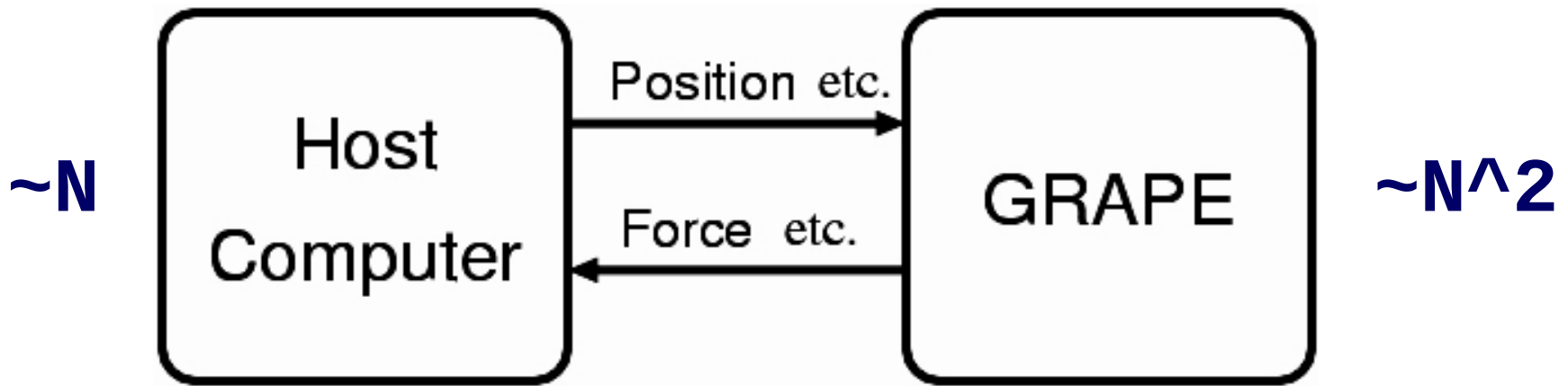
$$\frac{d^2 \vec{r}_i}{dt^2} = \vec{a}_i$$

<ftp://ftp.ari.uni-heidelberg.de/pub/staff/berczik/phi-GRAPE/>



北京大學
PEKING UNIVERSITY

Our own ϕ GRAPE/GPU N-body code



$$\vec{a}_i = \sum_{j=1; j \neq i}^N \vec{f}_{ij} \quad \vec{f}_{ij} = - \frac{G \cdot m_j}{(r_{ij}^2 + \epsilon^2)^{3/2}} \vec{r}_{ij}$$

Software

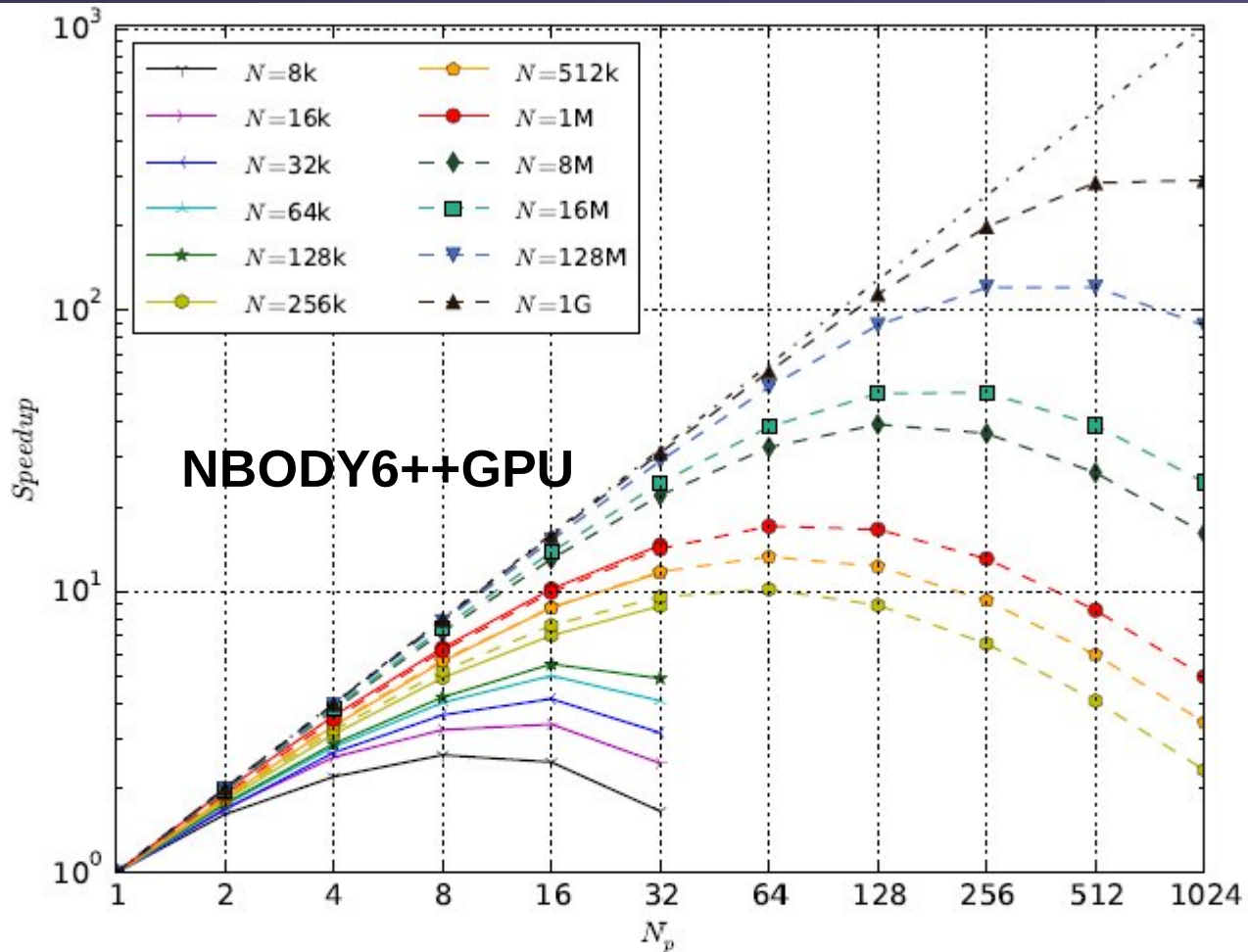
NBODY4, NBODY6, S.J.Aarseth, S. Mikkola, ...

(ca. 20.000 lines, since 1963):

- Hierarchical Individual Time Steps (HITS)
- Ahmad-Cohen Neighbour Scheme (ACS)
- Kustaanheimo-Stiefel and Chain-Regular. (KSREG) for bound subsystems of $N < 6$ (Quaternions!)
- 4th order Hermite scheme (pred/corr), Bulirsch-Stoer (for Chain)
- Stellar Evolution (single/binary) (w Hurley)

- NBODY6++, ϕ GPU, R. Spurzem, P. Berczik, T. Hamada, K. Nitadori, ...
- *(massively parallel codes, since 1999):*

- NBODY6++ (Spurzem 1999) using MPI
- Parallel ϕ GRAPE / ϕ GPU (Harfst et al. 2006, Spurzem et al. 2009, Berczik, Hamada et al. 2011 in prep.)
- NBODY6++/GPU-MPI (Wang, Spurzem, Aarseth, Berczik 2015)
- Parallel Binary Integration in Progress (KSREG)



Huang, Berczik, Spurzem, *Res. Astron. Astroph.* 2016, 16, 11.

Fig. 2 The speed-up (S) of NBODY6++ as a function of particle number (N) and processor number (N_p). Solid points are the measured speed-up ratio between sequential and parallel wall-clock time, dash lines predict the performance of larger scale simulations further. The symbols used in figure have the magnitudes: $1k = 1,024$, $1M = 1k^2$ and $1G = 1k^3$.

Summary

▪ Astrophysical High Precision N-Body – Star Clusters

DRAGON simulations of higher-density star cluster
Stellar Evolution, binaries, high density, nuclear star
Clusters, nuclear stellar disks

(Wang et al. 2015, 2016, Cai et al. 2015, Pang et al. 2015 RAA, Panamarev et al. 2017, 2018, 2019 ; Rizzuto et al. 2019...)

• Be careful about GW rate predictions:

LIGO/Virgo Observations very small number

Full modelling of star clusters very small number/or approximate

Detailed galaxy / star cluster population within 1 Gpc poorly known

Uncertainties in stellar evolution (kicks, common envelope, mergers...)

▪ Our next plans:

More DRAGON simulations / check Monte Carlo

Parameter Studies for Stellar Evolution problems

Gravitational Wave Prediction / low / high frequencies



中国科学院国家天文台

NATIONAL ASTRONOMICAL OBSERVATORIES, CHINESE ACADEMY OF SCIENCES



北京大学
PEKING UNIVERSITY